A Proposed Method for the Detection of Steel Moment Connection Fractures Using High-frequency, Transient Accelerations

By Janise E. Rodgers[1] and Mehmet Çelebi[1]

2005

Open-File Report 2005-1375

[1]U.S. Geological Survey, Menlo Park, California

U.S. DEPARTMENT OF THE INTERIOR
U.S. GEOLOGICAL SURVEY

Table of Contents

Table of Contents....2
List of Figures....3
List of Tables....4
Abstract....5
Introduction....6
Background....8
Dataset description....11
Effects of data sources and processing....14
  Data sources....14
  Data processing....14
Methods for transient detection and characterization....18
  Detection of transients....19
    Detection by visual inspection....19
    Detection using high-pass filtering....21
    Detection using the windowed Discrete Time Fourier Transform....24
    Detection using wavelet analysis....25
  Characterization of transients....29
    Characterization and identification of transient characteristics by visual inspection....29
    Characterization by frequency domain analysis....30
  Impact Transient Characterization by Experiment on FBA, SMA-1 and K2 Instruments....31
    GEOS Experiment....31
    SMA-1 Experiments....32
    K2 Experiments....34
  Summary of transient characteristics....35
Identification of likely transient cause....36
    Example: Burbank – Office Building #1....38
    Example: Woodland Hills – Canoga #1 and #2....38
Results for datasets....39
  Transients only....40
  Transients in combination with other damage indicators....41
Conclusions and Recommendations....43
Acknowledgments....44
References....44
Appendix A

List of Figures

Figure 1. Steel moment frame test specimen (top) and key to frame member abbreviations (bottom), Rodgers and Mahin (2004) 9
Figure 2. Acceleration transients predicted by analysis, cosine acceleration pulse with 1.2 seconds duration (Rodgers and Mahin, 2005) 10
Figure 3. Comparison of acceleration transients observed in the laboratory with those predicted by analysis, cosine acceleration pulse with 1.2 seconds duration (Rodgers and Mahin, 2005). DB = ductile baseline, BF = brittle fracture, and BP = 2 simultaneous fractures in 1st story, ideally ductile behavior in 2nd story 10
Figure 4. Comparison of corrected and uncorrected data from Los Angeles – Olympic Blvd. #2, Roof 15
Figure 5. Comparison of corrected and uncorrected data from Woodland Hills – Oxnard Blvd. #4, 6th floor 16
Figure 6. Digital image of a portion of the original analog record from Burbank – Office Building #1, roof 17
Figure 7. Uncorrected data obtained by digitization and processing of Burbank – Office #1 analog record 18
Figure 8. Acceleration time histories, Los Angeles - Olympic #2 20
Figure 9. High-pass filtering of uncorrected Los Angeles - Olympic #2 record 21
Figure 10. High-pass filtering of uncorrected Woodland Hills – Canoga #1 record 22
Figure 11. High-pass filtering of uncorrected Woodland Hills – Canoga #2 record 23
Figure 12. Spectrogram of wDTFT analysis of Los Angeles - Olympic #2 records 24
Figure 13. Time history (top), and wavelet transforms (middle and bottom) showing location of acceleration transients and wavelet coefficients in time, Los Angeles – Olympic #2. 26
Figure 14. Time history (top), and wavelet transforms (middle and bottom) showing location of acceleration transients and wavelet coefficients in time, Woodland Hills – Canoga #1. 27
Figure 15. Time history (top), and wavelet transforms (middle and bottom) showing location of acceleration transients and wavelet coefficients in time, Sherman Oaks – Ventura #6. 28
Figure 16. Time history (top), and wavelet transforms (middle and bottom) showing location of acceleration transients and wavelet coefficients in time, Woodland Hills – Canoga #2. 29
Figure 17. Acceleration response to direct impact of metal trash can on top of SMA-1 (Test 12) 33
Figure 18. Acceleration response to direct impact of metal trash can on top of K2 34
Figure 19. Flowchart for determining the likely cause of a high-frequency transient 37
Figure 20. Comparison of roof accelerations, Canoga #1 and #2 39

List of Tables

Table 1. Criteria used to separate data into subsets 12
Table 2. Damage bin definitions 12
Table 3. Data sets of steel buildings with recorded Northridge earthquake responses 12
Table 4. Prior studies on buildings in the dataset 13
Table 5. Key transient characteristics from visual identification 30
Table 6. Experiments performed on FBAs 32
Table 7. Experiments performed on SMA-1 32
Table 8. Qualitative results of SMA-1 impact tests 33
Table 9. Summary of transient characteristics 35
Table 10. Results of transient evaluation procedure 40
Table 11. Method success rate by set and damage bin 41
Table 12. Results for combination of indicators 42

A Proposed Method for the Detection of Steel Moment Connection Fractures Using High-frequency, Transient Accelerations

By Janise E. Rodgers[1] and Mehmet Çelebi[1]

[1]U.S. Geological Survey, Menlo Park, California

Abstract

The 1994 Northridge earthquake caused brittle fractures in the beam-to-column connections of numerous steel moment frame buildings. Since many buildings had little visible damage, most of these fractures were not detected until architectural finishes and fireproofing were removed in intrusive inspections weeks (or even months) later. Currently, the only way to determine if fractures have occurred in such cases is by intrusive inspection, which can be time-consuming and expensive. However, if a building is seismically instrumented, even sparsely (in some cases with a single tri-axial accelerograph at the roof only), the recorded acceleration response is available and can provide information that may indicate potential building damage. This report explores the possibility of going beyond traditional indicators of building damage that are obtained from accelerograms (such as fundamental period elongation) and examining indicators specific to fracture, impact and other types of sudden structural failure. Specifically, based on the equations of motion, sudden structural failures and impacts are expected to produce a transient dynamic response, both globally and locally, with frequency content higher than that of the predominant building response preceding it, due to the excitation of both member and structure higher modes by the failure/impact. In cases of substantial sudden damage (i.e. numerous connection fractures), this high-frequency, transient dynamic response is expected to be visible in the recorded acceleration response, provided certain conditions are satisfied.

Based on this expectation, a method for detecting steel moment connection fractures using fracture-generated high-frequency transient accelerations is proposed. The method is evaluated using a dataset containing strong motion data from the 1994 Northridge earthquake, and damage and inspection information from 24 steel moment frame buildings with varying degrees of connection fracture damage. The success rate of the method is high for heavily damaged buildings, relatively high for undamaged buildings, and moderate for moderately damaged buildings. However, the method fails for lightly damaged buildings. The success rate improves for moderately and heavily damaged buildings with the removal of records with excessive noise, indicating that too much noise can affect the success of the method. The proposed method is also evaluated in combination with more commonly used damage indicators, which gives a higher success rate at detecting damage occurrence.

Due to the very sparse instrumentation in most buildings in the dataset, the method is not able to determine specific fracture locations, though very general location determination (such as upper floors vs. lower floor) may be possible in the future in buildings with more accelerometers. However, it is anticipated that a very dense instrumentation scheme would be necessary to determine fracture locations down to the individual connections. Such high-density instrumentation schemes are not practical with current technology, though advances in cheaper and/or wireless instrumentation may permit such dense instrumentation in the future.

Introduction

In the aftermath of the 1994 Northridge earthquake, fracture damage was discovered in many steel moment frame buildings with welded connections. In most cases, this damage was not immediately discovered by walk-through visual inspections (ATC 1989), but rather by intrusive inspections, where the architectural finishes and fireproofing were removed (FEMA 2000a; Bertero 1994). A number of building owners performed intrusive inspections voluntarily soon after the earthquake, and eventually the City of Los Angeles and several other local jurisdictions required intrusive inspection and repair of connections for many welded steel moment frame (WSMF) buildings within certain geographical areas (FEMA 2000b).

Information on the damage sustained by WSMFs during the Northridge earthquake is available from both intrusive inspections and extensive research conducted in response to the fracture damage, most notably by the SEAOC-ATC-CUREe (SAC) Joint Venture (comprising the Structural Engineers Association of California (SEAOC), Applied Technology Council (ATC), and Consortium of Universities for Research in Earthquake Engineering (CUREE)). A number of case studies (SAC 1995a; Cohen 1996; Naeim 1997; Naeim et al. 1999), damage surveys (SAC 1995b; FEMA 2000b; Maison and Bonowitz 2003), and unpublished inspection reports provide detailed information. Inspection reports were required for compliance with mandatory inspection and repair ordinances. Also, due to a Los Angeles Building Code requirement for instrumentation in taller buildings (see Darragh et al. 1994)[1], a number of these damaged buildings were instrumented with a triaxial accelerograph at the roof at a minimum. Strong-motion records from many of these buildings are available from the California Strong Motion Instrumentation Program (CSMIP) (Shakal et al. 1994; Darragh et al. 1994, 1995) and the U.S. Geological Survey (USGS) (Porcella et al. 1994). Thus, the availability of both damage and inspection information and recorded accelerations made it possible to assemble the dataset used herein.

Following the Northridge earthquake, the FEMA 352 guidelines (FEMA 2000c) were developed to direct inspections of WSMFs with pre-Northridge connection details after future earthquakes. For strongly shaken buildings without severe, obvious damage, detailed evaluations with intrusive inspections are required. These guidelines permit a representative sample of connections to be inspected (though inspection of all connections is preferred), with the intent that significant fracture damage should be uncovered if it exists. The sample can be selected randomly, by rational analysis (for instance, time-history analysis of a computer model of the building), or by a prescribed combination of the two (e.g. 20% of the connections to be inspected are selected by rational analysis, and the remainder randomly). Even if a random sample is used, weeks or even months may pass before the inspections are complete and the presence or absence of fracture damage confidently determined.

Therefore, information on fracture damage which can be obtained very quickly after an earthquake is highly desirable both for making informed decisions on whether to re-occupy the building and as an aid for the FEMA 352 rational analysis method of selecting connections for inspection. Strong motion instruments can provide such key information on building response within a very short time of the earthquake, provided necessary arrangements have been made for the timely retrieval of records (such as telephone dial-up or real-time capabilities). Tools which harness recorded accelerations for the detection of brittle fracture damage are therefore highly desirable, as they can provide valuable early information on building performance. As a result, a number of more theoretical damage detection methods which perform various types of analyses on recorded response data have been proposed. These approaches are generally applicable to multiple types of structural systems and include those using probabilistic methods (e.g. Sohn and Law 1997; Köylüoğlu et al. 1998; Sohn et al. 2001), neural networks (e.g. Nakamura et al. 1998; Masri et al. 2000), wavelet analysis (e.g. Hou et al. 2000; Kim and Melhem 2003), or a combination (e.g. Marwala 2000; Sun and Chang 2002). However, these methods tend to be computationally intensive, and require advanced signal processing or analysis methods that are not commonly used by practicing engineers. Many of these methods could potentially be applied in a timely manner following an earthquake (since their application basically

[1] At the time, Los Angeles County mandated conformity with the Uniform Building Code (ICBO, 1967) recommendations for tri-axial instruments at the roof, mid-height, and base of buildings 6 stories and higher with floor area greater than 60,000 square feet, and all buildings 10 stories and higher. After 1982, only a single tri-axial instrument at the roof was required, but a maintenance agreement for the instrument was necessary.

consists of applying a computer algorithm to the data), but require substantial work prior to the earthquake to mathematically characterize the system.

In addition, almost all instrumented buildings are sparsely instrumented; that is, motions are captured at only a small number of the structural degrees of freedom. The sparseness of available data is problematic for many damage detection methods. However, the case will be made herein that in many instances widespread steel moment connection fracture damage can be detected within a reasonable degree of certainty using high-frequency, transient accelerations generated by fracture, even in minimally instrumented buildings. This represents a strong argument for instrumentation. However, if transients are to be used in the post-earthquake evaluation process, data should be made available in a timely manner. This is not always possible with analog instruments, as the time for digitization and processing often exceeds the owner's timetable for inspection, performance evaluation, and repair. Therefore, owners should upgrade their current code-mandated analog instruments to digital instruments. It is assumed that all new instruments will be digital, as manufacturers no longer produce analog recorders.

This study is based on the premise that sudden structural failures or impacts cause a transient dynamic response to occur. The frequency content of such a transient response is expected to be significantly higher than that of the building response immediately preceding it, due to the excitation of higher modes (including local member modes) and the propagation of elastic waves. Thus, steel moment connection fracture is expected to produce high-frequency, transient accelerations. For the sake of brevity, these high frequency, transient accelerations are referred to hereafter as either *high-frequency transients*, or simply *transients*. In the case of moment connection fracture, high-frequency transients are generated by several sources: (a) the sudden change in member (and therefore structure) stiffness and strength, resulting in sudden changes in global accelerations to satisfy the equations of motion (dynamic equilibrium); (b) the sudden change in member end conditions, resulting in excitation of local member vibration modes, which have much higher frequencies than the building as a whole, and (c) the sudden release of strain energy, resulting in elastic waves propagating away from the fracture in connected members. Transients in accelerations from sources (a) and (b) and in strain time histories from source (c) have been observed in laboratory tests of a steel moment frame (Rodgers and Mahin 2004, 2005). Analytical studies of single and multiple degree of freedom systems (Rodgers and Mahin 2005) also show the existence of transients from source (a). Significantly more complex analytical models would have been required to produce transients from sources (b) and (c).

For very sparsely instrumented structures, such as those in this study, transients from sources (b) and (c) will probably not be recorded unless the fractures occur in the instrumented story. However, it should be noted that experimental testing has not established the distance over which fracture transients from sources (b) and (c) can be detected in full-size structures with typical rolled shapes. This estimate is based on observed transients in a one-third scale structure with idealized connections whose geometry may reduce wave propagation distance (Rodgers and Mahin 2004) for details. In general, transients will be present in the acceleration records of instrumented structures if the following conditions are satisfied: (1) the damage is located sufficiently close to a sensor, (2) the extent and severity of the damage is such that the transient is measurable above the background noise level, and (3) the frequency of the transient is low enough to be recorded by the sensor. Understandably, there is significant interaction between conditions (1) and (2), since more severe damage, such as a number of concurrent fractures, will have a greater effect on the story and overall system behavior and will generate transients measurable over larger portions of the structure than less severe damage such as a single connection fracture.

The intent of this study is to demonstrate that particular high-frequency features in recorded accelerations can indicate the presence of brittle fractures in WSMF connections. These features can be used to quickly identify the possibility of fracture damage. Using a dataset of instrumented WSMFs with known damage due to the Northridge earthquake, a method is developed for discerning between transients likely caused by fracture from those likely due to other sources. The method is then evaluated using a second set of instrumented WSMFs. Method performance is evaluated by comparison with a basic damage ratio from the results of intrusive inspections.

Background

High-frequency transients are defined as short-lived acceleration waveforms with sudden onsets and high frequency content, which are of sufficient amplitude to be visually identifiable above the noise level of the record. For the purposes of this study, baseline (DC) offsets are excluded. As the name implies, the frequency content of these transient signals is significantly higher than in those portions of the time history surrounding them, and can range from ~25 Hz to frequencies higher than the Nyquist frequency (for digital instruments) or higher than can be resolved by high-resolution digitization (for analog instruments). Due to recording limitations, the upper end of this frequency range is not well defined. In many cases, the frequency content of the transient is too high to be resolved by the instrument, and the transient thus has a jagged appearance in the time domain (at normal timescales such as 1 second/cm). This appearance leads to transients being commonly referred to as "spikes" in the literature. The term "transients" is preferred here, as "spikes" connotes a particular waveform (the one-sided pulse), though high-frequency transients can have a number of different waveforms.

High-frequency transients have been observed in acceleration recordings from buildings and bridges with various structural systems, including steel, concrete, and base isolation. Many of these high-frequency transients have been interpreted as resulting from system-specific structural failures or impacts, though in some cases this interpretation was somewhat speculative. Transients present in the upper floor records from the non-ductile concrete Imperial County Services building during the 1979 Imperial Valley earthquake were attributed to the crushing of exterior columns (Rojahn and Mork 1982) and subsequent sudden loss of gravity load capacity. Transients in the recorded response of the base isolated Fire Command and Control building during the Northridge earthquake were attributed to impacts against an entry bridge which defeated the isolation moat in one direction (Nagarajaiah and Sun 2001). The possibility that transients are related to structural damage in steel buildings was raised in a study of Northridge-damaged, instrumented buildings (Huang et al. 1996, 1998).

Similarly, transients in the recorded response of the reinforced concrete I10/215 interchange bridge during the 1992 Landers and Big Bear earthquakes were attributed to interaction of the bridge superstructures at the hinges (Fenves and DesRoches 1994; Huang and Shakal 1995). The amplitudes of these transients were used to calculate the forces generated by pounding of adjacent portions of superstructure (Malhotra et al. 1994). Transients observed in records from the 101/156 Separation bridge (Kasai et al. 1992), another multi-segmented structure, have been attributed to hinge interaction as well.

In the laboratory, high-frequency transients have been observed in shaking table tests of a one-third scale steel moment-framed structure (Rodgers and Mahin 2005). Beam-column connection fractures were found to cause such transients. These observations were made during a larger study of steel moment frame behavior (Rodgers and Mahin 2004). The test specimen used is shown in Figure 1. Analytical results of a model of the test specimen with fracturing and ductile connection behavior are compared for the same excitation in Figure 2. Experimental time histories from the shaking table tests are compared with the analysis results in Figure 3.

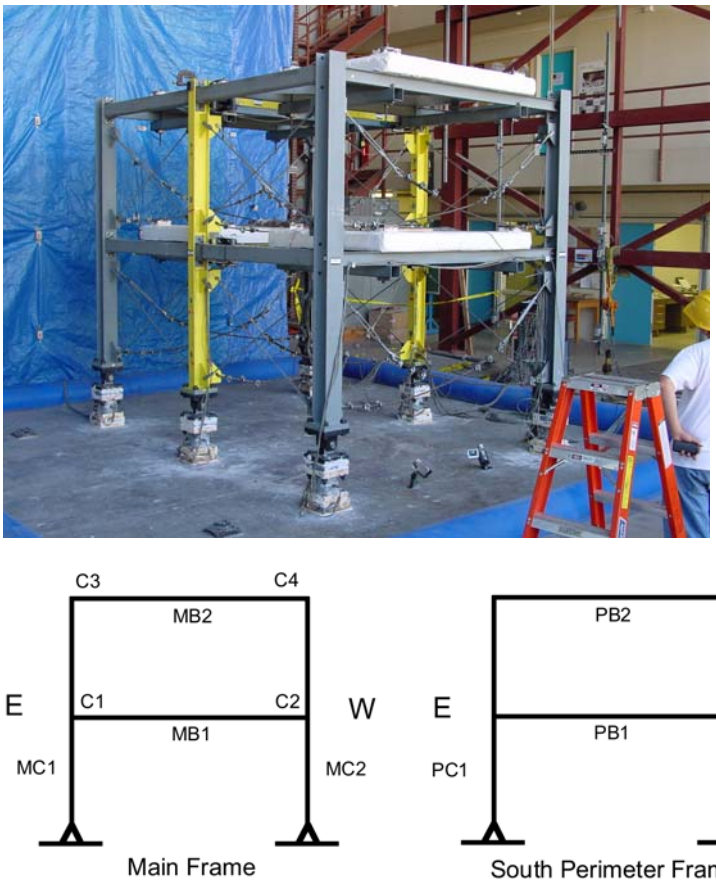

Figure 1. Steel moment frame test specimen (top) and key to frame member abbreviations (bottom), Rodgers and Mahin (2004)

The transient caused by fracture is evident in both the experimental and analytical results for the case with fracture, and is absent from the ductile cases. In this experimental series transients arising from sources other than fracture, such as engagement of the safety catch cable system, sudden spurious motions of the shaking table, and slip or severe buckling in ductile connections were observed to occur as well. These transients from other sources did not occur consistently, and most of these particular sources were related to the shaking table and test setup and will not be present in real WSMF buildings. However, other types of transients, such as those caused falling objects, may be present, and caution should be used when attributing transients to fracture.

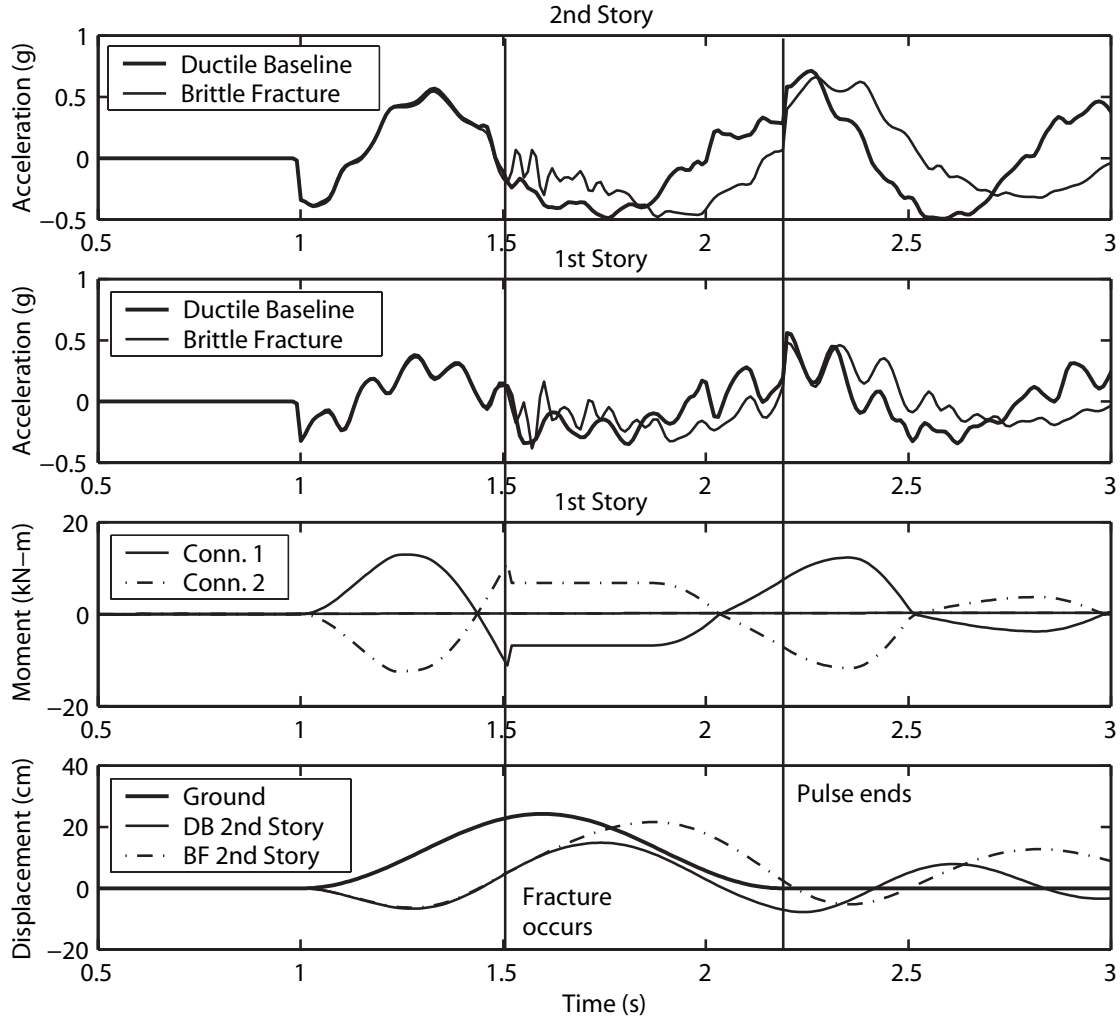

Figure 2. Acceleration transients predicted by analysis, cosine acceleration pulse with 1.2 seconds duration (Rodgers and Mahin, 2005)

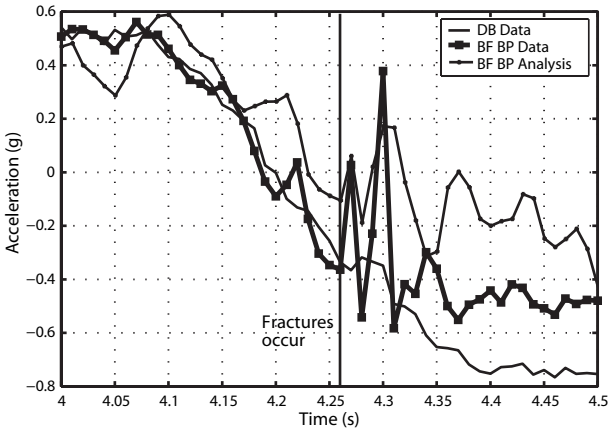

Figure 3. Comparison of acceleration transients observed in the laboratory with those predicted by analysis, cosine acceleration pulse with 1.2 seconds duration (Rodgers and Mahin, 2005). DB = ductile baseline, BF = brittle fracture, and BP = 2 simultaneous fractures in 1st story, ideally ductile behavior in 2nd story

High-frequency, low-amplitude transients in rotations at a fracturing connection were predicted by Uetani and Tagawa (1996) using a detailed analytical model of a 2-story, 2-bay frame with 138 degrees of freedom (DOF). These transients were not observed in the rotations of a simplified model of the same structure with only 2 DOF. Longitudinal accelerations were not reported in the paper. Very little information about the accelerations predicted by analysis is available for the numerous system behavior studies (see Rodgers and Mahin 2004 for a listing), which have been performed since Northridge. This is mostly due to the SAC project's emphasis on interstory drift and other response measures rather than acceleration, as well as a lack of studies conducted using connection hysteresis models which represent fracture explicitly. Explicit modeling of the sudden change in connection properties is necessary to capture transients analytically.

High-frequency transients can arise from a number of sources other than damage; hence, caution must be exercised when interpreting transients. A common-sense approach is recommended: (a) rule out transients caused by sources other than damage, within a reasonable degree of certainty; (b) determine that transient characteristics are consistent structural damage, and (c) use the presence of transients determined to have been most likely caused by damage in combination with other potential damage indicators, such as the amplitude of ground motion (or estimated ground motion) and building response, and changes in building vibration properties. Such an approach will be described in the following sections.

Dataset description

The strong motion dataset used in this study is limited to the Northridge earthquake and was assembled from three sources: (a) code-instrumented buildings with data retrieved and disseminated by CSMIP under an agreement with the City of Los Angeles, (b) code-instrumented buildings maintained as strong motion stations by USGS, and (c) USGS extensively-instrumented[2] buildings. Buildings were included in the dataset only if reliable damage information was available and measured accelerations were large enough that damage was considered likely. The criterion used for inclusion was horizontal acceleration of at least 0.15 g measured at the roof or an intermediate story (if instrumented), since base accelerations were not available for many of the code-instrumented buildings in the Los Angeles area. This level of acceleration was deemed a reasonable indication of strong shaking and permitted the inclusion of a number of buildings in areas where significant damage to WSMFs was observed. Plots of the recorded acceleration time histories for each building are located in Appendix A.

The majority of the dataset comes from code-instrumented buildings, since there were many more records from damaged and potentially damaged buildings available; records from over 400 code-instrumented buildings of all construction types were recovered after Northridge. In comparison, records were recovered from 57 CSMIP and 12 USGS extensively-instrumented buildings of all types. Due to its composition of primarily code-instrumented buildings, the dataset is heavily biased towards taller buildings, with the median building height being 12 stories. In contrast, the SAC database developed for loss estimation studies (Bonowitz and Maison, 2003) has a median building height of 4 stories, which is much more representative of the regional WSMF population. Unfortunately, there are no strong motion records available from low-rise WSMFs (less than 4 stories), and a limited number from mid-rise WSMFs (5-8 stories). However, the argument can be made that detection of fractures using recorded accelerations is more difficult in taller sparsely instrumented buildings than in shorter ones, since the instruments will tend to be further away from fractures, on average. So, at least based on fracture proximity alone, this dataset provides a greater challenge for the method.

The dataset was divided into three subsets as shown in Table 1. Set 1 contains primarily well-studied buildings with a range of observed damage, and is used to develop and refine the proposed method for detecting fracture damage. Sets 2a and 2b contain the remainder of the buildings and were used to test the method. Information about damage to

[2] For the purposes of this study, extensive instrumentation is defined as an array with more than 6 channels, with the capability to record both translational and torsional motions. The tri-axial instruments in code-instrumented buildings are not capable of measuring torsional response.

buildings in Sets 2a and 2b was not examined until after the analyses had been conducted, in order to provide a more rigorous test of the transient evaluation method. Set 2 can also be considered as a sample of buildings for which inspection recommendations are being made, with the proposed method used to help determine the likelihood of damage and thus the extent of inspections. (This scenario assumes a pre-*FEMA 267* inspection environment, such as that in existence immediately following Northridge).

Table 1. Criteria used to separate data into subsets

Dataset Name	A Priori Level of Knowledge	Peak Roof Acceleration
Set 1	Damage state known	> 0.3g
Set 2a	Damage state unknown	> 0.5 g
Set 2b	Damage state unknown	0.15 g to 0.5 g

In the case of Set 1, damage information was obtained from case studies available in the literature (e.g. SAC 1995a; Naeim et al. 1999) and verified using inspection reports and/or repair drawings by the consulting engineer. These buildings were grouped into the bins shown in Table 2 based on a damage ratio, which was defined as the number of damaged connections divided by the total number of inspected connections (Bonowitz and Maison 2003). Minor weld cracks only detectable with ultrasonic testing (FEMA designation W1) were not included, as these are considered by many researchers to be pre-existing conditions (see Paret 2000), and regardless, probably would not generate the sudden connection property changes necessary to cause acceleration transients.

Table 2. Damage bin definitions

Damage Bin	Damage Ratio*
None	0
Light	≤ 0.02
Moderate	≤ 0.10
Heavy	≤ 0.25
Severe	> 0.25

* number of damaged connections divided by the total number of inspected connections

Buildings included in the dataset are listed by subset in Table 3. The generic naming convention used by CSMIP is followed in order to maintain building anonymity.

Table 3. Data sets of steel buildings with recorded Northridge earthquake responses

Building Name	Stories	Data Source	Instrument Layout	Damage Ratio	Damage Bin *a priori*	A_{roof_max} (g)
Set 1						
North Hollywood - Lankershim #2	8	CSMIP	Code	0.00	None	0.36
Sherman Oaks - Ventura Blvd. #6	15	CSMIP	Code	0.00	None	0.48
Alhambra – Office Building #1	13	USGS	Extensive	0.00	None	0.14
Tarzana - Ventura Blvd, #10	10	CSMIP	Code	0.02	Light	0.52
Burbank – Office Building #1	8	USGS	Code	0.08	Moderate	0.61*
Encino - Ventura Blvd. #12	19	CSMIP	Code	0.04	Moderate	0.64
Woodland Hills - Canoga Ave. #1	17	CSMIP	Code	0.09	Moderate	0.39
Woodland Hills - Oxnard Blvd. #4	13	CSMIP	Code	0.09	Moderate	0.33
Woodland Hills - Canoga Ave. #2	17	CSMIP	Code	0.12	Heavy	0.49
Los Angeles - Olympic Blvd. #2	11	CSMIP	Code	0.17	Heavy	1.07
Set 2a						
Los Angeles - Olympic Blvd. #1	9	CSMIP	Code	0.00	Unknown	0.69
Los Angeles - Olympic Blvd. #3	12	CSMIP	Code	0.06	Unknown	0.70
Los Angeles - Olympic Blvd. #4	12	CSMIP	Code	0.14	Unknown	0.55
Los Angeles - Wilshire Blvd. #1	24	CSMIP	Code	0.00	Unknown	0.63

Building Name	Stories	Data Source	Instrument Layout	Damage Ratio	Damage Bin *a priori*	A_{roof_max} (g)
Woodland Hills – Office Bldg. #1	12	USGS	Code	0.17	Unknown	0.51*
Set 2b						
Encino – Office Building #1	12	USGS	Code	0.01	Unknown	0.40*
Los Angeles – Office Building #3	14	USGS	Code	0.00	Unknown	0.32*
Los Angeles – Office Building #4	18	USGS	Code	0.00	Unknown	0.15*
Los Angeles - Wilshire Blvd. #7	14	CSMIP	Code	0.00	Unknown	0.34
Northridge - Oakdale Ave. #1	10	CSMIP	Code	0.23	Unknown	0.46
Sherman Oaks - Ventura Blvd. #7	22	CSMIP	Code	0.17	Unknown	0.46
Woodland Hills - Oxnard Blvd. #1	11	CSMIP	Code	0.06	Unknown	0.41
Woodland Hills - Oxnard Blvd. #2	20	CSMIP	Code	0.03	Unknown	0.31
Woodland Hills – Oxnard Blvd. #5	11	CSMIP	Code	0.15	Unknown	0.33

* Peak value from uncorrected data (corrected data not available)

A number of the buildings with records used in the above data sets have been examined extensively by other investigators as part of post-Northridge studies conducted by the SAC Joint Venture and others. In addition, the CSMIP code buildings are listed in Huang et al. (1998). Studies available in the literature are listed in Table 4. Unpublished reports by engineering consultants documenting the results of investigations performed to satisfy a mandatory inspection and repair ordinance in Los Angeles, described in FEMA 355-E (FEMA 200b), exist for a number of the buildings as well. In addition, damage surveys were performed after the Northridge earthquake by several investigators (SAC 1995b, FEMA 2000b, Bonowitz and Maison 2003). These surveys typically covered fairly large samples of buildings and were intended for use in studying broad trends rather than extracting information for specific buildings. Due to the small size of the dataset used herein, information from survey sources was corroborated with either published case studies or unpublished inspection reports before use.

Table 4. Prior studies on buildings in the dataset

Building	Studies performed
Set 1	
Alhambra – Office Building #1	Cohen (1996) Sanli and Çelebi (2002) Rodgers, Sanli and Çelebi (2004)
Encino – Ventura Blvd. #12	Naeim, Lobo, Skliros, and Sgambelluri (1999)
Los Angeles – Olympic Blvd. #2	Naeim, DiJulio, Benuska, Reinhorn and Li (1995) Huang, Malhotra, and Shakal (1996, 1998)
North Hollywood – Lankershim #2	Naeim, Lobo, Skliros, and Sgambelluri (1999)
Sherman Oaks – Ventura Blvd. #6	Naeim, Lobo, Skliros, and Sgambelluri (1999)
Tarzana – Ventura Blvd. #10	Naeim, Lobo, Skliros, and Sgambelluri (1999)
Woodland Hills – Canoga Ave. #1	Huang, Malhotra, and Shakal (1996, 1998)
Woodland Hills – Canoga Ave. #2	Anderson and Filippou (1995) Filippou (1995) Paret and Sasaki (1995) Huang, Malhotra, and Shakal (1996, 1998) Chi, El-Tawil, Deierlein, and Abel (1998)
Woodland Hills – Oxnard Blvd. #4	Uang, Yu, Sadre, Bonowitz, Youssef, and Vinkler (1995) Huang, Malhotra, and Shakal (1996, 1998) Maison and Kasai (1997) Bonowitz and Maison (1998) Lobo, Skokan, Huang, and Hart (1998) Tsai, Chung, and Wang (1998) Kunnath, Nghiem, and El-Tawil (2004)

Building	Studies performed
Set 2b	
Los Angeles – Office Bldg. #3	Astaneh-Asl, Mojtahedi, McMullin, Shen, and D'Amore (1998)

Effects of data sources and processing

Data sources

Most of the data used herein comes from what are referred to as "code" instrumented buildings (see footnote on page 7). All of the records used in this study came from analog instruments, and were subsequently digitized. The code stations were instrumented with tri-axial Kinemetrics SMA-1* instruments, while the extensively instrumented USGS stations were equipped with Kinemetrics CRA-1* recorders connected to individual force-balance accelerometers (FBAs). Both uncorrected (Volume 1) and corrected (Volume 2) data are available for CSMIP code stations (Darragh et al. 1994, 1995) and the extensively instrumented UGSS station (Porcella et al. 1994). Uncorrected (V1) data are available for the USGS code stations (Porcella et al. 1994).

Data processing

Since high-frequency transients are unusual signals, the effects of procedures (Shakal et al. 2004; Stephens and Boore 2004) used to process the data used in this study were examined. For example, it was noted that some common strong motion processing procedures, namely decimation and low-pass filtering, can reduce the amplitude of, or in some cases entirely eliminate, transients from corrected records. Figure 4 and Figure 5 show comparisons between uncorrected (Volume 1) and corrected (Volume 2) data from two records with significant high-frequency transients. The corrected data has been decimated from 200 samples per second (sps) to 50 sps, and has been low-pass filtered according to standard CSMIP processing procedures. In both cases, the amplitude of the transients is decreased by processing, and in the case of the vertical component in Figure 5, the transient is removed almost entirely. In these cases and all others in this study, processing did not introduce or amplify transients.

Therefore, an immediate conclusion is that the uncorrected (V1) data should be used for transient detection, and thus should be made available to the user community. If further investigations are to be performed using the corrected (V2) data, such as frequency-domain analysis or system identification, a comparison such as those shown in Figure 4 and Figure 5 is recommended to assess the effects of processing on the transients. This step was also recommended for records containing transients by prior investigators (Rojahn and Mork 1982; Mau and Revadigar 1994).

* Use of trade, firm, or product names does not imply endorsement by the U.S. Government or the authors.

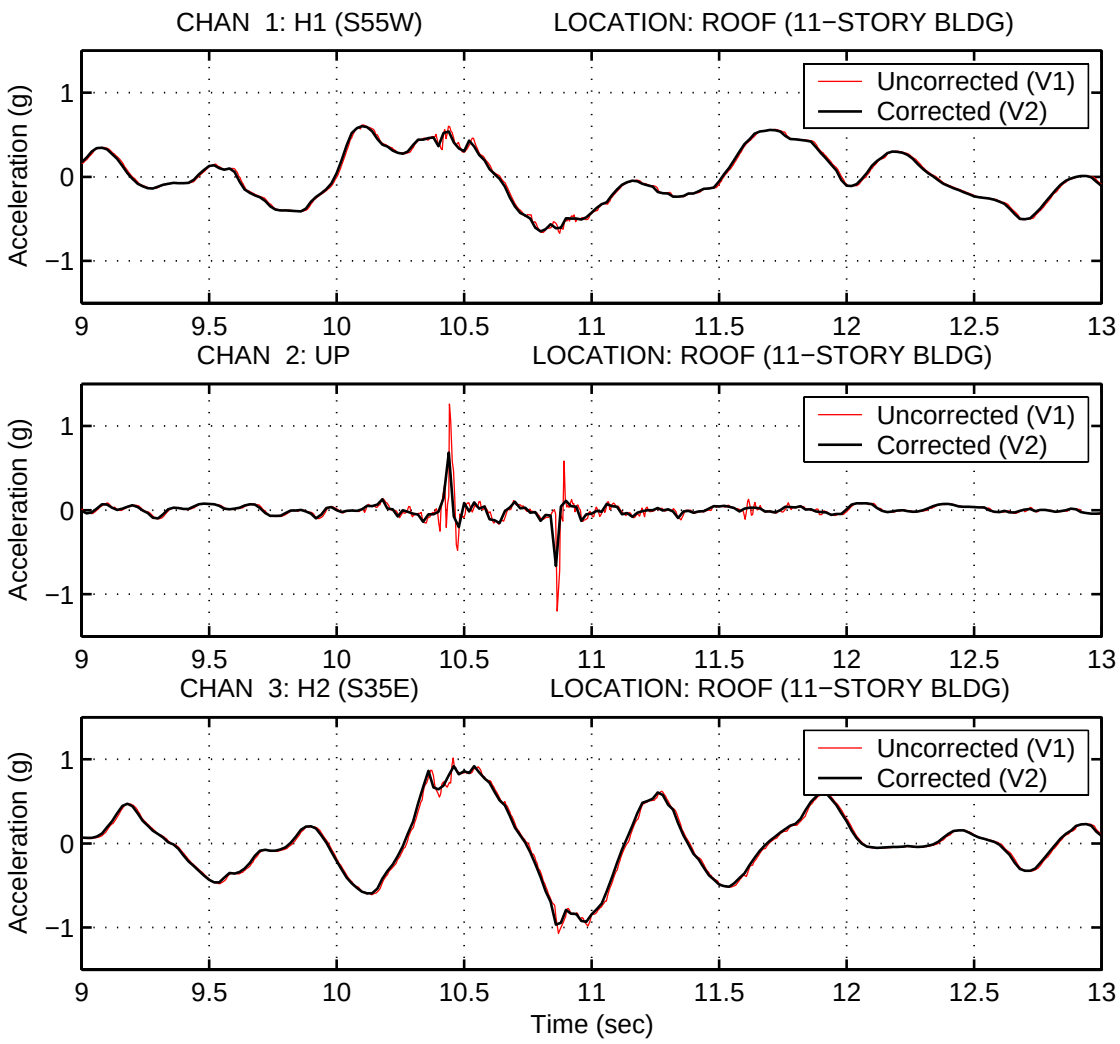

Figure 4. Comparison of corrected and uncorrected data from Los Angeles – Olympic Blvd. #2, Roof

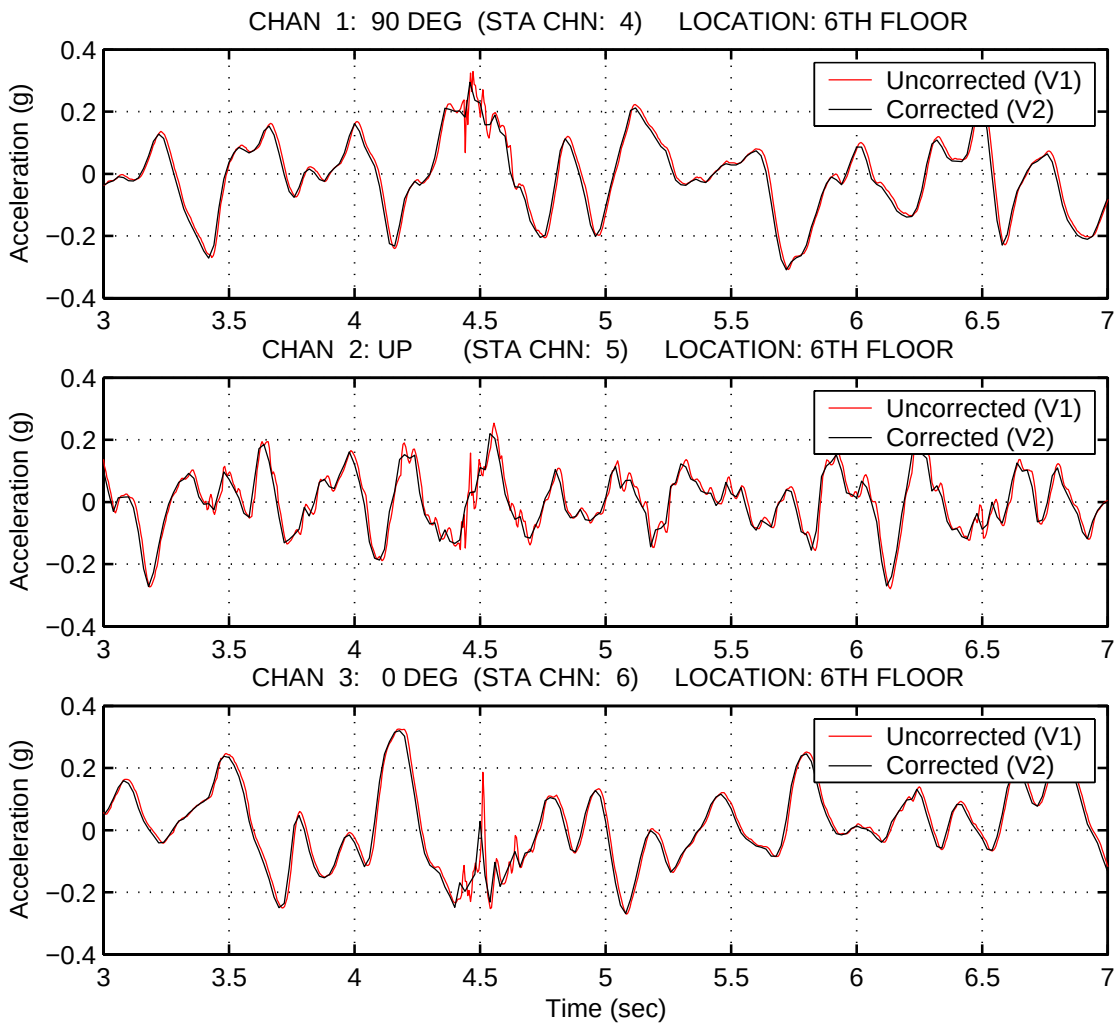

Figure 5. Comparison of corrected and uncorrected data from Woodland Hills – Oxnard Blvd. #4, 6th floor

In addition, a researcher should determine how the digitization of the analog records affected any potential transients by examining the original records (or good copies) if they are available. In particular, very high frequencies may not be reproduced in the digitization, even if the quality is very high, due to the finite width of the traces. Also, portions of records containing transients may be difficult to digitize due to large amplitudes and trace crossings. An example of an analog record containing large amplitude transients and trace crossings is shown in Figure 6. The corrected and uncorrected data resulting from digitization of this record are shown in Figure 7. It is clear that the digitization does not fully capture the high-frequency response, but it provides significant clarification of the maximum amplitudes for each trace, which are difficult to determine from simple visual inspection of the analog record. Additional valuable information, such as whether the timing or fixed traces were disturbed, is available only from the analog records. The use of such information will be discussed in later sections.

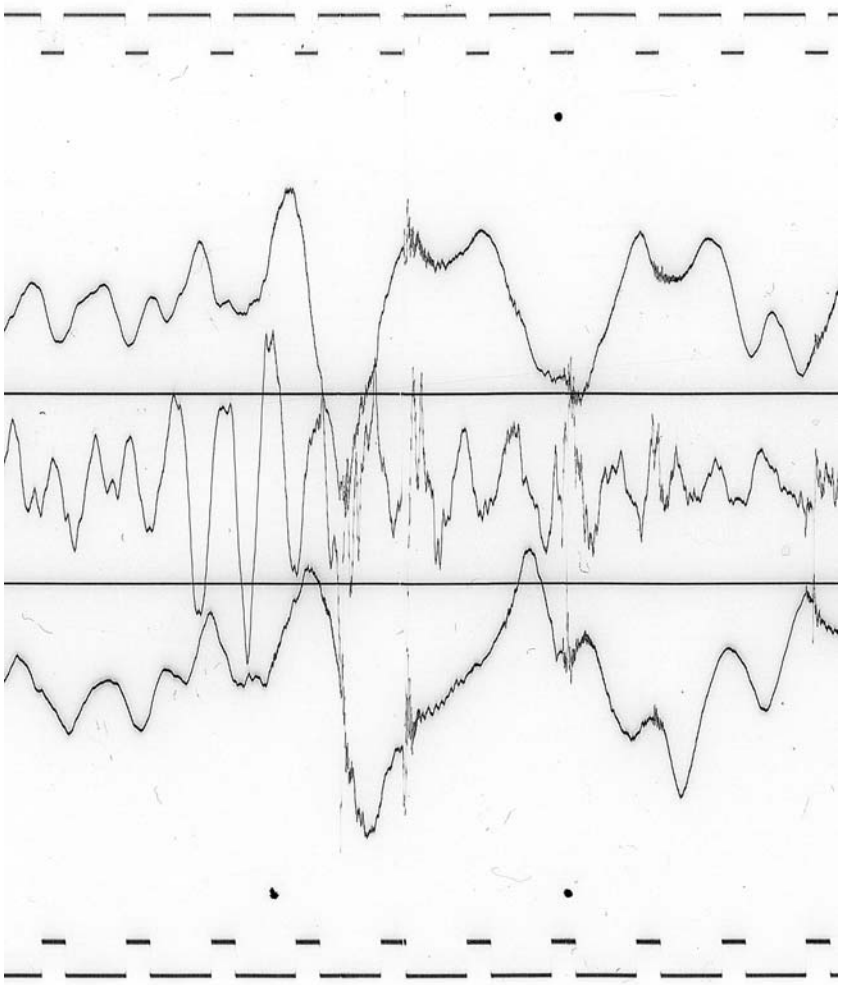

Figure 6. Digital image of a portion of the original analog record from Burbank – Office Building #1, roof

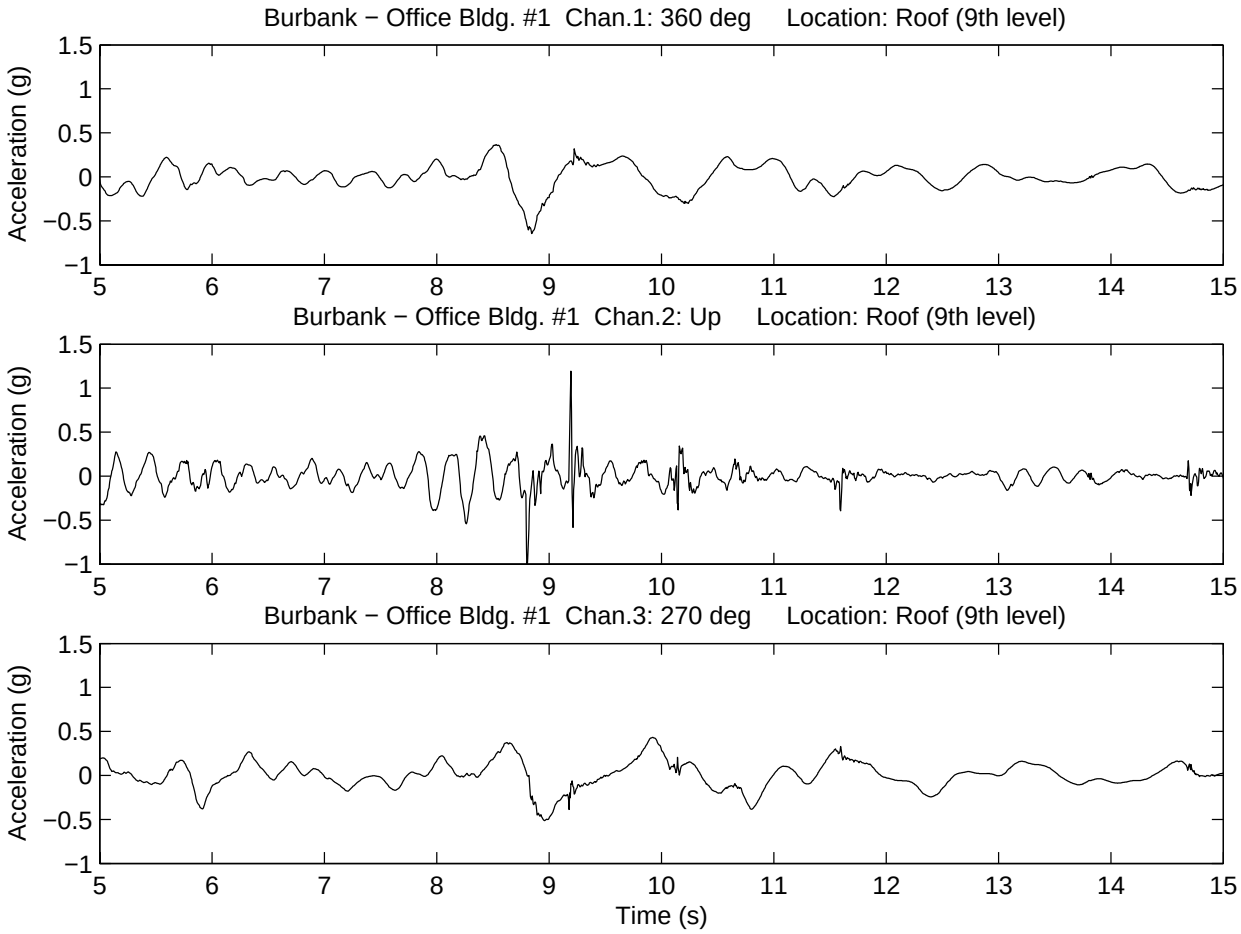

Figure 7. Uncorrected data obtained by digitization and processing of Burbank – Office #1 analog record

Methods for transient detection and characterization

Several methods for transient detection and characterization are explored in this study, and are described in the following section. Detection and characterization are treated as separate endeavors. A transient must be detected first; at this stage of the process, no attempt is made to determine its source. A transient is detected by identifying the simple characteristics which define it as such: (a) amplitude sufficient to differentiate the transient from the background noise level of the record, (b) frequency content significantly higher than that of the portions of the signal immediately preceding and following it, and (c) brief duration (typically << 1 second). After a transient has been detected, the process enters the characterization phase, where pertinent characteristics of the transient are determined, with the end goal being to determine the source within a reasonable degree of certainty.

Detection of transients in accelerograms recorded on analog instruments is accomplished in the most practical and efficient manner by visual inspection of the filtered and unfiltered acceleration time series using a sufficiently expanded timescale (such as 1 sec/cm). Detection capability can be significantly enhanced by making comparisons of filtered and unfiltered versions of the signal, and such comparisons are recommended, especially for noisy signals. If both uncorrected (V1) and corrected (V2) data are available, they can be plotted together as in Figure 4, since the low-pass filtering applied to the latter tends to accentuate the difference in high-frequency content between the two traces. This type of simple comparison also has the advantage of preserving the lower-frequency portion of the signal, and therefore shows the transients in the context of the predominant building response. Also, no signal processing is required on the part of the user. A related approach that requires slightly more effort on the part of the

user involves comparing the uncorrected signal with no filtering applied to the same signal with high-pass filtering applied. This approach permits the isolation of the higher-frequency components of the record, which include the transients of interest (if present) and noise. This approach is recommended for noisy signals, since high-pass filtering can be very helpful in determining whether transients that rise above the noise level are present.

Transformation of the digitized acceleration signal using the windowed Discrete Time Fourier Transform (wDTFT) or the wavelet transform (WT) can provide quantitative information on changes in the frequency content of the signal with time. However, such transformed signals must still be inspected visually for the indicators of transients. These methods can also accentuate the noise in a record, which can lead to false positives. Automated detection using wavelets is possible, but is significantly more complicated than visual identification (even with filtering), and provides information that is in most cases at best equal in quality to that obtained from visual inspection, at least in terms of detection capability alone. For high-resolution records from digital instruments, it is possible that signal processing approaches to detection such as the wDTFT, WT, or a filtering/correlation scheme may be more efficient than visual inspection, though it is anticipated that noise will still be problematic. However, the dataset contains no high-resolution digital recordings on which such approaches might be tested.

Characterization of transients, specifically determination of unique and identifying features, was primarily accomplished by visual inspection as well. Due to the physical limitations of digitization and the resulting inability to resolve the frequency content of many transients, wavelet and frequency domain analysis were not particularly helpful in characterization. Accurate characterization using signal processing techniques is not possible if the transient signal is not captured accurately in digital form to begin with. However, in the future, signal processing techniques may provide useful information when applied to high-resolution digital records, which are capable of capturing the high-frequency content of transients.

It was particularly difficult to distinguish between transients likely caused by damage and those likely caused by the impact of an object falling on the instrument. Due to the significant amount of time that has elapsed since the collection of the analog records following the Northridge earthquake, evidence from the instrument's environment and the instrument technicians was not available. Thus, the only source of reliable source of information for determining if falling object impact occurred was the record itself. A lack of published impact test data from analog instruments of the type that recorded most of the data used herein led to several experiments being conducted. These experiments involved dropping different objects on or near the instrument, and a description of the tests and results is presented later in this section. Since the primary instrument of interest was an analog one, the limitations of digitization in resolving the frequency content of high-frequency transients were encountered here as well. Accurately capturing the frequency content of high-frequency transients in the analog records was deemed impossible after several digitization attempts, due to physical overlap of the traces. Thus, as was the case for other transients recorded on these instruments, frequency-domain and wavelet analysis, and other signal processing approaches were not helpful due to a lack of accuracy in the signal being analyzed. For this reason, visual identification was instead used to identify the distinguishing characteristics of impact-generated transients. For records from digital instruments, it may be possible to obtain key information from frequency-domain or wavelet analyses if the sampling rate is high enough that all of the pertinent frequencies can be resolved.

Detection of transients

Detection by visual inspection

In most cases, high-frequency transients, if present in an acceleration time-history trace, are readily identifiable visually, as is the case in both Figure 4 (a large transient) and in Figure 5 (a much smaller transient). The amplitude of the transient relative to the underlying signal is important for detection by visual inspection. Transients must be visible above the background noise level of the record. Naturally, transients with large relative amplitudes are easier to spot. Both the number and location of fractures and the amplitude of the underlying building response affect relative amplitudes. Record processing also affects relative amplitudes since low-pass filtering typically reduces

transient amplitudes. Comparison of filtered and unfiltered data can facilitate the identification of transients, as shown in Figure 8 for the Los Angeles – Olympic #2 record.

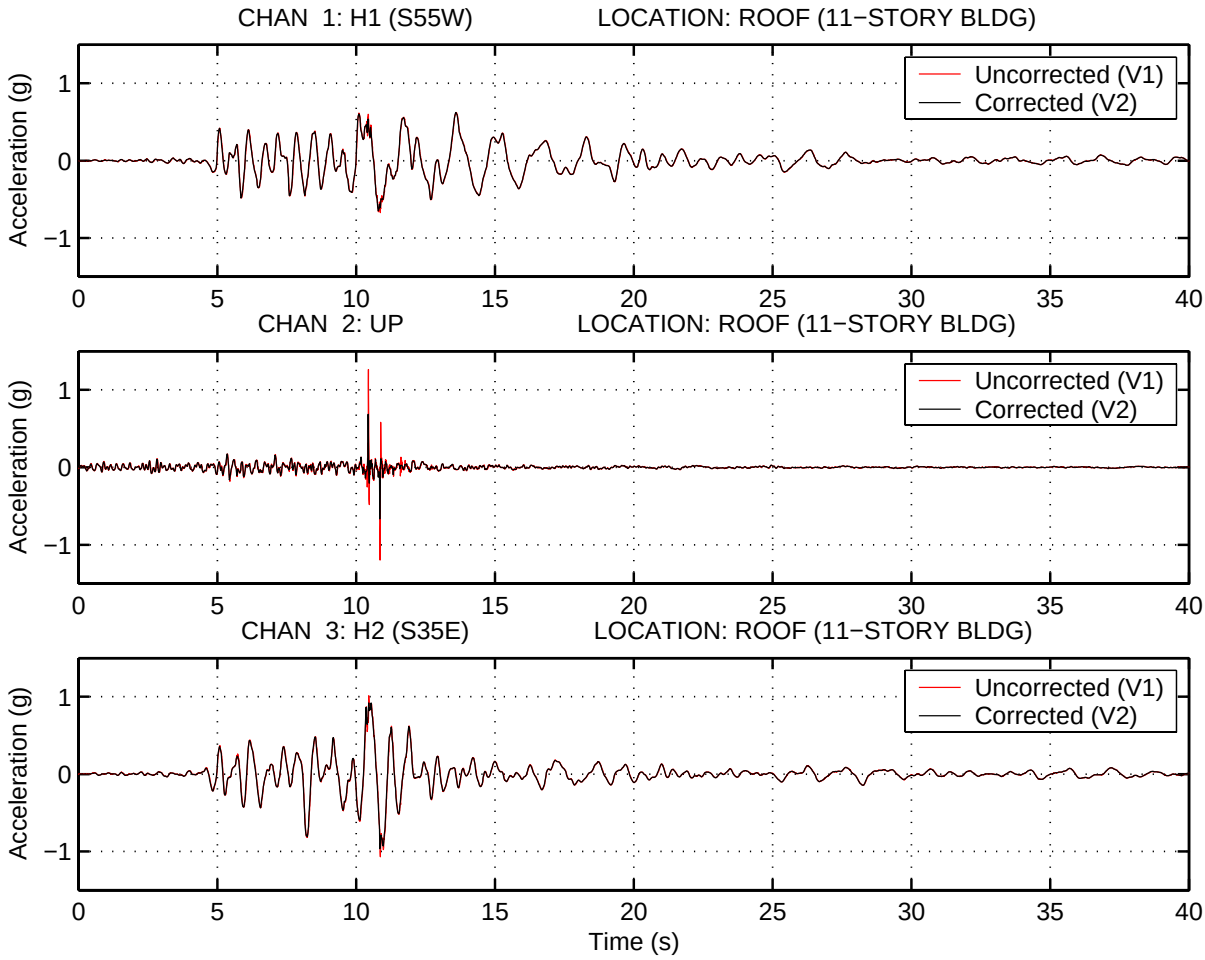

Figure 8. Acceleration time histories, Los Angeles - Olympic #2

The frequency content of the transient is also key for detection by visual inspection. The frequency content of a transient is much higher than that of the signal immediately preceding and following it, typically anywhere from 5 to 500 (or even more) times the predominant frequencies in the underlying signal. The high-frequency portion of the record (which includes the transient) can be isolated by high-pass filtering, which will be discussed in the next section. The brief duration of a transient is also important; most transients last only a small fraction of a second. A sustained high-frequency signal, on the other hand, is generally noise or some type of local resonant response, such as that of the floor slab when excited by operating machinery.

In addition, a reasonable time scale must be used in figures for visual identification of transients. Use of a time scale which is sufficiently expanded to distinguish between higher mode response and transients is necessary, as the former can look like the latter if the time axis is compressed. For visual identification of transients in the dataset records, as standard time axis of 20 seconds with a 22 cm (8.5 inch) length was used, giving a scale of approximately 0.9 sec/cm (2.4 sec/inch). Timescales were further expanded in sections of the record where transients were present, such as in Figure 4.

Transients of very large amplitude are present in the vertical record for the Los Angeles – Olympic Blvd. #2 building, as shown in Figure 8. It is possible that these vertical transients may have been caused by the numerous

column flange fractures in upper story connections. Photographs of column flange fracture damage and a detailed damage summary can be found in Naeim et al. (1995). This is only one possible explanation; others include constructive interference of flexural waves or a sudden change in the deflected shape of affected beams due to a change in end fixity caused by fracture, resulting in vertical accelerations.

Detection using high-pass filtering

The higher frequency components of an acceleration time history are isolated when the record is high-pass filtered. Comparisons of the original signal and the signal after high-pass filtering can facilitate the location of transients within the time history. An example of this type of comparison is shown in Figure 9 for the Los Angeles – Olympic #2 record. This signal contains a visually evident transient signal between 10 and 11 seconds, and a low level of background noise. The transient signal is clearly evident in the high-pass filtered records.

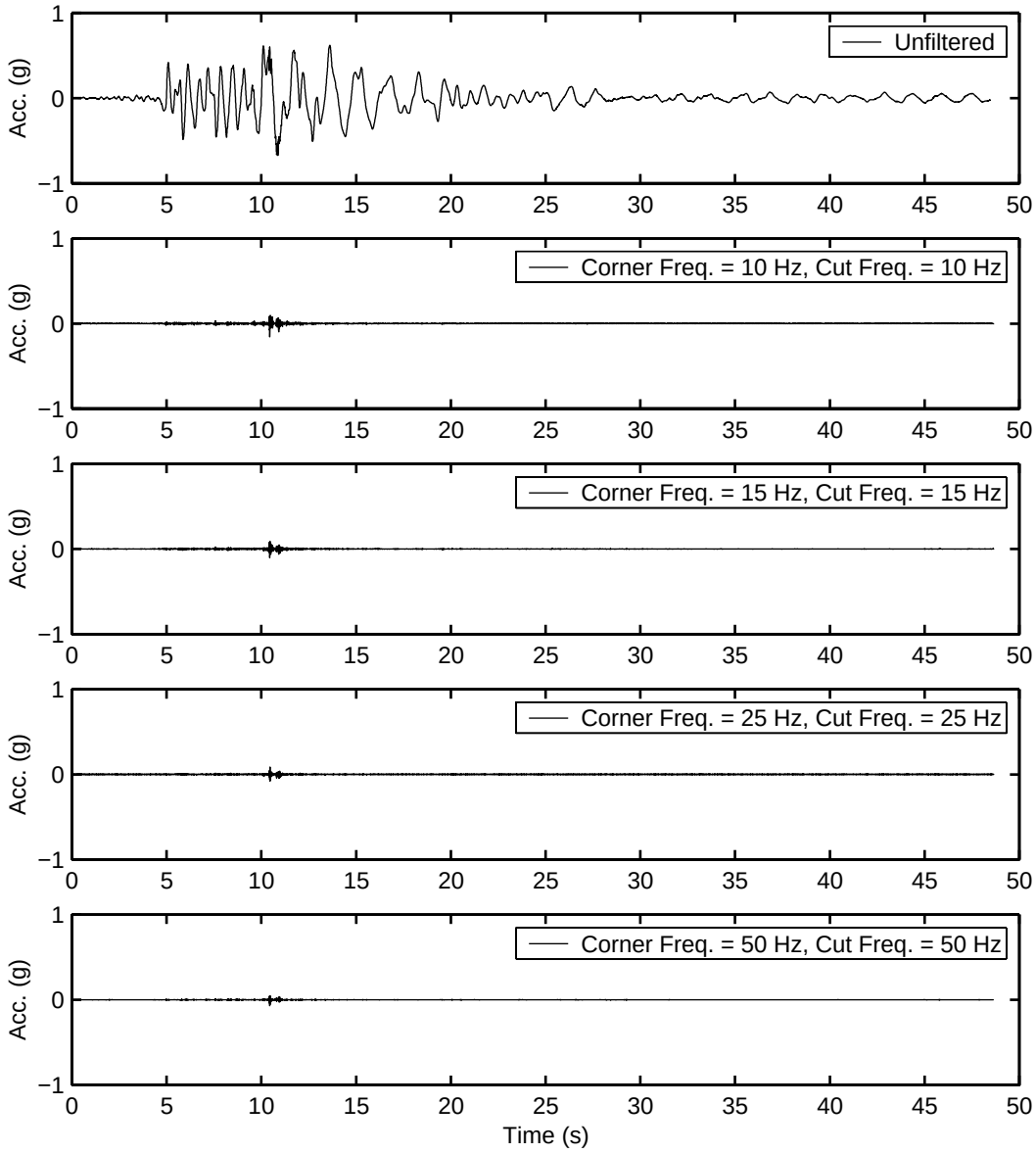

Figure 9. High-pass filtering of uncorrected Los Angeles - Olympic #2 record

For noisy signals, the detection of transients is more difficult, and the line between detection and characterization can become blurred. The Woodland Hills – Canoga building records have a relatively high level of background noise. The same comparison between filtered and unfiltered signals is shown in Figure 10 for Canoga #1 and Figure 11 for Canoga #2. For Canoga #1, there is no clearly defined transient signal that rises above the background noise level. One could possible make the case for a transient signal at about 9.5 seconds, but the amplitude of the signal in question is not appreciably larger than that of the background noise signals in the first few seconds of the record. In contrast, in the Canoga #2 record, there is a clearly indicated transient signal at about 5 seconds that rises significantly above the background noise level.

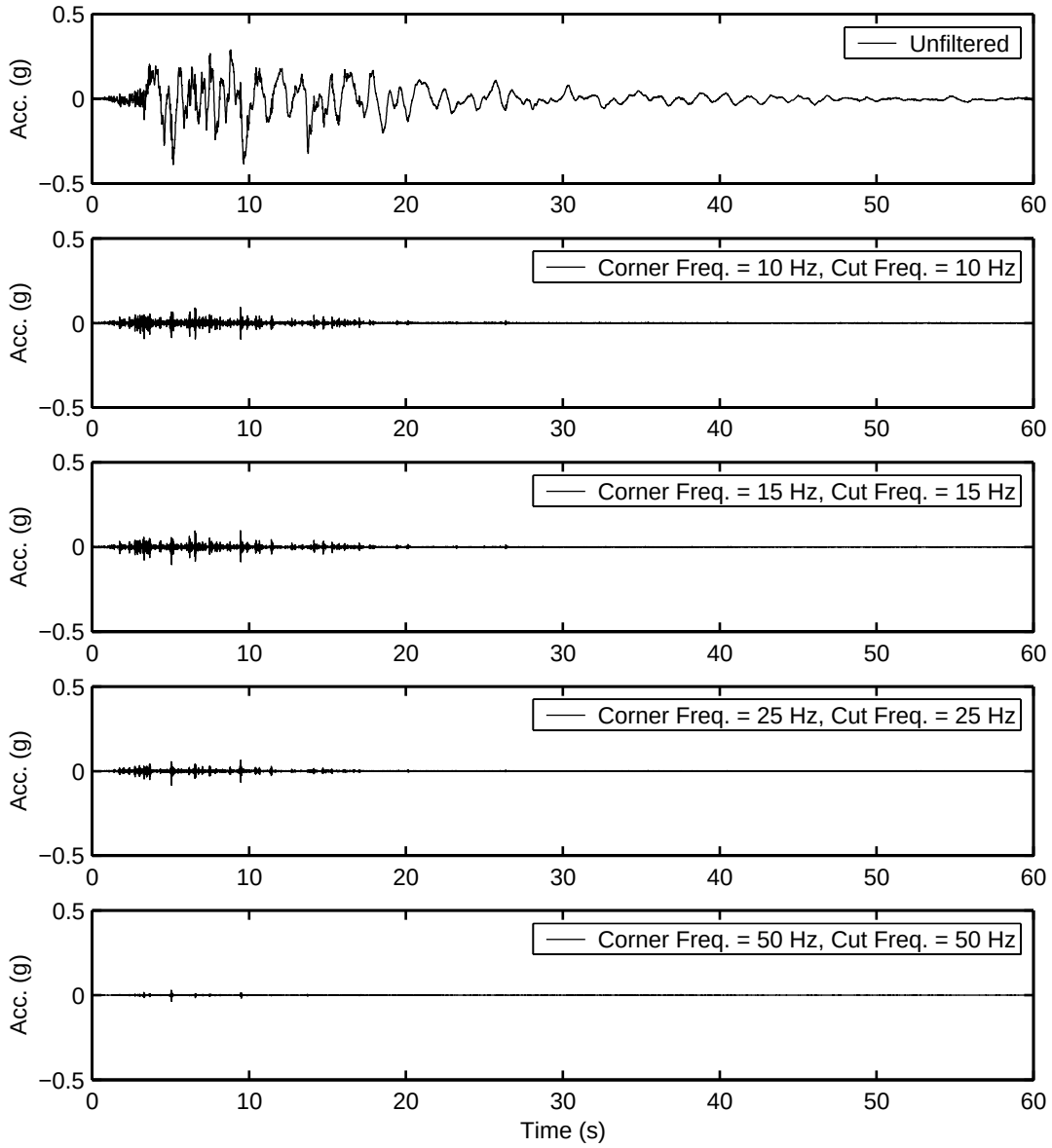

Figure 10. High-pass filtering of uncorrected Woodland Hills – Canoga #1 record

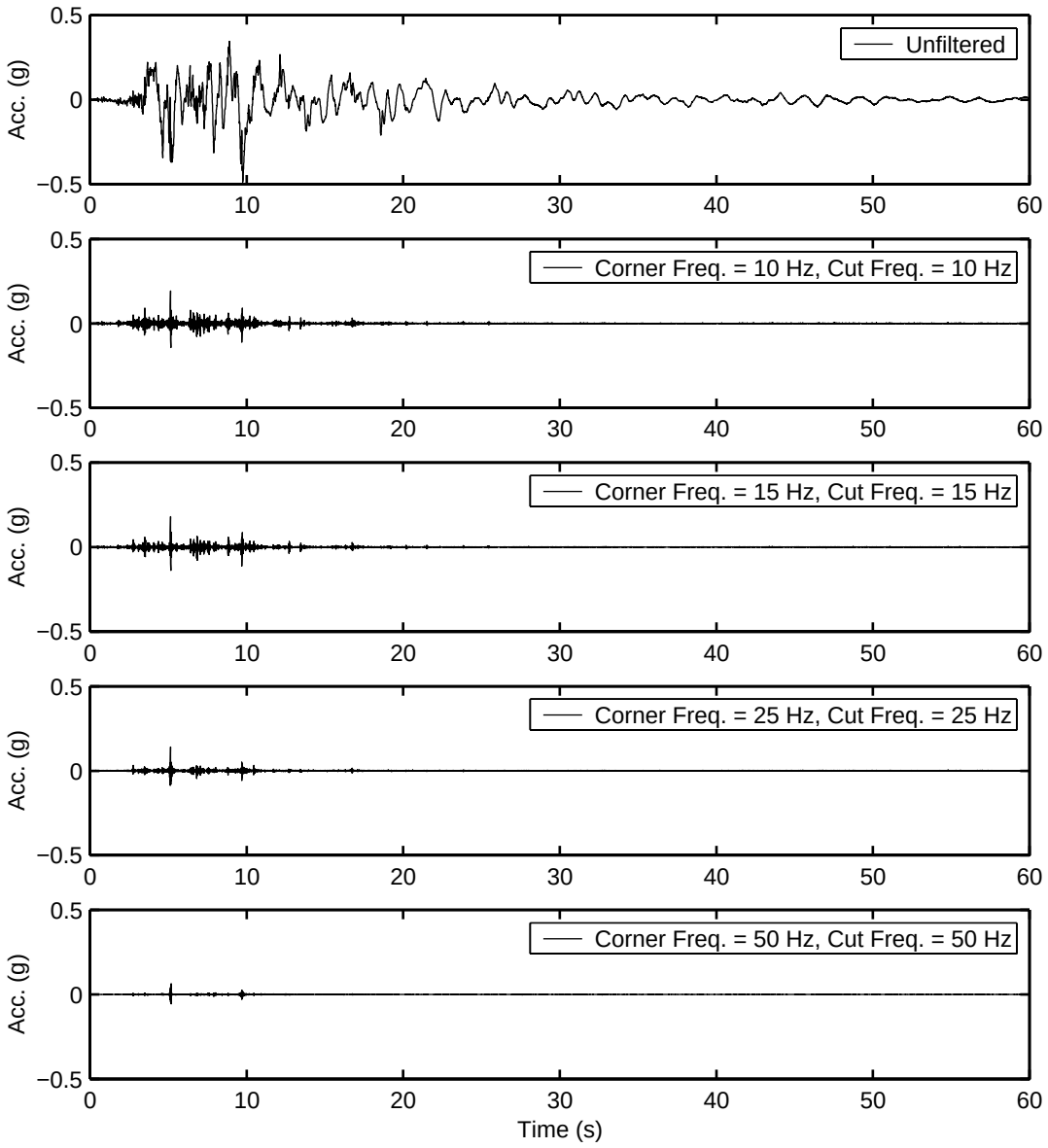

Figure 11. High-pass filtering of uncorrected Woodland Hills – Canoga #2 record

A very simple high-pass digital filter with equal cut and corner frequencies was applied to the signal in the frequency domain. This filter was chosen for simplicity and for the purpose of illustration, and more complex filtering schemes can certainly be employed if desired. For the signals in question (uncorrected CSMIP code station data), the Nyquist frequency was 100 Hz. Filter cutoffs of 10, 15, 25, and 50 percent of the Nyquist frequency were examined. From the few signals examined, it appears that there is no "ideal" percentage of the Nyquist frequency that will best isolate transients from background noise in the record. The cutoff frequency with the best "performance" appears to depend on the relative amplitudes and frequency contents of the transient signals of interest and the noise in the record. Therefore, filtering with a range of cutoff frequencies, as demonstrated here, is recommended. High-pass filtering is perhaps most helpful in cases where low-amplitude, high-frequency transients are present in signal with low levels of background noise. Such filtering can also help to determine whether clearly defined transient signals are present in noisy records. In these cases, a visual comparison of uncorrected (V1) and corrected (V2) data may not be conclusive, and high-pass filtering and the subsequent visual inspection of the filtered signal can help resolve the issue of whether transients are present or not.

Detection using the windowed Discrete Time Fourier Transform

An acceleration time-history can be transformed into joint time-frequency format using the windowed Discrete Time Fourier Transform (wDTFT). This format allows the presentation of time and frequency information simultaneously, and shows changes in the frequency content of a record over time. The vertical component of Los Angeles – Olympic #2 record contains two very large transients, as shown in Figure 8. These transients are easily identified visually even at the very compressed timescale shown. The wDTFTs of these records are plotted in spectrogram format in Figure 12. This plot accentuates the high frequency content of the records, most significantly the vertical component record, around 10 seconds into the time history. This indicates the presence of transients, but the occurrence time is not as well defined as it is in the actual time history. Also, a number of smaller burst of high frequency, most likely indicative of noise, are present at many other times during the record. Interpretation of these small bursts as transients could lead to the erroneous conclusion that there are many transients throughout the record. In the interest of avoiding false positives, the wDTFT must be compared to the original time series. Visual inspection of both the wDTFT and the acceleration time series are thus necessary, with the acceleration time series being more authoritative. The end result is that an extra analysis has been performed, and it provides no more information as to whether a transient is actually present or not.

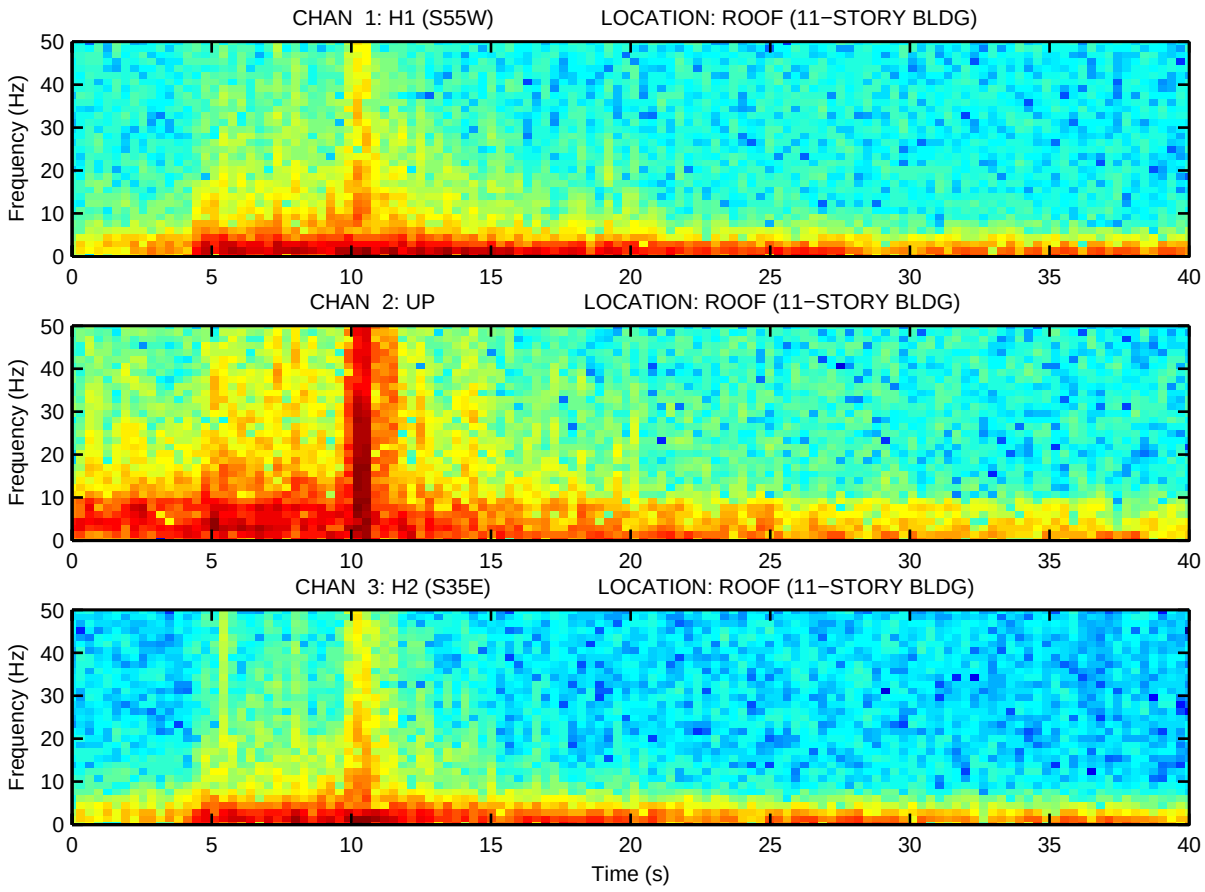

Figure 12. Spectrogram of wDTFT analysis of Los Angeles - Olympic #2 records

Detection using wavelet analysis

Wavelets provide another means of examining time and frequency information simultaneously. However, visual inspection of the wavelet transforms of signals has some of the same shortcomings as the visual inspection of wDTFTs of signals. In particular, noise can be enhanced, and the original time history must still be consulted for verification. However, in contrast to the wDTFT, wavelets can locate the presence of transients in time with much better resolution, and the indicator of a transient can be much more clearly defined. This makes the automated detection of transients possible, though there are some significant practical problems to overcome. Additionally, wavelet analysis is unfamiliar to most structural engineers, and it requires specialized computer software (or the willingness to write it).

The theory of wavelets is well-covered elsewhere (e.g. Walker 1999) and will not be repeated here. The applicability of wavelets to detection of damage (such as an abrupt loss of stiffness) in structures subjected to earthquakes was proposed by Hou et al. (2000). This reference provides a good summary of wavelet analysis, and uses an example with fracturing springs to demonstrate the utility of the wavelet transform for detection of sudden stiffness loss, such as that caused by fracture. However, they also conclude that the noise level can adversely affect the ability of the wavelet transform to detect damage.

The wavelet transform permits the decomposition of a signal into an averaged (or trend) signal and a detail (or fluctuation) signal. The detail sub-signal contains information on sudden changes in the original signal, making it particularly well-suited for transient detection. Multi-resolution analysis (MRA) is accomplished by decomposing the first averaged signal into the second averaged and detail signals, and so on, until the n-level averaged and detail signals are obtained. An n-level MRA results in n detail signals which contain higher scale and lower frequency content as n increases. For this reason, only detail signals with low values of n are of interest when examining high-frequency transients.

Transient detection is accomplished using the wavelet transform with a thresholding algorithm. The n-level wavelet transform of the original signal in question is calculated, with the observation that $n = 2$ provides relatively good results. Next, the wavelet coefficients with amplitude greater than the threshold are identified. To distinguish transients from other signal features, a high threshold, such as 50-70% of the maximum wavelet coefficient amplitude, should be used. In addition, the number of values exceeding the threshold should be checked to avoid false positives in cases with many similar coefficients due to background noise. Low-noise signals without transients may also have many coefficients with similar amplitude, however. The number of wavelet coefficients exceeding the threshold should typically be less than five, though this depends on signal length. Due to the oscillatory nature of many transients, a number of large-value wavelet coefficients may be generated along the duration of the transient. For detection purposes, however, it is only necessary to record one of these values. This algorithm was implemented using the Wavelab Version 802 toolbox (Donoho, et al. 1999) for use with the software package Matlab (The MathWorks, 2002). A typical result for a signal with low noise is shown in Figure 13.

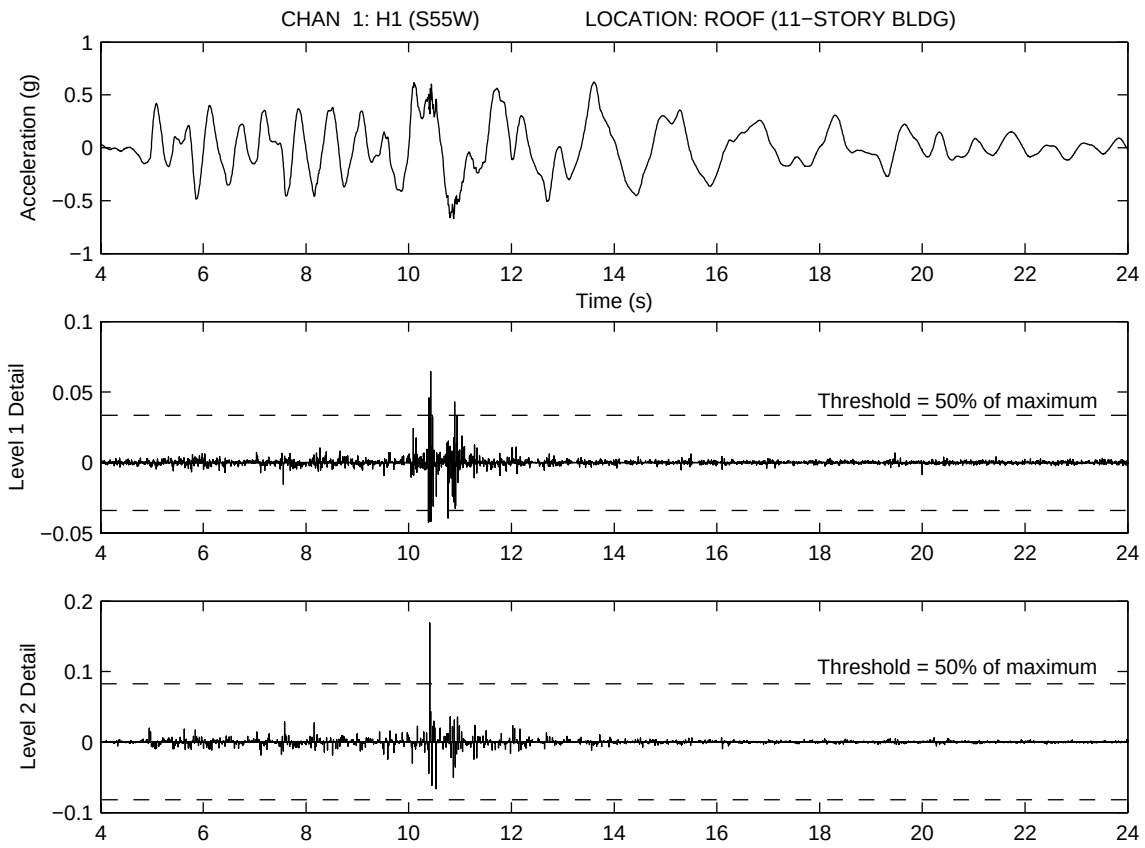

Figure 13. Time history (top), and wavelet transforms (middle and bottom) showing location of acceleration transients and wavelet coefficients in time, Los Angeles – Olympic #2.

The results in Figure 13 show that the thresholding algorithm works well for a low-noise signal with a well-defined transient. However, this transient is also readily apparent from visual inspection of the time history. In terms of detection capability, nothing is gained by going to the trouble of performing wavelet analysis in this case. If we examine signals with a significant amount of noise, such as the responses of the Woodland Hills – Canoga buildings, and clean signals (those with no transients and little noise), such as Sherman Oaks – Ventura #6, other difficulties present themselves. Figure 14 shows the results of the algorithm for Woodland Hills – Canoga #1, while Figure 15 shows the results for Sherman Oaks – Ventura #6. Both the noisy and clean signal produce a number of wavelet coefficients that exceed the threshold. There is no large-amplitude, dominant wavelet coefficient which would indicate the presence of a transient which is distinct from the background noise, except in the Level 2 Detail of the clean signal, which is a false positive. Also, a number of the coefficients that exceed the threshold do so in only one of the detail signals, rather than both. In this case, the original time history would still need to be consulted to verify that the wavelet coefficients were associated with transients rather than background noise. Again, if only detection capabilities are considered, wavelet analysis does not provide additional benefits which outweigh the effort expended to perform the analysis.

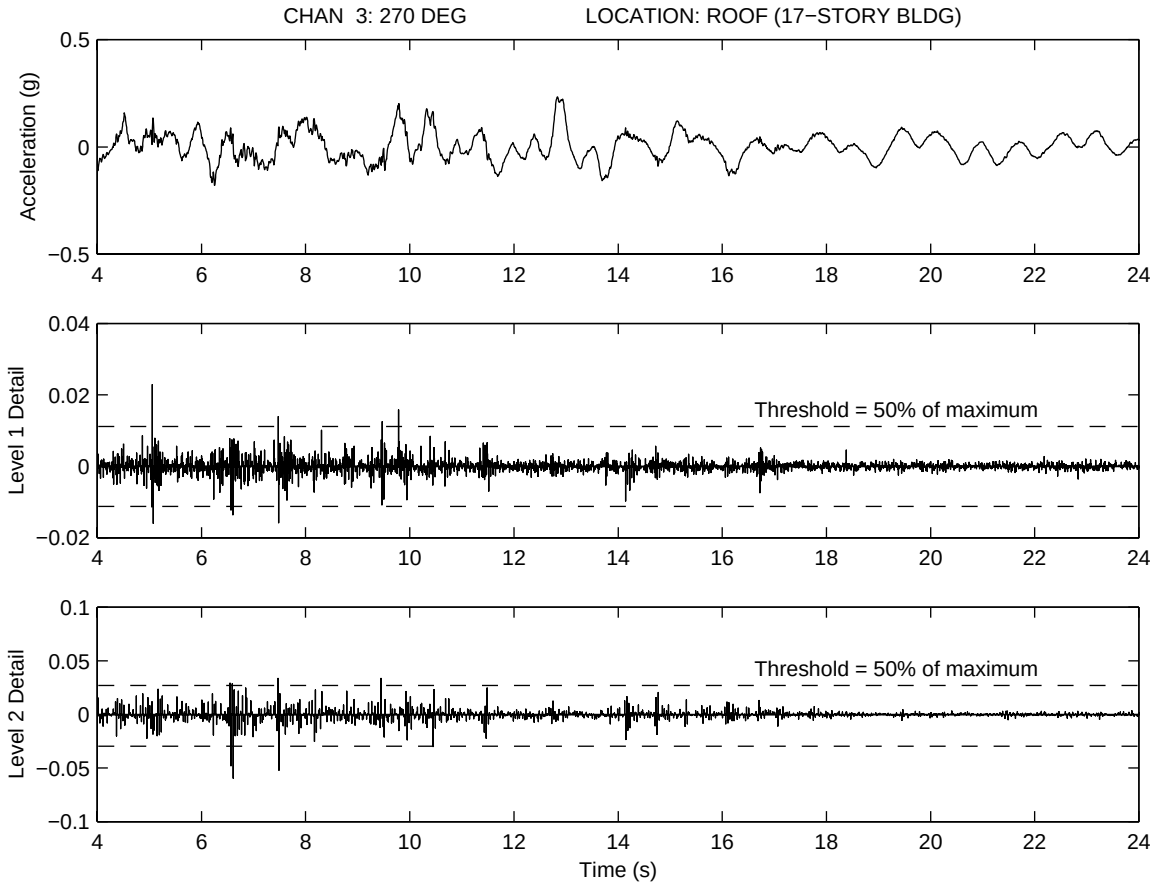

Figure 14. Time history (top), and wavelet transforms (middle and bottom) showing location of acceleration transients and wavelet coefficients in time, Woodland Hills – Canoga #1.

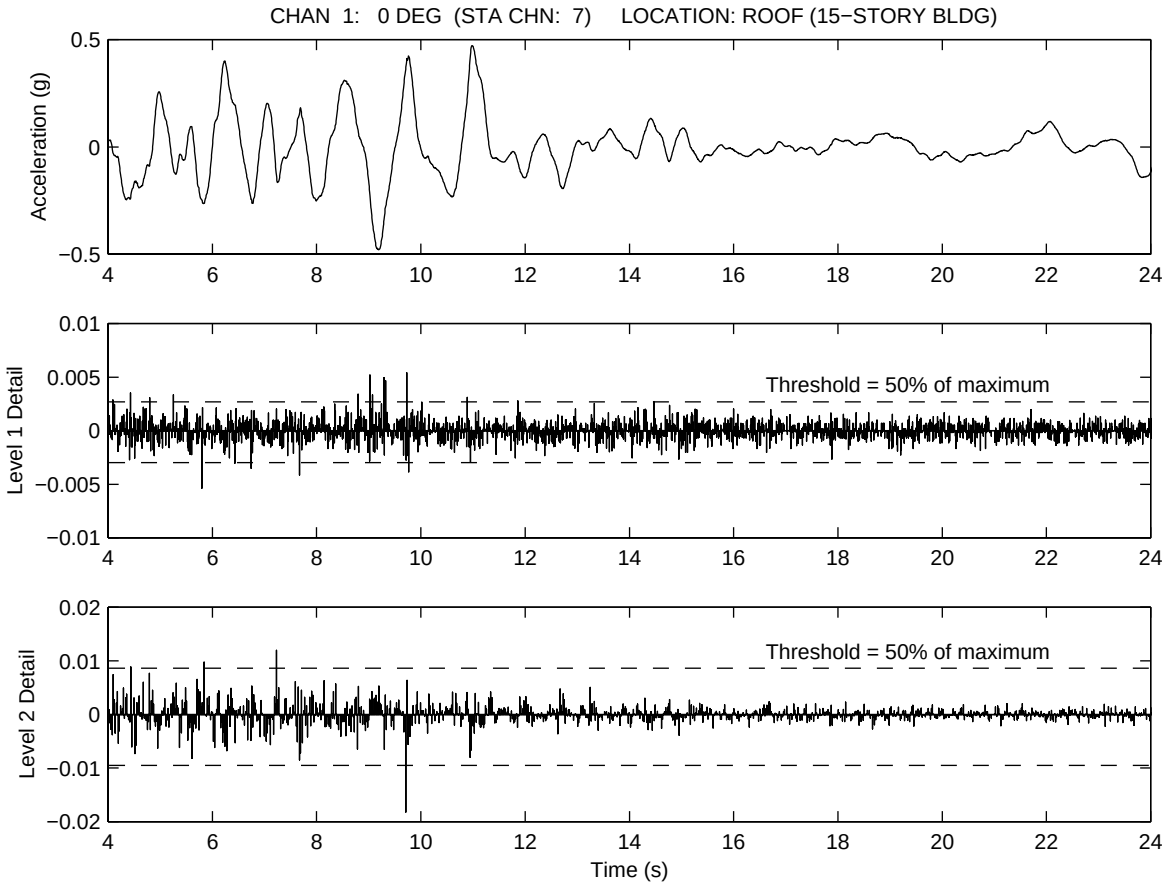

Figure 15. Time history (top), and wavelet transforms (middle and bottom) showing location of acceleration transients and wavelet coefficients in time, Sherman Oaks – Ventura #6.

In the case of Canoga #2, wavelet analysis is more helpful when used as a tool to distinguish between background noise and transients likely caused by damage. The large-amplitude, dominant coefficient present at approximately 5 seconds in the Level 1 and 2 detail plots in Figure 16 provides evidence that a transient which rises above the noise level is present. This is much more obvious in the wavelet analysis than in the acceleration time history, especially when compared with Canoga #1. However, very similar results can be obtained by high-pass filtering of the acceleration time history (see Figure 11), which is a much simpler procedure.

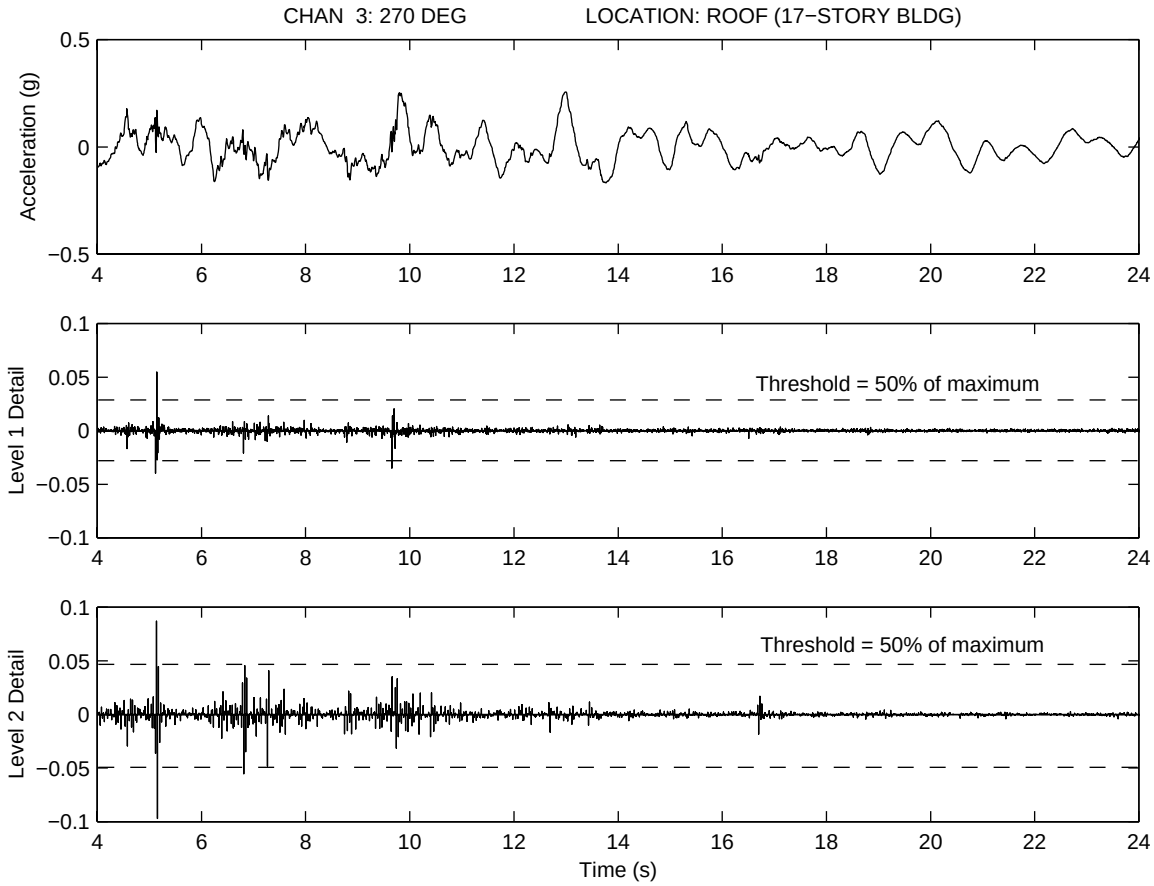

Figure 16. Time history (top), and wavelet transforms (middle and bottom) showing location of acceleration transients and wavelet coefficients in time, Woodland Hills – Canoga #2.

Characterization of transients

Characterization and identification of transient characteristics by visual inspection

The results of visual transient identification for both uncorrected (V1) and corrected (V2) data are shown in Table 5. These results include transient existence (detection) and key transient characteristics which are visually identifiable and play an important role in determining the likely cause of the transient (characterization). Such characteristics include transient presence during the strong shaking portion of the record only, in multiple channels at the same level, and at multiple levels in the structure. It should be noted that the causes of the transients in Table 5 have not yet been identified, and they may be a result of instrument malfunction or another source other than fracture. These results of visual identifications will be used in a procedure for determining the likely cause of the transient, which is described in later sections.

Table 5. Key transient characteristics from visual identification

Building Name	Transients Present			During strong shaking only	Multiple channels	Multiple levels
	Analog	V1 Data	V2 Data			
Set 1						
N. Hollywood – Lankershim #2	Yes	Yes	Possible	Yes	Yes	Possible
Sherman Oaks – Ventura #6	Not available	No	No	N/A	N/A	N/A
Alhambra – Office Bldg. #1	No	No	No	N/A	N/A	N/A
Tarzana – Ventura #10	Yes	Yes	Possible	Yes	No	No
Burbank – Office Bldg. #1	Yes	Yes	Not available	Yes	Yes	N/A
Encino – Ventura #12	Yes	Yes	Yes	Yes	Yes	No
Woodland Hills – Canoga #1	Yes	Yes	Yes	No	Yes	N/A
Woodland Hills – Oxnard #4	Yes	Yes	Yes	Yes	Yes	No
Woodland Hills – Canoga #2	Yes	Yes	Yes	No	Yes	N/A
Los Angeles – Olympic #2	Yes	Yes	Yes	Yes	Yes	N/A
Set 2a						
Los Angeles – Olympic #1	Yes	Yes	No	Yes	Yes	N/A
Los Angeles – Olympic #3	Yes	Yes	No	No	Yes	N/A
Los Angeles – Olympic #4	Yes	Yes	Possible	Yes	Yes	N/A
Los Angeles – Wilshire #1	Yes	Yes	No	Yes	Yes	N/A
Woodland Hills – Office Bldg. #1	Yes	Yes	Not available	No	Yes	N/A
Set 2b						
Encino – Office Bldg. #1	Yes	Yes	Not available	No	Yes	N/A
Los Angeles – Office Bldg. #3	Yes	Yes	Not available	Yes	Yes	N/A
Los Angeles – Office Bldg. #4	Yes	Yes	Not available	No	No	N/A
Los Angeles – Wilshire #7	Yes	Yes	Possible	Yes	Yes	N/A
Northridge – Oakdale #1	Yes	Yes	No	No	Yes	N/A
Sherman Oaks – Ventura #7	Not available	Yes	Possible	No	No	N/A
Woodland Hills – Oxnard #1	Yes	Not available	Yes	Yes	Yes	N/A
Woodland Hills – Oxnard #2	No	No	No	N/A	N/A	N/A
Woodland Hills – Oxnard #5	Yes	Not available	Not available	Yes	Yes	N/A

Characterization by frequency domain analysis

The frequency content of transients can provide important clues to transient origin. This of course assumes that the frequency content of a transient signal are accurately represented, either by digitization of the analog record or by a digital recorder with a high sampling rate. Unfortunately, this is not the case for the analog records used in this study; typically, some high-frequency information is omitted during the digitization. Thus, frequency-domain characteristics of these signals are used with caution. However, the frequency content of the signal, typically determined from a plot of the Fourier amplitude spectrum, can still be helpful in identifying some types of noise, where the frequencies generated by the transient source are known. An example of this is electromagnetic interference, which produces spectral peaks at 60 Hz and its multiples.

Another case where frequency domain analysis can be helpful, at least theoretically, is in the case of transients generated by a falling object striking the instrument. Since an object falling on the instrument is an impact load, the signal produced will contain essentially the impulse response of the instrument. Theoretically, since the frequency response of an instrument is generally known (or at least the first several frequencies are), the recorded transient can be analyzed in the frequency domain and the results compared with the frequencies expected from the instrument's impulse response. However, in practice this may not be feasible due to difficulties in properly resolving the frequency content of the signal, particularly for analog instruments. In the case of the SMA-1, discussed in further detail in subsequent sections, the impact excites some very high instrument response frequencies which cannot be resolved by digitization, even at 1200 dots per inch (dpi). In these cases, frequency domain analysis is not helpful, since the original signal cannot be digitized accurately to begin with. Rather, visual estimates of the response

frequency (typically a range of frequencies) combined with observation of characteristics such as beating or disturbance of the fixed and timing traces are used to help determine whether the transient was generated by an impact.

Impact Transient Characterization by Experiment on FBA, SMA-1 and K2 Instruments

Due to the significant amount of time which has elapsed between retrieval of the Northridge records from the study buildings and this study, it was deemed virtually impossible to determine if object impact occurred based on either (a) visual observation of the instrument environment (since post-earthquake cleanup and other changes have occurred, and there is typically no documentation of the immediate post-earthquake state of the instrument and its environment), or (b) the recollection of technicians who retrieved records. In future events, these methods would be very effective in determining if an object impact was likely to have occurred, since the instrument's environment could be easily documented with photographs. However, for the purposes of this study, the only reliable evidence is found in the signals themselves. If a falling object impacts the instrument, the signal generated should be distinct from the background earthquake response signal and from other types of high-frequency, transient signals. Determining the distinguishing characteristics of an impact signal requires data from impact tests on operating instruments. Three simple tests are described below. As a starting point, general characteristics of impact signals were observed using the digital test setup in the General Earthquake Observation System (GEOS) laboratory at USGS, consisting of a floor-mounted triaxial force-balance accelerometer (FBA) connected to a GEOS recorder (Borcherdt et al. 1985). These tests were performed by dropping or sliding a series of ordinary objects onto the FBAs (Chris Dietel, 2004 pers. comm.).

Data on the impact response of the analog instruments most commonly deployed in the study buildings (the Kinemetrics SMA-1[*]) were scarce, as published studies focused on overall behavior and characterization of the instrument response in the frequency range of interest, usually less than 25 Hz (e.g. Trifunac 1971). Since FBAs differ in several significant ways from the SMA-1, it was determined that impact tests on SMA-1 would be necessary to resolve concerns about the response of the instrument case and effects of impact on the fixed and timing traces, which could not be resolved using the digital GEOS setup. The goals of these experiments were threefold: (1) assess the response of the instrument to impact, (2) excite and capture higher-mode instrument response, and (3) determine characteristic signals associated with different types of impacts. For comparison purposes, the tests were repeated on a modern standalone digital instrument (the Kinemetrics K2[*]). These experiments were performed on instruments in the USGS inventory (Leroy Foote, 2004, pers. comm.).

GEOS Experiment

A simple experiment was performed to observe the signals generated by (a) dropping objects onto the top of a tri-axial force-balance accelerometer, (b) sliding objects into the side of the accelerometer, and (c) dropping objects next to the accelerometer. Tests performed are listed in Table 6. In each case, characteristic large two or three-sided pulses resulted, with a much smaller amplitude free vibration response following. If the dropped object bounced, there was a set of spikes for each impact, with smaller spikes for subsequent impacts. In the case of objects dropped on top of the instrument, the horizontal accelerations were approximately the same magnitude as the vertical acceleration, or larger. For the objects sliding into the side of the instrument, the horizontal accelerations were larger by at least a factor of 2. For objects dropped next to the instrument, the vertical response was larger than the horizontal by at least a factor of two. More irregular high-frequency response at lower amplitude was seen following the spikes, particularly for heavier objects. These experiments provided several key observations which can be used to characterize object impacts on FBAs in the time domain. The most important of these is that two-sided or three-sided pulses of similar amplitude occur in all components in the case of a direct top impact. For the other cases, the pulses occur in all components but the relative amplitudes depend on the location of the impact.

[*] Use of trade, firm, or product names does not imply endorsement by the U.S. Government or the authors.

Table 6. Experiments performed on FBAs

#	Test Type	Object to drop or slide	Drop height	Horizontal distance from SMA-1
1	Direct top impact	Pencil	2 ft	0
2	Direct top impact	Screwdriver	2 ft	0
3	Direct top impact	Light cardboard box	2 ft	0
4	Direct side impact	Screwdriver	n/a	1-2 ft
5	Direct side impact	Light cardboard box	n/a	1-2 ft
6	Direct side impact	Ladder	n/a	1-2 ft
7	Impact next to instrument	Large crescent wrench	2 ft	1 ft
8	Impact next to instrument	Ladder	2 ft	1 ft
9	Impact next to instrument	Standard metal trash can	2 ft	1 ft

SMA-1 Experiments

A variety of common objects were dropped onto, dropped next to, or slid into the side of, an SMA-1* attached to a tile over slab-on-grade floor. Experiments performed are listed in Table 7. Object drop orientations were consistent from test to test. Tests were performed in sequence with the instrument triggered to remove any startup effects. The response to the direct top impact of a metal trash can (Test 12) is shown in Figure 17. Several interesting characteristics of impact responses were observed, and are listed in Table 8. Beating, or a similar-appearing phenomenon, was observed during free vibration decay in every test for which the recorded response was large enough to be visible. The beat frequency was observed to be approximately 25 Hz in the vertical and transverse directions and 50 Hz in the longitudinal direction. The largest amplitude response was observed to occur in either the vertical or transverse components for top impacts. For large impact-generated transients, both fixed and timing traces were typically disturbed. In cases where the object was dropped on the floor near the instrument, a visibly apparent response was recorded only when the object was dropped quite close to the instrument. This suggests that falling objects would either need to impact on or very close to the instrument (or be very heavy if farther away) to affect the measured response.

Table 7. Experiments performed on SMA-1

#	Test Type	Object to drop or slide	Height drop from	Horizontal distance from SMA-1
1	Direct side impact	Roll of electrical tape	n/a	1 m
2	Direct side impact	Ream of copy paper	n/a	1 m
3	Direct side impact	Standard metal trash can	n/a	1 m
4	Impact next to instrument	Pencil	1 m	1 m
5	Impact next to instrument	Ream of copy paper	1 m	1 m
6	Impact next to instrument	Standard metal trash can	1 m	1 m
7	Impact next to instrument	Pencil	1 m	0.5 m
8	Impact next to instrument	Ream of copy paper	1 m	0.5 m
9	Impact next to instrument	Standard metal trash can	1 m	0.5 m
10	Direct top impact	Pencil	1 m	0
11	Direct top impact	Ream of copy paper	1 m	0
12	Direct top impact	Standard metal trash can	1 m	0
13	Direct top corner impact*	Pencil	1 m	0
14	Direct top corner impact*	Ream of copy paper	1 m	0
15	Direct top corner impact*	Standard metal trash can	1 m	0

* Object dropped on corner of instrument, rather than at centroid.

* Use of trade, firm, or product names does not imply endorsement by the U.S. Government or the authors.

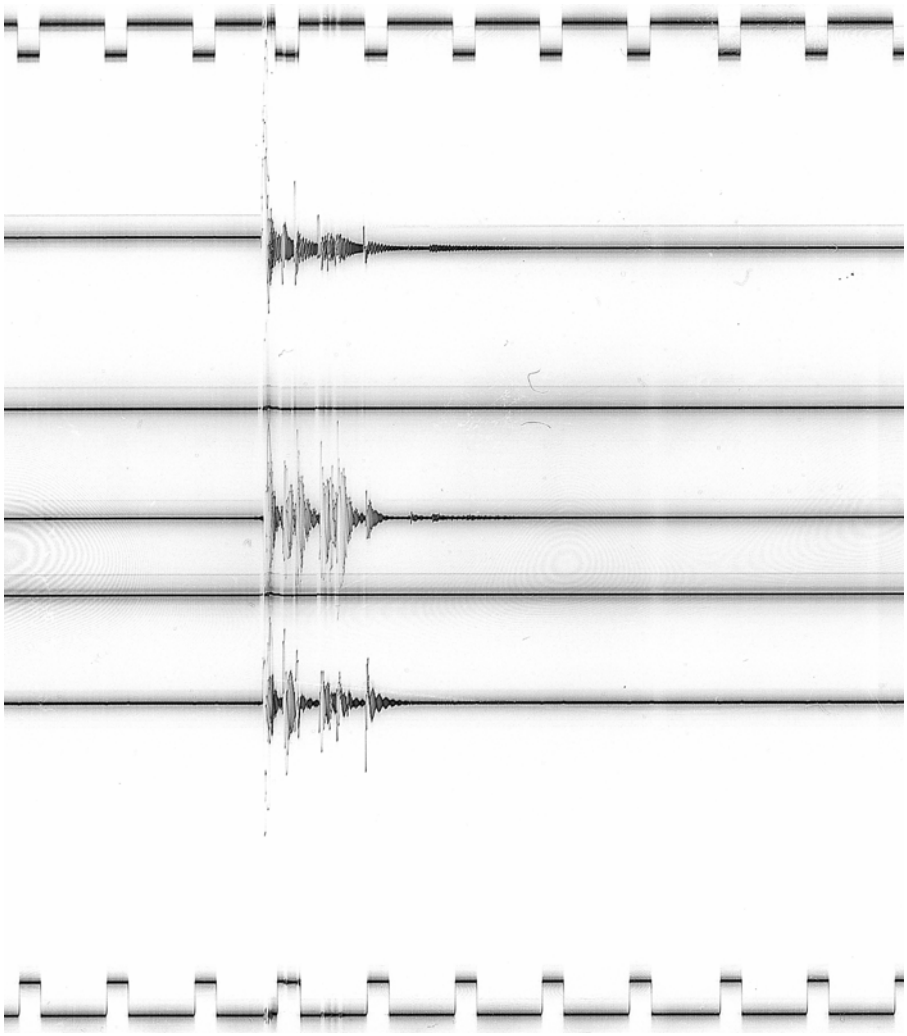

Figure 17. Acceleration response to direct impact of metal trash can on top of SMA-1 (Test 12)

Table 8. Qualitative results of SMA-1 impact tests

#	Fixed traces disturbed	Timing traces disturbed	Beating	2-sided pulse	Largest signal	Over range	Permanent offset of trace
1	N	Y	Y	Y	Transverse	N	N
2	Y	Y	Y	Possible	Transverse	Y	Y - Longitudinal
3	Y	Y	Y	Y	Transverse	Y	Y- Longitudinal
4	No visible recorded response						
5	N	N	Y	Y	Transverse	N	N
6	N?	N?	Y	N	Vertical	N	N
7	No visible recorded response						
8	No visible recorded response						
9	N	N	Y	N	Vertical	N	N
10	N	N	Y	Y	Vertical	N	N
11	Y	Y	Y	Y	Vertical or Transverse	Possible	Y - Longitudinal

#	Fixed traces disturbed	Timing traces disturbed	Beating	2-sided pulse	Largest signal	Over range	Permanent offset of trace
12	Y	Y	Y	Y	Signals over range	Y	Y - Longitudinal
13	No visible recorded response						
14	Y	Y	Y	Y	Transverse	Y	Y - Longitudinal
15	Y	Y	Y	Y	Signals over range	Y	N

K2 Experiments

The experiments performed on the SMA-1 described in the previous section were repeated on a Kinemetrics K2* instrument. The K2 is a modern digital accelerograph, and many of these instruments are currently deployed as part of the USGS strong motion observation network. The response of the K2 was much more similar to that of the FBA than the SMA-1, and was dominated by a very high amplitude, two or three sided pulse of very short duration, as shown in Figure 18. Virtually no free vibration was observed after the initial pulse-like response. This pulse-like response was observed in all components, but tended to be larger in the vertical component for most cases of top or nearby impact, though this was not always the case. The amplitude of the response drops off substantially with increasing horizontal distance for objects dropped near the instrument. The K2 was observed to be more sensitive to nearby object impacts than the SMA-1, though responses for objects dropped one meter away were small. Thus, the recorded response is not expected to be affected by object impacts unless they occur very close to the instrument, or the object is very large.

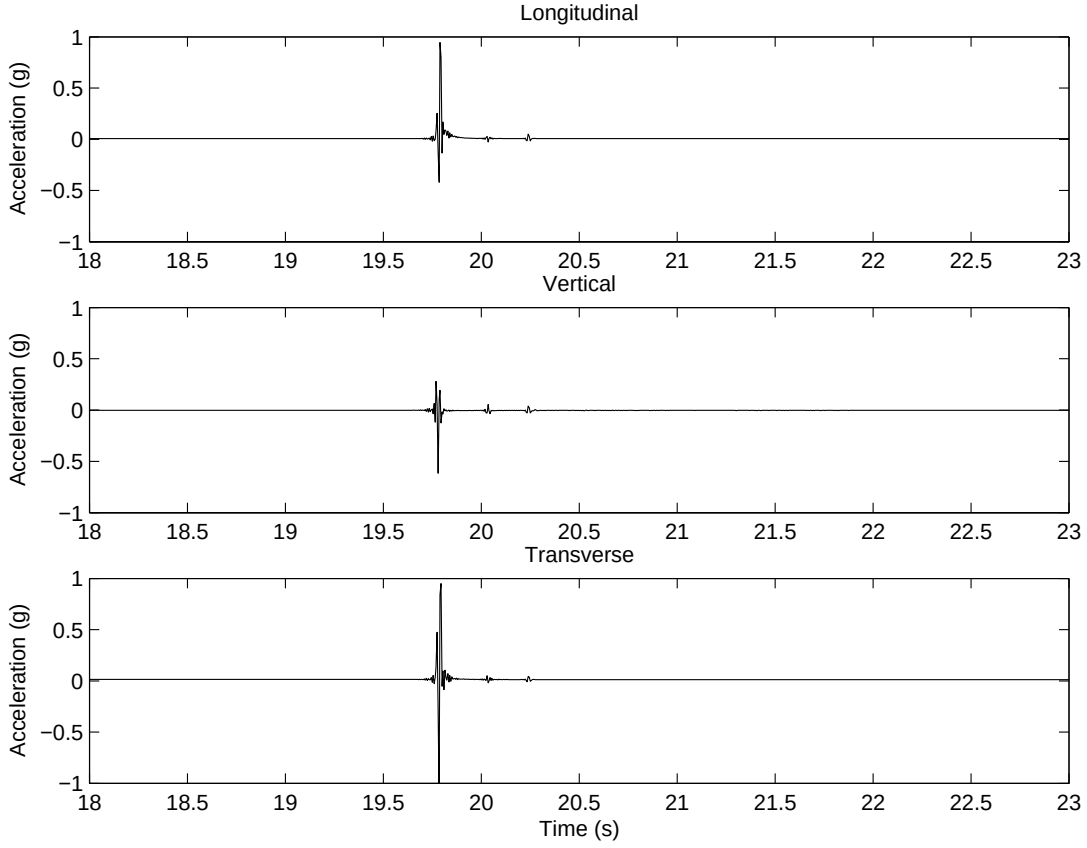

Figure 18. Acceleration response to direct impact of metal trash can on top of K2

* Use of trade, firm, or product names does not imply endorsement by the U.S. Government or the authors.

Summary of transient characteristics

Different transient sources produce transients that have differing and distinguishing characteristics, which are identified during the process of transient characterization. Characteristics associated with transients from each source considered in this study are summarized in Table 9. Relations between sources and transient characteristics were obtained from experimental data (falling object impact and sudden structural damage), digital signal processing literature (white noise, electromagnetic interference, pop noise) and the institutional "knowledge base" at the USGS (all other sources), built over many years of accelerogram processing by data processing experts and scientists.

Table 9. Summary of transient characteristics

Transient source	Characteristics	
	Analog instrument	Digital instrument
Fracture or other sudden structural damage	Occurs during the strong shaking portion of the record only Occurs in all co-located channels simultaneously Fixed and timing traces typically not disturbed even though transient is large No beating	Occurs during the strong shaking portion of the record only Occurs in all co-located channels simultaneously
Mounting failure	Sudden change to very long period signal which does not resemble building or ground response	same
Instrument malfunction	Can be moderate or high amplitude Does not only occur during strong shaking May include DC offsets	same
Local member response	Recurring low-amplitude harmonic signals with consistent frequency content occurring throughout the record	same
White noise	Low-amplitude white noise signal (meaning a random signal containing approximately equal amounts of all frequencies) occurring throughout the record	same
Electromagnetic interference	Recurring low-amplitude harmonic signals with frequencies at multiples of 60 Hz occurring throughout the record	same
Pop noise	n/a	One-sided pulse Only one data point in pulse
Falling object impact	Beating (or similar-appearing phenomenon) Excitation of very high instrument and/or case response frequencies Decay of harmonic response noticeably slower than for digital instruments Large response amplitude (even over range) for large objects, small for small objects Disturbance of both fixed and timing traces if transient amplitude is large (i.e. greater than the distance between traces) Large response amplitudes in all components Vertical component amplitude not necessarily largest	Large amplitude two-sided pulse Very little to no harmonic response following pulse Large response amplitudes in all components Vertical component amplitude not necessarily largest Over range for larger objects

Identification of likely transient cause

Since high-frequency transients can be caused by a number of phenomena, identification of the cause of a particular transient requires some effort. The "process of elimination" approach is recommended, since it is necessary to first determine whether the transient is an artifact of the instrument or its environment (i.e. falling objects) before interpreting it as structural response. The process is best illustrated by a flowchart, such as the one shown in Figure 19.

After a transient has been visually identified in uncorrected (V1) data, causes other than damage are ruled out, one by one. The instrument and its immediate environment are evaluated first, beginning with proper function of the instrument. Instrument malfunctions are generally evident in the recorded data, but some malfunctions, such as minor stalls in film advancement in analog recorders, are sometimes less evident. If there is doubt about proper instrument function, the data file header should be examined (stalls should be noted), and the original analog record (or a good copy) should be obtained and examined in the case of analog instruments. Also, if the instrument has only malfunctioned because it went over-range, this does not rule out damage as a cause. It is possible that very high acceleration amplitudes were caused by damage or building impact.

It is important that the immediate environment of the instrument be evaluated also. This includes the instrument mounting and possible falling objects that could have hit the instrument or landed nearby. Since it is often impossible or impractical to visually inspect the instrument's environment in cases involving older records (such as the ones used in this study), this determination must be made using the record alone. Fortunately, both mounting failure and falling object impact often produce characteristic signals in the recorded response. If impact is considered possible, the original analog record or a good copy should be examined, as some key impact-signal characteristics are not well resolved, or not resolved at all, by digitization.

When and if impact and mounting failure have been ruled out, characteristics of the time series are used to determine if local vibration, noise, or an unknown local cause is to blame. The visually identifiable characteristics in Table 5, which include transient presence during the strong shaking portion of the record only, in multiple channels at the same level, and at multiple levels in the structure, are used in this step. Local member vibration, such as that caused by mechanical equipment in operation, is often relatively easy to detect from the signal alone, as it tends to cause a consistent frequency to occur for significant portions of the record (usually most conspicuous in the vertical component, due to out-of-plane floor diaphragm vibration). If available, knowledge of the location of the instrument can be helpful in cases where local member behavior is suspected of affecting the response, however. Such information includes the type of member to which the instrument is mounted (floor slab vs. beam) and the proximity of elevators and other mechanical equipment which can cause vibrations. Transients which do not contain enough points (four at 200 sps), particularly in records from digital instruments, may be due to pop noise, recording or playback errors, or analog-to-digital conversion errors. Transients which are present at times outside of the strong shaking portion of the record and are not present in other channels in the same level are likely to have resulted from causes other than damage.

If no other likely cause has been found for the transient at this point, all of the major causes except for damage or structure pounding impact (distinct from falling object impact) have been either ruled out or determined to be unlikely. Unlike moment connection fractures, pounding damage is generally readily apparent from visual inspection of the exterior of the building. Pounding results in damage to the exterior finishes at the point(s) of impact. The reader is referred to Nagarajaiah and Sun (2001) for an example of the pounding. Other information contained in the recorded building response can provide clues as to whether significant structural damage has occurred. The results of a windowed Discrete Time Fourier Transform (also called moving window Fourier analysis) can also be used to help determine if there has been a substantial elongation (>30%) of the structure fundamental period. In almost all cases, such elongation indicates significant structural damage has occurred.

Figure 19. Flowchart for determining the likely cause of a high-frequency transient

Example: Burbank – Office Building #1

Using the flowchart in Figure 19, the likely cause of the transients in the Burbank – Office Building #1 record is determined. A scanned image of the portion of the original analog record containing the transients is shown in Figure 6, while the uncorrected, digitized record is shown in Figure 7. The transients in this portion of the record are large, especially in the vertical component, and are easy to detect by visual inspection of both the analog and uncorrected data. Following the flowchart, the data file and headers are examined, and no instrument malfunctions are found. Next, the instrument and its environment are examined, and no mounting failures are found. However, based on the uncorrected data, a determination of whether the transient is due to falling object impact is inconclusive. The original analog record shown in Figure 6 is examined, and is found to be missing key characteristics of an impact signal. If the cause of a transient of this size were object impact, disturbance of the fixed and timing traces, such as that shown in Figure 17, would be expected. Also missing are large amplitude signals in the longitudinal and transverse components, and beating in the response following the transient. Thus, falling object impact is considered an unlikely source for the transients in the record.

Next, the time series containing the transient is examined and it is determined that transients only occur during the strong shaking portions of the record, that there are at least four points in the transient waveforms, and that the transients occur simultaneously in all channels. These steps eliminate noise as a likely cause. Based on the evaluation of the records using the flowchart, the likely cause of the transients in the Burbank – Office Building #1 record is damage. Since only the roof record is available, no comparisons with other instruments are possible, and it is not possible to determine if transients occur simultaneously in the accelerations at other floors.

Example: Woodland Hills – Canoga #1 and #2

The flowchart above is intended to identify the most likely cause of transients found in a particular record. However, it is important to realize that more than one type of transient may exist in a particular record. A record containing transients caused by connection fracture may also contain transients from local vibration or noise. This situation is illustrated by a pair of nominally identical 17-story buildings, Woodland Hills – Canoga #1 and #2. The roof records for both buildings are compared in Figure 20, and contain transients in both corrected and uncorrected data. Following the flowchart, the instruments in both buildings functioned properly, the instrument mounts did not fail, and it is unlikely that either instrument was struck by a falling object. However, significant high-frequency, low amplitude transients occur throughout the first half of the records, not only during strong shaking. Per the flowchart, the original analog records are examined and a recurring frequency is found in both cases, indicating local noise or vibration.

However, the record from the more heavily damaged Canoga #2 contains several larger amplitude transients during the strong shaking portion of the record, which rise above the “noise level” defined by the smaller-amplitude transients. While transients occur in the Canoga #1 record at the same time as the larger transients occur in the Canoga #2 record, they are not appreciably larger than the “noise level”. These observations are especially apparent when the records are high-pass filtered, as shown in Figure 10 for Canoga #1 and Figure 11 for Canoga #2. Thus, the smaller transients in the Canoga #1 record cannot reliably be attributed to fracture due to the noise in the record. Again following the flowchart, the transients in the Canoga #1 record are attributed to local noise, while the larger transients in the Canoga #2 record are evaluated using the remainder of the flowchart. The other causes are ruled out, so the most likely possibility is that the larger transients in the Canoga #2 record were caused by fracture. However, since judgment plays a role in the use of the flowchart, caution must be used in making such interpretations. In records with significant local vibrations or noise, transients should not be attributed to fracture unless they are high-amplitude and satisfy all other flowchart criteria.

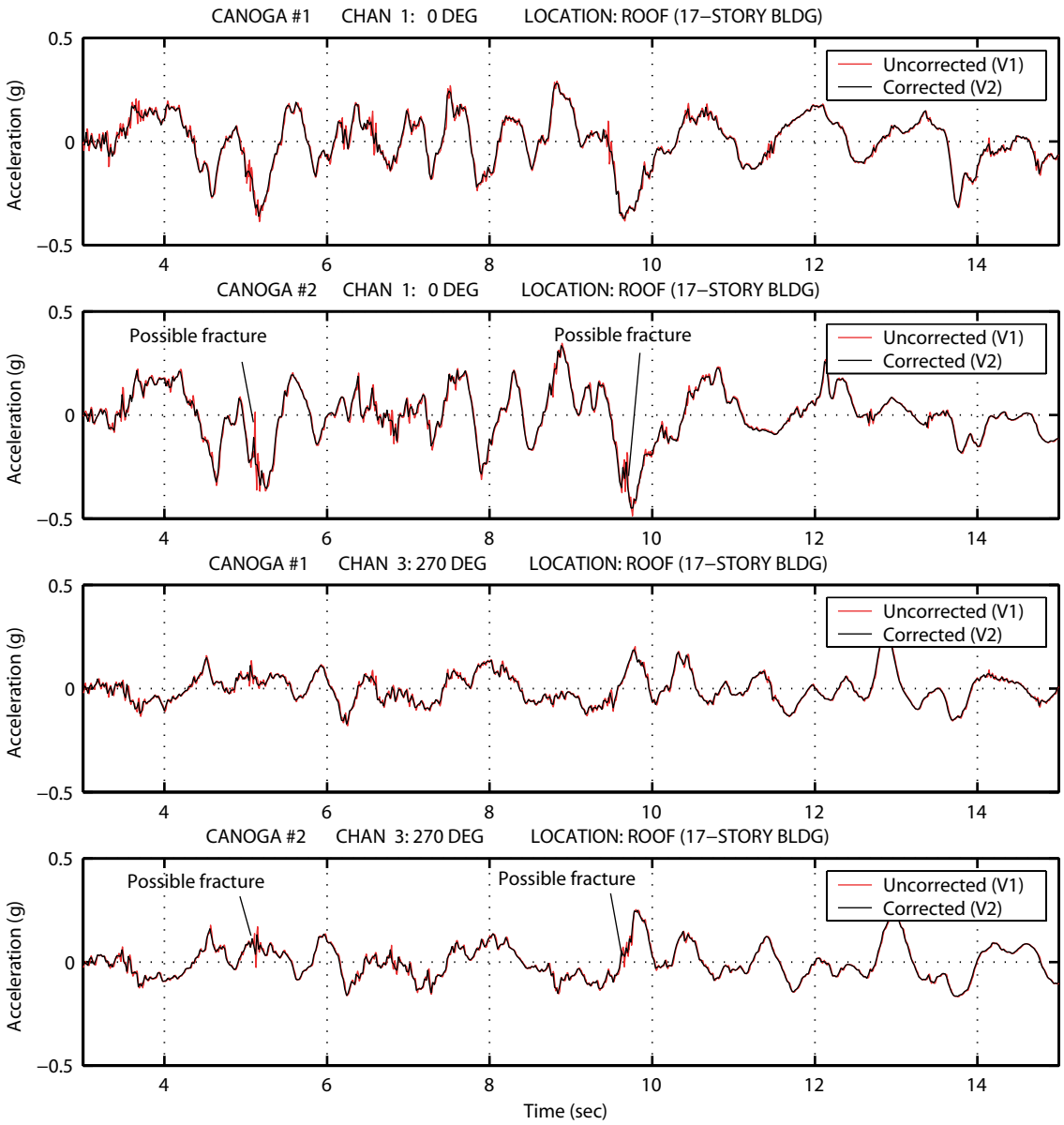

Figure 20. Comparison of roof accelerations, Canoga #1 and #2

Results for datasets

The effectiveness of the high-frequency transients procedure in detecting fracture damage is examined and validated using the datasets. The results of this approach, termed the “transients only” method, are then combined with other commonly used indicators of possible moment frame damage, including ground shaking intensity, elongation of fundamental period and estimated interstory drift. This combined method is examined for Set 1, in order to present an example of how information from the transients method might be combined with other information from strong motion data which would typically be available to engineers in a real event.

Transients only

The method for detecting and determining the likely cause of high-frequency acceleration transients described in the previous section was developed and refined using the data in Set 1, and tested using the data in Set 2. The damage information for Set 2 was not examined prior to their evaluation using the developed method. This was done to remove a potential source of bias from the method assessment process. The records in the dataset with visually identifiable transients (in the uncorrected data) were evaluated using the procedure outlined in Figure 19. The results of the evaluation are shown in Table 10, and the method success rate is broken down by set and damage bin in Table 11.

Table 10. Results of transient evaluation procedure

Building Name	Transient Present	Attributed to fracture	Cause if not fracture	Damage Bin	Damage Ratio	Inspection Ratio	Method Successful
Set 1							
N. Hollywood - Lankershim #2	Yes	Yes	-	None	0.00	0.18	No **
Sherman Oaks - Ventura #6	No	N/A	-	None	0.00	0.23	Yes
Alhambra – Office #1	No	N/A	-	None	0.00	0.06	Yes
Tarzana - Ventura #10	Yes	No	Higher modes	Light	0.02	0.13	No *
Burbank – Office Building #1	Yes	Yes	-	Moderate	0.08	0.92	Yes
Encino - Ventura #12	Yes	Yes	-	Moderate	0.04	1.00	Yes
Woodland Hills - Canoga #1	Yes	No	Noise	Moderate	0.09	1.00	No *
Woodland Hills - Oxnard #4	Yes	Yes	-	Moderate	0.09	1.00	Yes
Woodland Hills - Canoga #2	Yes	Yes	-	Heavy	0.12	1.00	Yes
Los Angeles - Olympic #2	Yes	Yes	-	Heavy	0.17	0.99	Yes
Set 2a							
Los Angeles - Olympic #1	Yes	Yes	-	None	0.00	0.14	No **
Los Angeles - Olympic #3	Yes	No	Instrument	Moderate	0.06	0.86	No *
Los Angeles - Olympic #4	Yes	Yes	-	Heavy	0.14	0.99	Yes
Los Angeles - Wilshire #1	Yes	No	Noise	None	0.00	0.10	Yes
Woodland Hills - Office Bldg. #1	Yes	Yes	-	Heavy	0.17	1.00	Yes
Set 2b							
Encino – Office Bldg. #1	Yes	No	Noise	Light	0.01	0.25	No
Los Angeles – Office Bldg. #3	Yes	No	Noise	None	0.00	0.14	Yes
Los Angeles – Office Bldg. #4	Yes	No	Noise	None	0.00	0.10	Yes
Los Angeles - Wilshire #7	Yes	No	Higher modes	None	0.00	0.31	Yes
Northridge - Oakdale #1	Yes	Yes	-	Heavy	0.23	1.00	Yes
Sherman Oaks - Ventura #7	Yes	No	Instrument	Heavy	0.17	0.60	No *
Woodland Hills - Oxnard #1	Yes	Yes	-	Heavy	0.11	1.00	Yes
Woodland Hills - Oxnard #2	No	N/A	-	Moderate	0.03	0.97	No *
Woodland Hills - Oxnard #5	Yes	Yes	-	Heavy	0.15	1.0	Yes

* Failure is false negative
** Failure is false positive

Table 11. Method success rate by set and damage bin

Results	All results			Buildings with excessive instrument response or excessive noise omitted		
	Total buildings	Successes	Success rate (%)	Total buildings	Successes	Success rate (%)
By Set						
Set 1	10	7	70	8	6	75
Set 2a	5	3	60	4	3	75
Set 2b	9	6	67	8	6	75
By Bin						
Heavy	8	7	88	6	6	100
Moderate	6	3	50	4	3	75
Light	2	0	0	2	0	0
None	8	6	75	8	6	75
All	24	16	67	20	15	75

As shown in Table 11, the overall success rate of the method is 67% when all buildings are considered. Success rates for the three subsets fall between 60 and 70%, indicating that the sets are relatively well-balanced. However, success rates vary considerably with damage bin. For buildings in the "Heavy" damage bin, the success rate is substantially higher than the overall rate at 88% for all buildings. Rates for the "Moderate" and "None" bins are substantially lower and somewhat higher than the overall rate, respectively. The success rate for the "Light" bin is zero, indicating that the method fails to detect light damage. When buildings with excessive instrument response or noise are removed from the dataset, the success rates increase for the "Heavy" and "Moderate" bins, and remain the same for the "Light" and "None" bins. The overall rate rises to 75%, indicating that the success rate of the method can be diminished by noisy records, though this effect is not particularly large.

The general trend indicated by the above results is that the method is useful in detecting significant fracture damage, but fails at detecting a small number of fractures, which is to be expected. Also important, the method is useful in identifying cases where there is no damage. The argument can be made that only significant fracture damage will impact important performance states such as life safety and continued occupancy (Luco and Cornell 2000), and that there are really only two damage states that matter: significant damage and minor/no damage. If the "Heavy" and "Moderate" damage bins used in this study are grouped into the "significant damage" state, and the "Light" and "None" bins are grouped in the "minor/no damage" state, the method works well for determining which general state the building belongs in. Thus, the results of the high-frequency transients method provide a valuable additional piece of information to incorporate into decision-making on inspection scope and continued occupancy.

Transients in combination with other damage indicators

Combinations of damage indicators have been used by several investigators (Revadigar and Mau 1999; Marwala 2000) to provide more robust assessments of whether or not damage has occurred. In addition, it is typical for engineers in real post-earthquake situations to combine the different pieces of information at their disposal using their professional judgment in order to arrive at a recommendation. As a very simple example of this approach might be used, the results of the transient evaluation procedure described previously are combined with several indicators commonly used to identify potential moment frame damage in either sparsely instrumented or, in the case of ground motion intensity, un-instrumented buildings. These indicators are:

- Peak ground accelerations (measured or estimated from SAC contour maps) which exceed threshold values of 25% and 50% g
- Elongation of the fundamental period of the structure (calculated from measured accelerations by windowed Discrete Time Fourier Transform) which exceed threshold values of 25% and 50%.
- Average interstory drift ratio (estimated from building height and calculated or estimated roof drift) which exceeds a threshold value of 0.6% (150% of the assumed working stress drift of 0.4%)

For buildings without base records, peak ground acceleration estimates were obtained from contours developed by Woodward-Clyde consultants (SAC, 1995b). Roof drifts were estimated to be equal to roof displacements for buildings without base records, a reasonable approximation for flexible moment frames (Jennings, 1997). Threshold value exceedance was used instead of a damage index with each indicator (with the exception of fracture transient presence), both for simplicity and due to the approximate nature of the estimates of the indicator quantities. This permitted simple Boolean expressions (True or Yes = 1, False or No = 0) to be used for each indicator resulting in 1 if the threshold was exceeded, and 0 otherwise.

In order to arrive at a damage predictor, the indicators were combined using a very simple linear combination with equal weights for each indicator. For cases with two threshold values, each threshold was given half the weight of the overall indicator. The damage predictor value is computed using the following Boolean expression:

DP = 0.25[Fracture transient present + (Avg. drift ratio > 0.6%)] + 0.125[(PGA > 0.25g) + (PGA > 0.5g) + (T1 elongation > 25%) + (T1 elongation > 50%)]

This expression equals 1 if damage is most likely and 0 if damage is least likely, based on the indicators chosen. Larger values also indicate it is more likely that the damage will be more significant. This is primarily due to the period elongation indicator, which is a measure of the amount of damage, in addition to an indicator of the existence of damage. Results of this combination are shown in Table 12. This is a very simple combination scheme, and is used only for the purpose of illustrating the basic idea of the combination approach. It is anticipated that better results can be obtained with a more refined scheme which uses better estimates of some damage indicators. One possibility is a fuzzy logic approach, such as the one proposed by Revadigar and Mau (1999).

Table 12. Results for combination of indicators

Building Name	Fracture Transient	PGA > 0.25 g	PGA > 0.5 g	T_1 elong. > 25%	T_1 elong. > 50%	Est. avg drift > 0.6%	Damage predictor value	Damage Bin	Method Successful
Set 1									
N. Hollywood - Lankershim #2	Yes	Yes	No	No	No	No	0.38	None	Yes
Sherman Oaks - Ventura #6	No	Yes	Yes	No	No	Yes	0.5	None	No
Alhambra – Office #1	No	No	No	No	No	No	0	None	Yes
Tarzana - Ventura #10	No	Yes	Yes	No	No	Yes	0.5	Light	No
Burbank – Office Bldg #1	Yes	Yes*	No*	Yes	No	n/a	0.75	Moderate	Yes
Encino - Ventura #12	Yes	Yes	Yes	No	No	No	0.5	Moderate	Yes
Woodland Hills - Canoga #1	No	Yes*	No*	Yes	No	Yes	0.5	Moderate	Yes
Woodland Hills - Oxnard #4	Yes	Yes	Yes	Yes	No	Yes	0.88	Moderate	Yes
Woodland Hills - Canoga #2	Yes	Yes*	No*	Yes	Yes	Yes	0.88	Heavy	Yes
Los Angeles - Olympic #2	Yes	Yes*	No*	Yes	Yes	Yes	0.88	Heavy	Yes

* Estimated based on contours by Woodward-Clyde (SAC 1995b)

An 80% success rate results if the method is considered successful when DP greater than or equal to 0.5 in cases with “Moderate” or “Heavy” damage, and less than 0.5 for cases with “Light” or “None” levels of damage. However, this does not address the result that DP = 0.5 for cases in the “None”, “Light”, and “Moderate” damage bins. Consider a slightly more refined scheme, where DP<0.25 in cases with no damage, $25 \leq DP < 50$ in cases with “Light” damage, $50 \leq DP < 75$ in cases with “Moderate” damage, and $DP \geq 75$ for “Heavy” damage. If this scheme is used instead, the success rate drops to 50%. The combined method does not predict damage levels very well, though it is fairly good at predicting whether or not damage will occur.

If the results from the fracture transients approach are removed from the combination, and the three remaining indicator types given weights of 1/3 each, a success rate of 70% results for the simple Method 1 used above, though some notable false positives exist for Sherman Oaks – Ventura #6 and Tarzana – Ventura #10. If the slightly more

refined evaluation scheme in Method 2 is used, the success rate is 60%. These results suggest that the addition of information from the high-frequency transients method helps improve the success rate of predicting if fracture damage occurs, but does not improve the success rate in determining the level of damage. However, in cases of strongly shaken but undamaged buildings (such as Sherman Oaks – Ventura #6), the high frequency-transients method can provide information which counterbalances ground motion-based damage indicators.

Conclusions and Recommendations

Costly and time-consuming intrusive inspections are currently the only way to reliably determine if a particular connection in a steel moment frame has fractured. This type of damage can be extremely difficult to detect with commonly used post-earthquake visual inspection methods (ATC, 1989). However, it has been demonstrated herein that high-frequency, transient signals in the recorded acceleration responses of steel moment frames provide a promising indicator of the existence of connection fracture damage, though not of the locations of individual fractures. Further assessment of the proposed method by both experimental and analytical means is recommended. However, this study is a significant first step towards the development of a practical connection fracture damage detection method, and demonstrates that strong motion accelerograms, which are easily recorded using existing technology, have the potential to provide a key piece of additional information for post-earthquake safety decisions.

However, caution must be used in interpreting records containing high-frequency transients, since transients can arise from a number of other sources. Because of this, a procedure for enhancing the certainty with which transient sources can be identified has been developed using a set of well-inspected instrumented buildings with known damage states. This procedure was then tested using a second set of well-inspected instrumented buildings with damage states unknown a priori. The success rate of the high-frequency transient method of detecting fractures was found to be high in buildings with heavy damage, relatively high in buildings with no damage at all, and moderate in buildings with moderate damage. However, the method failed for buildings with light damage (< 2% of connections fractured). The removal of records with excessive noise or instrument response improved the success rate for buildings with moderate and heavy damage. This result suggests that the method's success rate can be affected by the noise level of the records, though the effect is not necessarily large.

This or a similar procedure is recommended for use in evaluating records with high-frequency transients from welded steel moment-frame buildings before proceeding to use these transients as a potential damage indicator. It is also recommended that transients be used as a potential damage indicator in conjunction with other available information related to potential damage, as well as other tools for damage detection. A combined method using transients and other indicators, such as peak ground acceleration and period elongation, had a higher overall success rate at predicting damage occurrence than either the transients-only method or a method which omitted transients. The combination method employed was very simple, and it is anticipated that improved performance could be obtained by method refinement and the use of improved estimates for the other damage indicators.

Due to the very sparse instrumentation in almost all buildings in the dataset, specific fracture locations could not be determined. It is expected that very general location determination (such as upper floors vs. lower floor) may be possible in buildings with many more accelerometers. However, it is anticipated that a very dense instrumentation scheme would be necessary to determine fracture locations down to the individual connections. Such high-density instrumentation schemes are neither practical nor feasible with current technology. Nevertheless, advances in cheaper and/or wireless instrumentation may permit such dense instrumentation in the future.

A lack of high-frequency transients in the acceleration time-history provides evidence that substantial fracture damage did not occur, and provides a significant incentive for owners to instrument their buildings, provided that inspections may be reduced. However, if transients are present a more thorough inspection may be required. In this case, the records can be used along with other information about structural performance to determine the most likely regions for damage occurrence.

Since transients are high-frequency, unusual signals, some common strong motion processing procedures can reduce the amplitude of or in some cases entirely eliminate transients from corrected records. These processing procedures include decimation and low-pass filtering. Because of this, researchers should have access to uncorrected data, and uncorrected data should be used for transient detection and characterization. Since use of uncorrected data is recommended, analysis for transient presence can be carried out quickly following an earthquake, as the processed records are not required. In cases where data was recorded on analog instruments, researchers should also be able to obtain access to the original film records to both help establish likely transient cause in cases where there is significant uncertainty and to confirm the quality of the digitization.

Recommendations for future research in this area include both experimental and analytical studies which further the understanding of the dynamic response of full-scale steel moment frames with fracturing connections. Measurement or computation of accelerations in such studies is necessary to confirm the findings of this study, which used very sparsely instrumented buildings. Further work on transient characterization is also necessary, particularly for records from digital instruments. It is anticipated that some of the signal processing tools which were not helpful in characterization of transients in the digitized analog records used in this study (due to resolution limitations) would be effective for high-resolution digital records. In addition, optimal instrumentation schemes for capturing transient acceleration responses following fracture still need to be determined. It is expected that some progress on fracture damage localization can be made with data from more dense instrumentation systems, and the balance between density and the quality of results obtained should be explored further.

Finally, despite the significant repair work following the Northridge earthquake and the substantial changes in the way steel moment frames are designed and constructed, the building stock in many areas of high earthquake hazard still contains numerous steel moment frames with connections vulnerable to brittle fracture. From a hazard reduction point of view, it is important to investigate and understand the behavior of these buildings. Individual building owners can also benefit from the deployment of seismic instruments in their properties, since the valuable information recorded during strong-motion events, including high-frequency, transient accelerations, can facilitate post-event safety decisions.

Acknowledgments

Strong motion records, building information, and information on data processing and instrument performance were provided by Moh Huang, Vladimir Grazier, and their colleagues at the California Strong Motion Instrumentation Program and Chris Stephens at USGS. Information on instrument performance and impact response was provided by Bill Rihn and Ian Standley of Kinemetrics, Inc. and Leroy Foote, Ron Porcella, Chris Deitel, Roger Borcherdt, and Malcolm Johnston of USGS. The assistance of the following persons in gathering damage information is also greatly appreciated: Bruce Maison of East Bay Municipal Utility District, Tom Sabol of Englekirk and Sabol Consulting Engineers, Kelvin Chang of the City of Burbank, Terrance Paret and Kent Sasaki of Wiss, Janney, Elstner Associates, Inc., Peter Maranian and Gregg Brandow of Brandow & Johnston Associates, Sea Fan of Los Angeles Department of Building and Safety, Farzad Naeim of John A. Martin & Associates, Brian Cochran of Brian L. Cochran & Associates, Owen Hata of Nabih Youssef & Associates, Albert Chen of Black & Veatch, Inc., and James Anderson of the University of Southern California. Helpful comments by the USGS internal reviewers were also greatly appreciated.

References

Anderson, J.C. and F.C. Filippou (1995). Dynamic response analyses of the 17-story Canoga building, in *SAC 95-04*, SAC Joint Venture, Sacramento, California.

Astaneh-Asl, A., Modjtahedi, D., McMullin, K. Shen, J.-H. and E. D'Amore (1998). Stability of damaged steel moment frames in Los Angeles, *Engineering Structures*, 20(4-6), 433-446.

ATC (1989), Procedures for postearthquake safety evaluation of buildings, *ATC-20*, Applied Technology Council, Redwood City, California.

Bertero V.V., Anderson, J.C., and H. Krawinkler (1994). Performance of steel building structures during the Northridge earthquake, *Report UCB/EERC-94/09*, Earthquake Engineering Research Center, University of California, Berkeley.

Bonowitz, D. and B.F. Maison (1998). Are steel frames safe? Probabilistic seismic evaluation of existing WSMF buildings, *Proceedings, Sixth U.S. National Conference on Earthquake Engineering, Seattle, Washington*, Earthquake Engineering Research Institute, Oakland, California.

Bonowitz, D. and B.F. Maison (2003). Northridge welded steel moment-frame damage data and its use for rapid loss estimation, *Earthquake Spectra*, 19(2), 335-364.

Borcherdt, R.D., Fletcher, J.B, Jensen, E.G., Maxwell, G.L., Van Schaack, J.R., Warrick, R.E., Cranswick, E., Johnston, M.S., and R. McLearn (1985), A general earthquake observation system (GEOS), *Bulletin of the Seismological Society of America*, 75, 1783-1825.

Chi, W.-M., El-Tawil, S., Deierlein, G.G., and J.F. Abel (1998). Inelastic analyses of a 17-story steel framed building damaged during Northridge, *Engineering Structures*, 20(4-6), 481-495.

Cohen, J.M. (1996). Seismic vulnerability analysis of steel framing with deep spandrel beams, *Professional Paper 96-16*, Los Angeles Tall Buildings Structural Design Council, Los Angeles, California.

Darragh, R., Cao, T., Grazier, V., Shakal, A., and M. Huang (1994). Los Angeles code-instrumented building records from the Northridge, California earthquake of January 17, 1994: Processed release no. 1, *Report No. OSMS 94-17*, California Strong Motion Instrumentation Program, Sacramento, California.

Darragh, R., Huang, M., Cao, T., Grazier, V., and A. Shakal (1995). Los Angeles code-instrumented building records from the Northridge, California earthquake of January 17, 1994: Processed release no. 2, *Report No. OSMS 95-07*, California Strong Motion Instrumentation Program, Sacramento, California.

Donoho, et al. (1999). Wavelab version 802, freeware computer program available from http://www-stat.stanford.edu/~wavelab/, Stanford University, California.

Fenves, G. and R. DesRoches (1994). Response of the northwest connector in the Landers and Big Bear earthquakes, *Proceedings, SMIP94 Seminar on Seismological and Engineering Implications of Recent Strong-Motion Data, Los Angeles*, California Strong Motion Instrumentation Program, Sacramento, California, 61-74.

FEMA (2000a). Recommended seismic design criteria for new steel moment-frame buildings, *FEMA-350,* prepared by the SAC Joint Venture for the Federal Emergency Management Agency, Washington, DC.

FEMA (2000b). Past performance of steel moment-frame buildings in earthquakes, *FEMA-355E,* prepared by the SAC Joint Venture for the Federal Emergency Management Agency, Washington, DC.

FEMA (2000c). Recommended postearthquake evaluation and repair criteria for welded steel moment-frame buildings, *FEMA-352,* prepared by the SAC Joint Venture for the Federal Emergency Management Agency, Washington, DC.

Filippou, F.C. (1995). Nonlinear static and dynamic analysis of a 17-story building with FEAP-STRUC, in *SAC 95-04*, SAC Joint Venture, Sacramento, California.

Hou, Z., Noori, M., and R. St. Amand (2000). Wavelet-based approach for structural damage detection, *Journal of Engineering Mechanics*, 126(7), 677-683.

Huang, M.J. and A.F. Shakal (1995). CSMIP instrumentation and records from the I10/215 interchange, *Earthquake Spectra*, 11(2), 193-215.

Huang, M.J., Malhotra, P.K., and A.F. Shakal (1996). Strong-motion records from buildings damaged in earthquakes, *Proceedings, SMIP96 Seminar on Seismological and Engineering Implications of Recent Strong-Motion Data, Sacramento*, California Strong Motion Instrumentation Program, Sacramento, California, 99-116.

Huang, M.J., Malhotra, P.K., and A.F. Shakal (1998). Strong motion records from steel buildings damaged in the 1994 Northridge earthquake, *Proceedings, 6th U.S. National Conference on Earthquake Engineering, Seattle, Washington*, Earthquake Engineering Research Institute, Oakland, California.

Jennings, P. (1997). Use of strong-motion data in earthquake-resistant design, *Proceedings, SMIP97 Seminar on Seismological and Engineering Implications of Recent Strong-Motion Data, Sacramento*, California Strong Motion Instrumentation Program, Sacramento, California.

Kasai, K., Liu, W.D., and V. Jeng (1992). Effect of relative displacements between adjacent bridge segments, *Proceedings, SMIP92 Seminar on Seismological and Engineering Implications of Recent Strong-Motion Data*, California Strong Motion Instrumentation Program, Sacramento, California.

Kunnath, S.K., Nghiem, Q., and S. El-Tawil (2004). Modeling and response prediction in performance-based seismic evaluation: case studies of instrumented steel moment-framed buildings, *Earthquake Spectra*, 20(3), 883-915.

Lobo, R.F., Skokan J. M., Huang, S.C., and G.C. Hart (1998). Three dimensional nonlinear analysis of a 13-story steel building with weld connection damage, *Proceedings, Fourth Conference on Tall Buildings in Seismic Regions*, Los Angeles Tall Buildings Structural Design Council, Los Angeles, California.

Maison, B.F., and K. Kasai (1997). Analysis of Northridge damaged thirteen-story WSMF building, *Earthquake Spectra*, 13(3), 451-473.

Malhotra, P.K., Huang, M.J., and A.F. Shakal (1994). Interaction at separation joints of the I10/215 bridge during earthquakes, *Proceedings, SMIP94 Seminar on Seismological and Engineering Implications of Recent Strong-Motion Data, Los Angeles*, California Strong Motion Instrumentation Program, Sacramento, California, 49-59.

Marwala, T. (2000). Damage identification using committee of neural networks, *Journal of Engineering Mechanics*, 126(1), 43-50.

Naeim, F., DiJulio, R., Benuska, K., Reinhorn, A. and C. Li (1995). Evaluation of seismic performance of an 11-story steel moment frame building during the 1994 Northridge earthquake, in *SAC 95-04*, SAC Joint Venture, Sacramento, California.

Naeim F., Lobo, R.M., Skliros, K., and M. Sgambelluri (1999). Seismic performance of four instrumented steel moment resisting buildings during the January 17, 1994 Northridge earthquake, *Proceedings, SMIP98 Seminar on Utilization of Strong Motion Data, Oakland*, California Strong Motion Instrumentation Program, Sacramento, California.

Nagarajaiah, S. and X. Sun (2001). Base isolated FCC building: impact response in Northridge earthquake, *Journal of Structural Engineering*, 127(9), 1063-1076.

Paret, T.F., and K.K. Sasaki (1995). Analysis of a 17-story steel moment frame building damaged by the Northridge earthquake, in *SAC 95-04*, SAC Joint Venture, Sacramento, California.

Porcella, R.L., Etheredge, E.C., Maley, R.P., and A.V. Acosta (1994). Accelerograms recorded at USGS national strong motion network stations during the Ms=6.6 Northridge, California earthquake of January 17, 1994, *Open File Report 94-141*, U.S. Geological Survey, Menlo Park, California.

Revadigar, S., and S.T. Mau (1999). Automated multicriterion building damage assessment from seismic data, *Journal of Structural Engineering*, 125(2), 211-217.

Rodgers, J.E. and S.A. Mahin (2005). Transient dynamic response caused by connection fracture in steel moment frames, in preparation for submission to Earthquake Engineering and Structural Dynamics.

Rodgers, J.E., and S.A. Mahin (2004). Effects of connection hysteretic degradation on the seismic behavior of steel moment resisting frames, *Report No. PEER-2003/13*, Pacific Earthquake Engineering Research Center, Richmond, California.

Rojahn, C. and P. Mork (1982). An analysis of strong-motion data from a severely damaged structure – the Imperial County Services Building, El Centro, California, *Professional Paper 1254*, Geological Survey, U.S. Department of Interior, 357-375.

SAC (1995a). Technical report: analytical and field investigations of buildings affected by the Northridge earthquake of January 17, 1994, *Report No. SAC 95-04*, SAC Joint Venture, Sacramento, California.

SAC (1995b). Technical report: surveys and assessment of damage to buildings affected by the Northridge earthquake of January 17, 1994, *Report No. SAC 95-06*, SAC Joint Venture, Sacramento, California.

Sanli, A.K. and M. Celebi (2002). Earthquake damage detection of a thirteen story building using recorded responses, *Proceedings, 3rd International Workshop on Structural Health Monitoring*, Stanford University, Stanford, California.

Shakal, A.F., Huang, M.J., Darragh, R., Cao, T., Sherburne, R., Malhotra, P., Cramer, C., Sydnor, R., Graizer, V., Maldonado, G., Petersen, C. and J. Wampole (1994). CSMIP strong-motion records from the Northridge, California earthquake of 17 January 1994, *Report No. OSMS 94-07*, California Strong Motion Instrumentation Program, Sacramento, California.

Shakal, A.F., Huang, M.J., and V. Graizer (2004). CSMIP strong-motion data processing, *Proceedings, COSMOS Invited Workshop on Record Processing Guidelines*, Consortium of Organizations for Strong Motion Observation Systems, Richmond, California.

Stephens, C.D. and D.M. Boore (2004). ANSS/NSMP strong-motion record processing and procedures, *Proceedings, COSMOS Invited Workshop on Record Processing Guidelines*, Consortium of Organizations for Strong Motion Observation Systems, Richmond, California.

The MathWorks, Inc. (2002). MATLAB Version 6.5, computer program, available from The MathWorks, Inc., Natick, Massachussetts.

Tsai, Chung and Wang, 11ECEE

Uang, C.M., Yu, Q.S., Sadre, A., Bonowitz, D., and N. Youssef (1995). Performance of a 13-story steel moment-resisting frame damaged in the 1994 Northridge earthquake, in *SAC 95-04,* SAC Joint Venture, Sacramento, California.

Walker, J.S. (1999). *A primer on wavelets and their scientific applications*, Chapman & Hall/ CRC, Boca Raton, Florida.

Appendix A – Acceleration Time Histories for 1994 Northridge earthquake main shock

Set 1

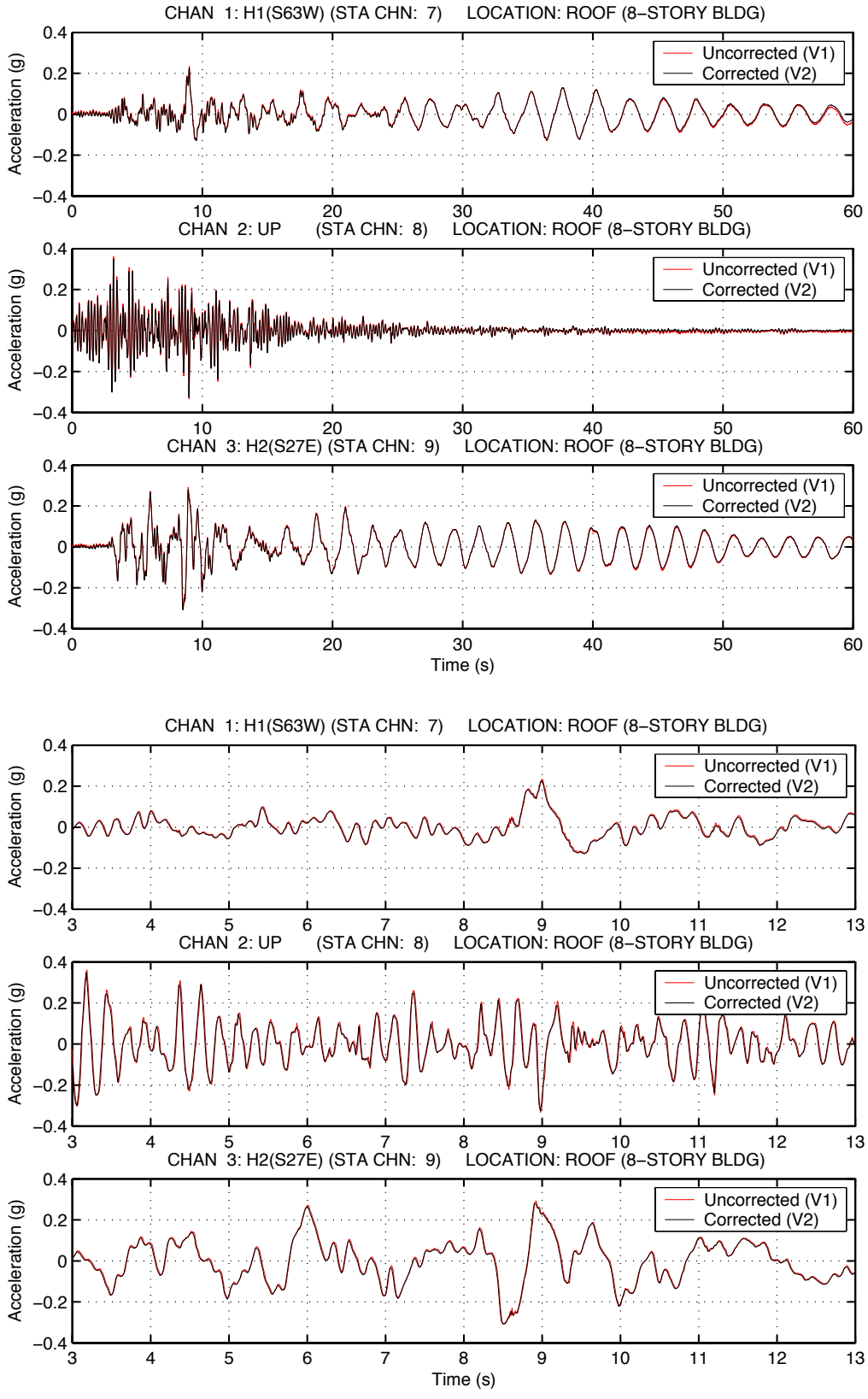

Figure A - 1. Corrected and uncorrected roof acceleration, North Hollywood – Lankershim #2, full record (top) and close-up of transients (bottom)

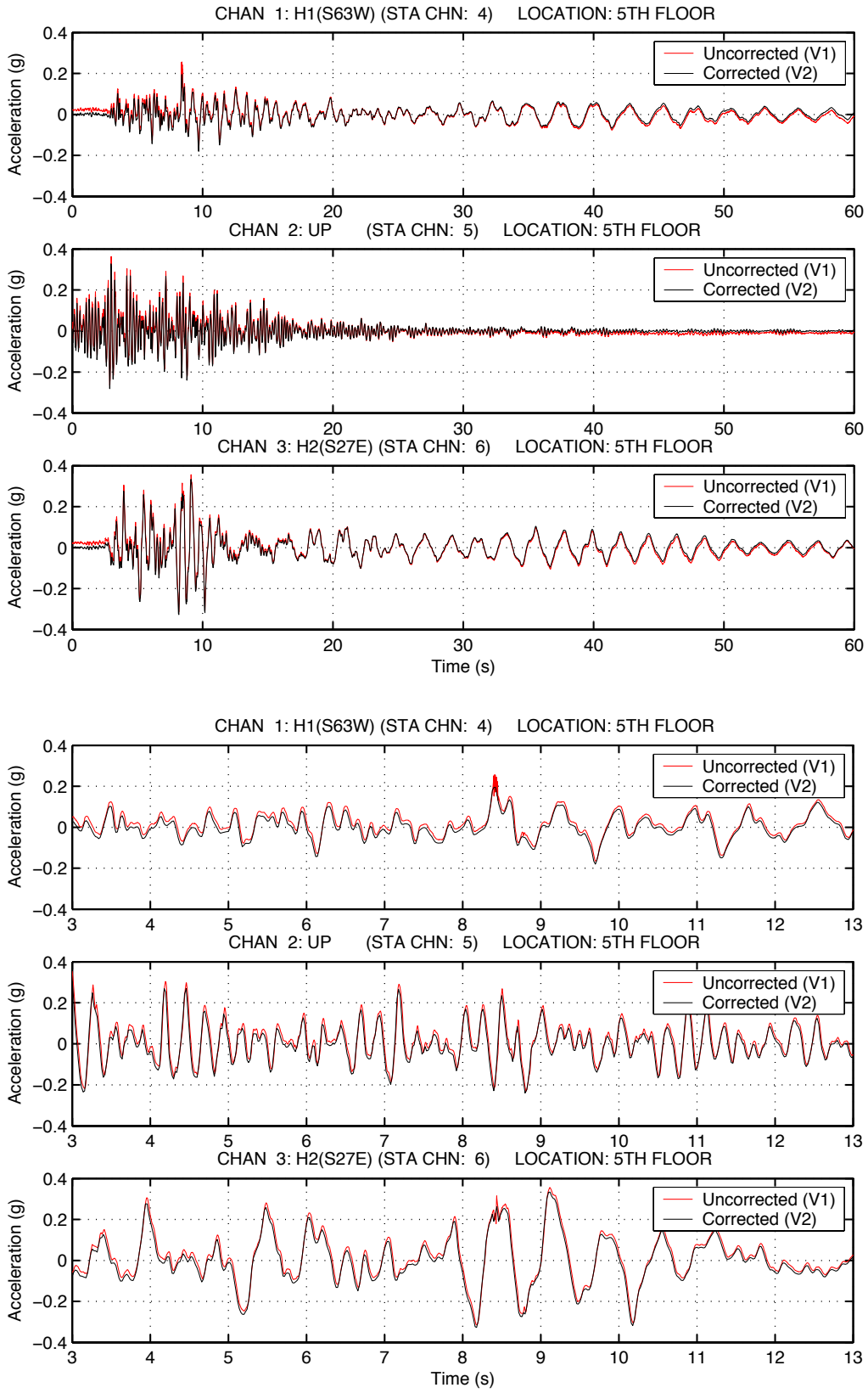

Figure A - 2. Corrected and uncorrected mid-height acceleration, North Hollywood – Lankershim #2, full record (top) and close-up of transients (bottom)

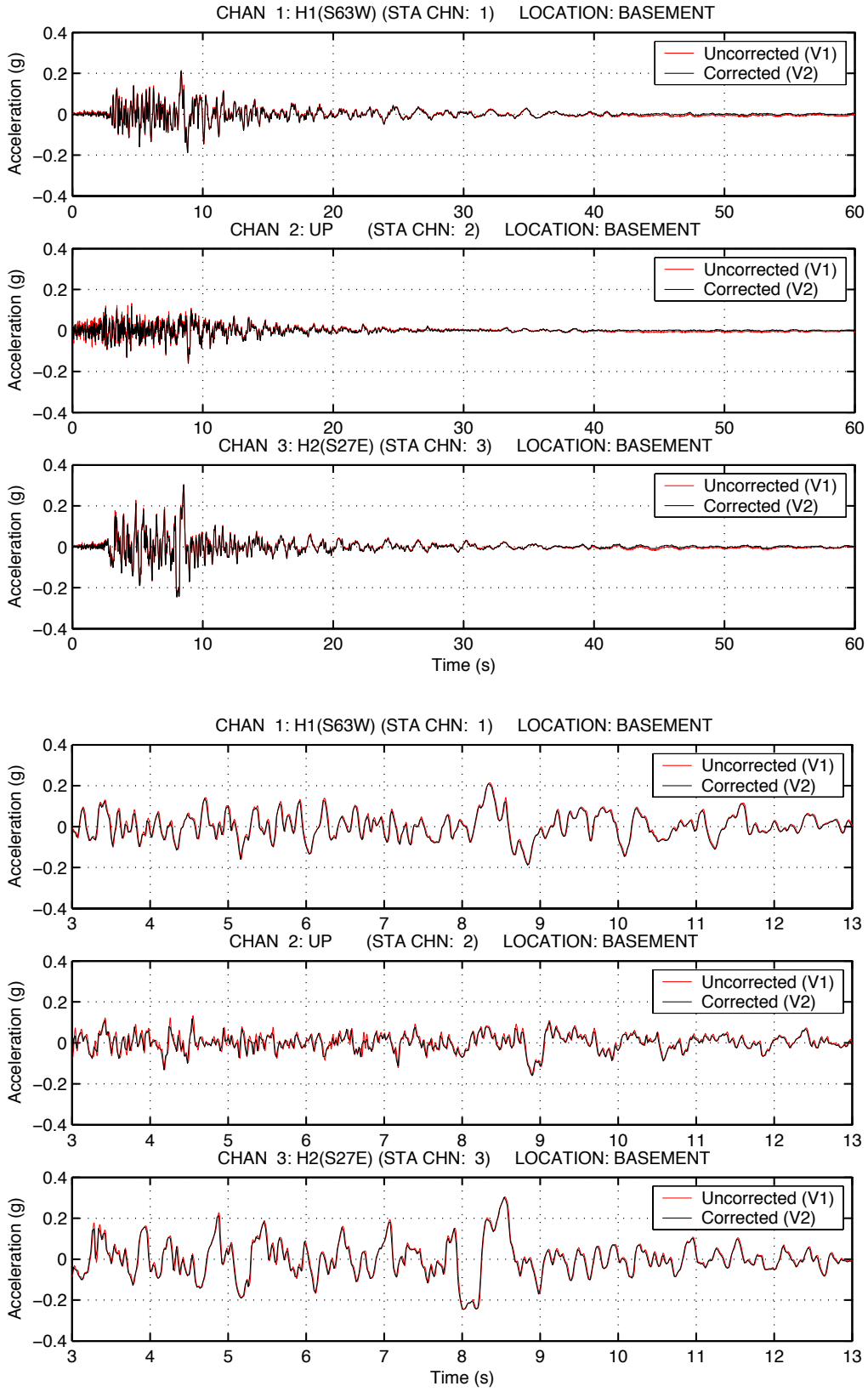

Figure A - 3. Corrected and uncorrected base acceleration, North Hollywood – Lankershim #2, full record (top) and close-up of transients (bottom)

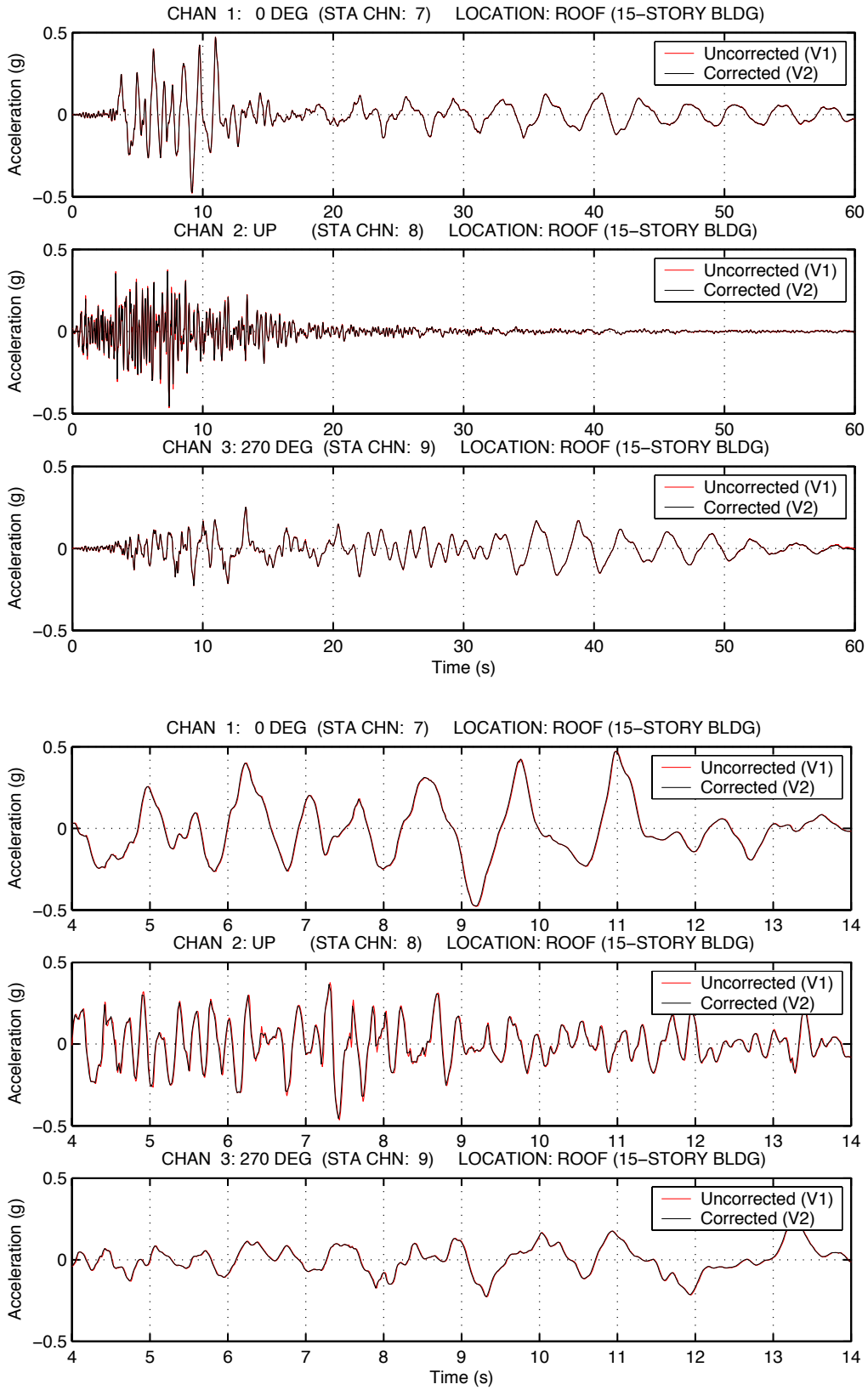

Figure A - 4. Corrected and uncorrected roof acceleration, Sherman Oaks – Ventura #6, full record (top) and close-up of transients (bottom)

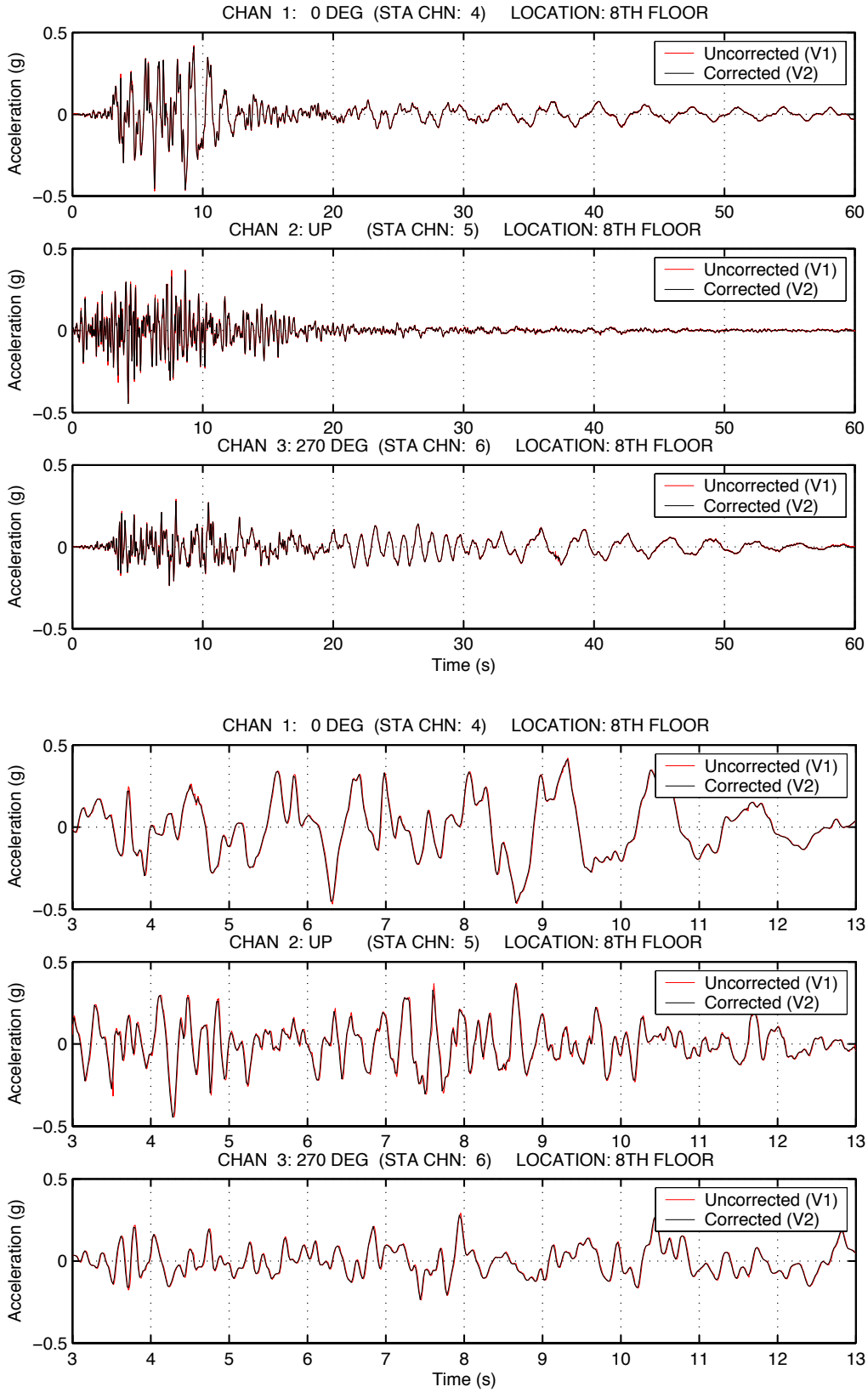

Figure A - 5. Corrected and uncorrected mid-height acceleration, Sherman Oaks – Ventura #6, full record (top) and close-up of transients (bottom)

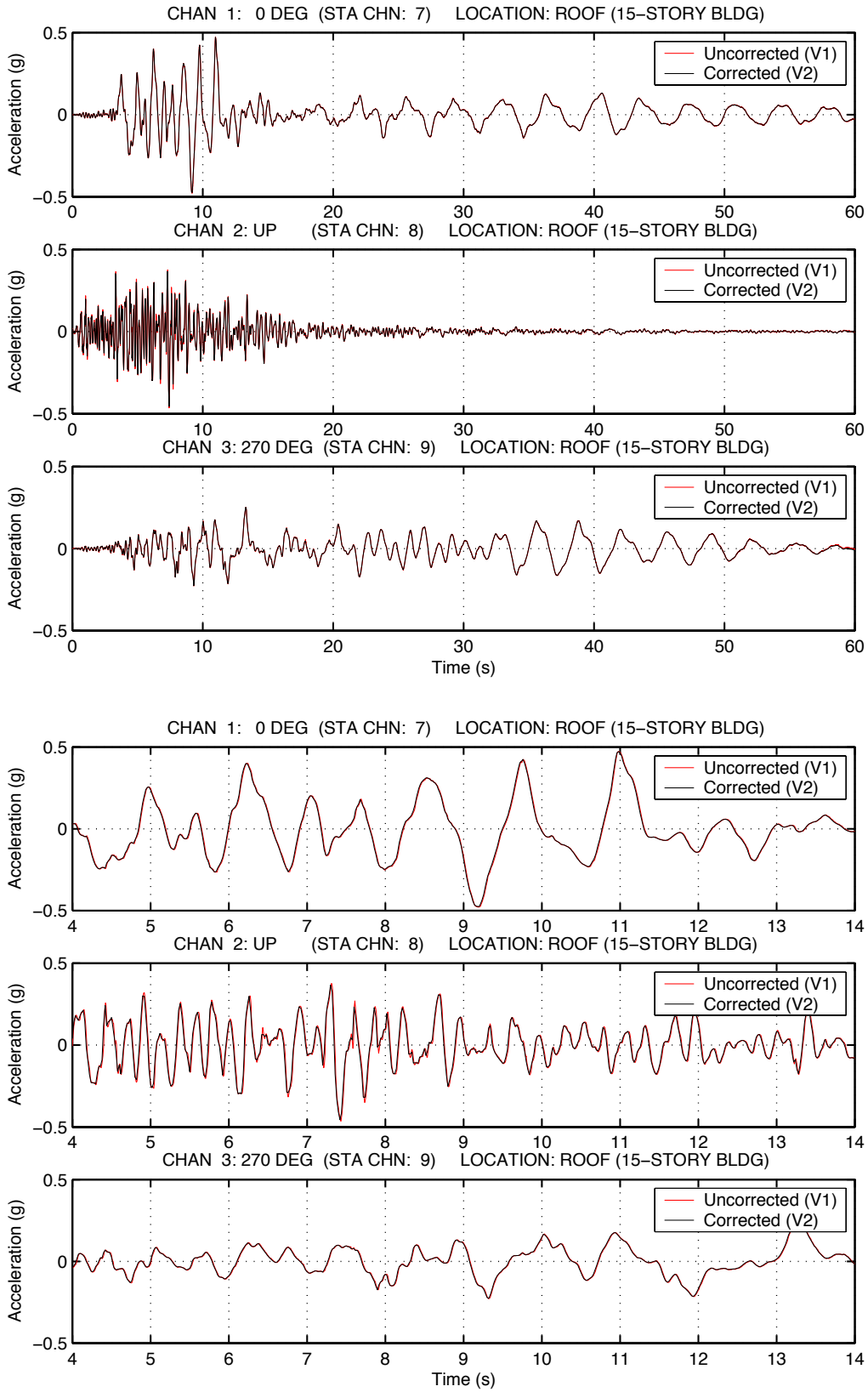

Figure A - 6. Corrected and uncorrected base acceleration, Sherman Oaks – Ventura #6, full record (top) and close-up of transients (bottom)

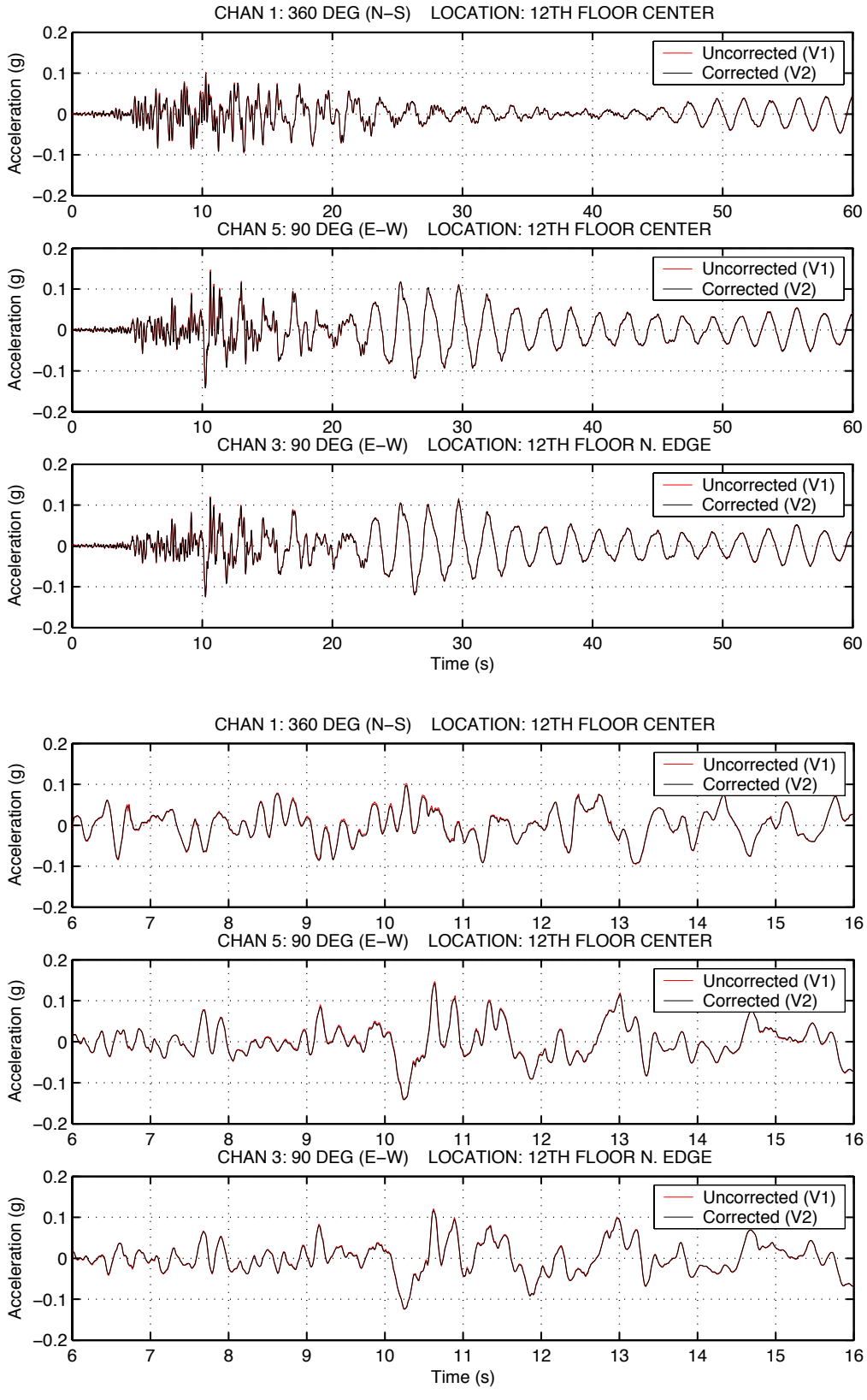

Figure A - 7. Corrected and uncorrected 12th floor acceleration, Alhambra – Office Building #1, full record (top) and close-up of transients (bottom)

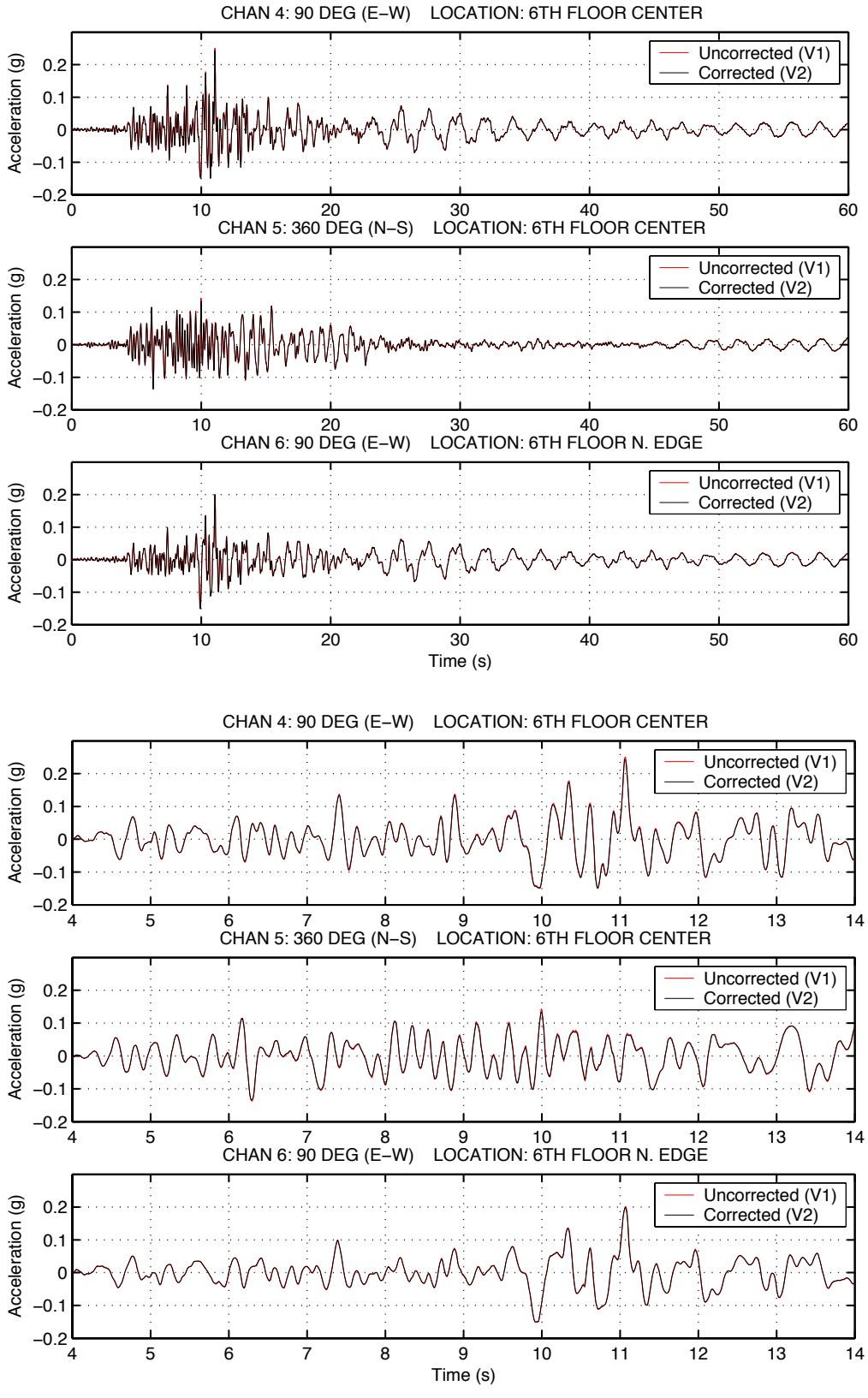

Figure A - 8. Corrected and uncorrected 6th floor acceleration, Alhambra – Office Building #1, full record (top) and close-up of transients (bottom)

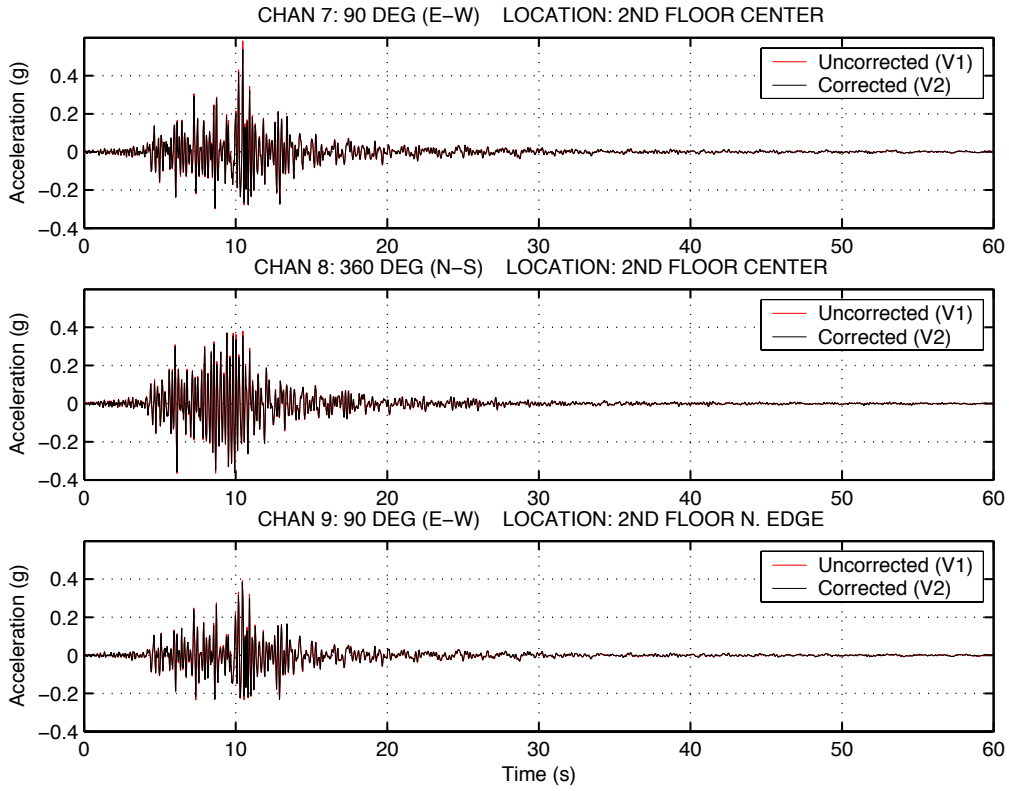

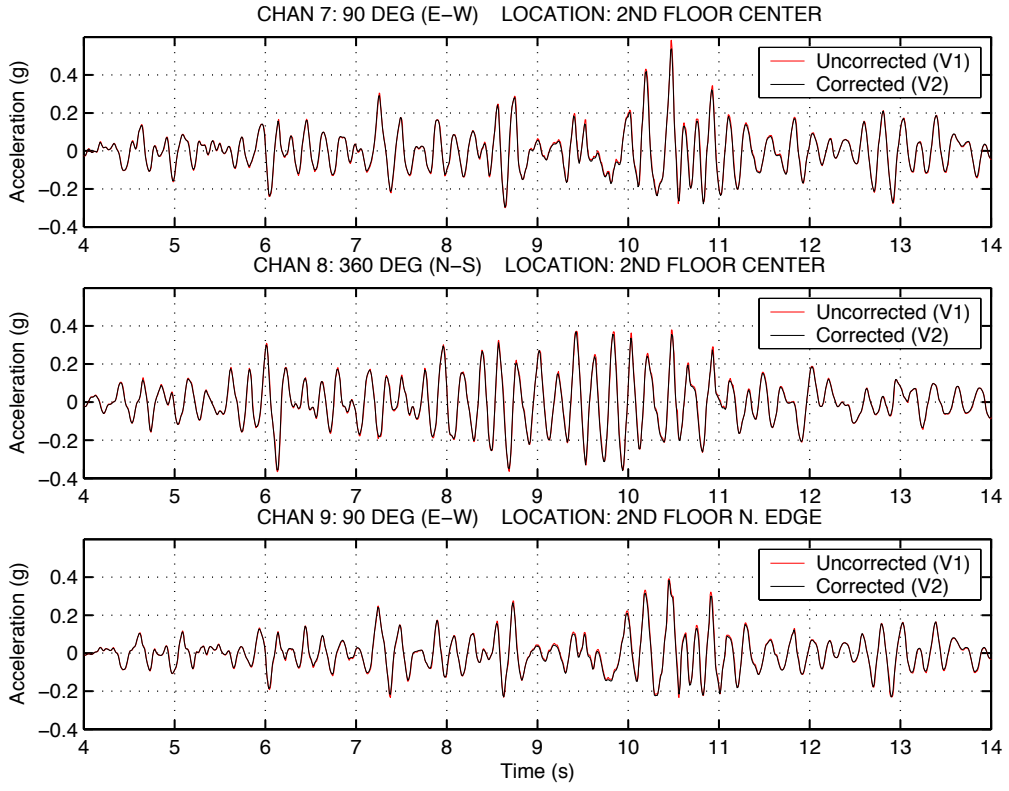

Figure A - 9. Corrected and uncorrected 2nd floor acceleration, Alhambra – Office Building #1, full record (top) and close-up of transients (bottom)

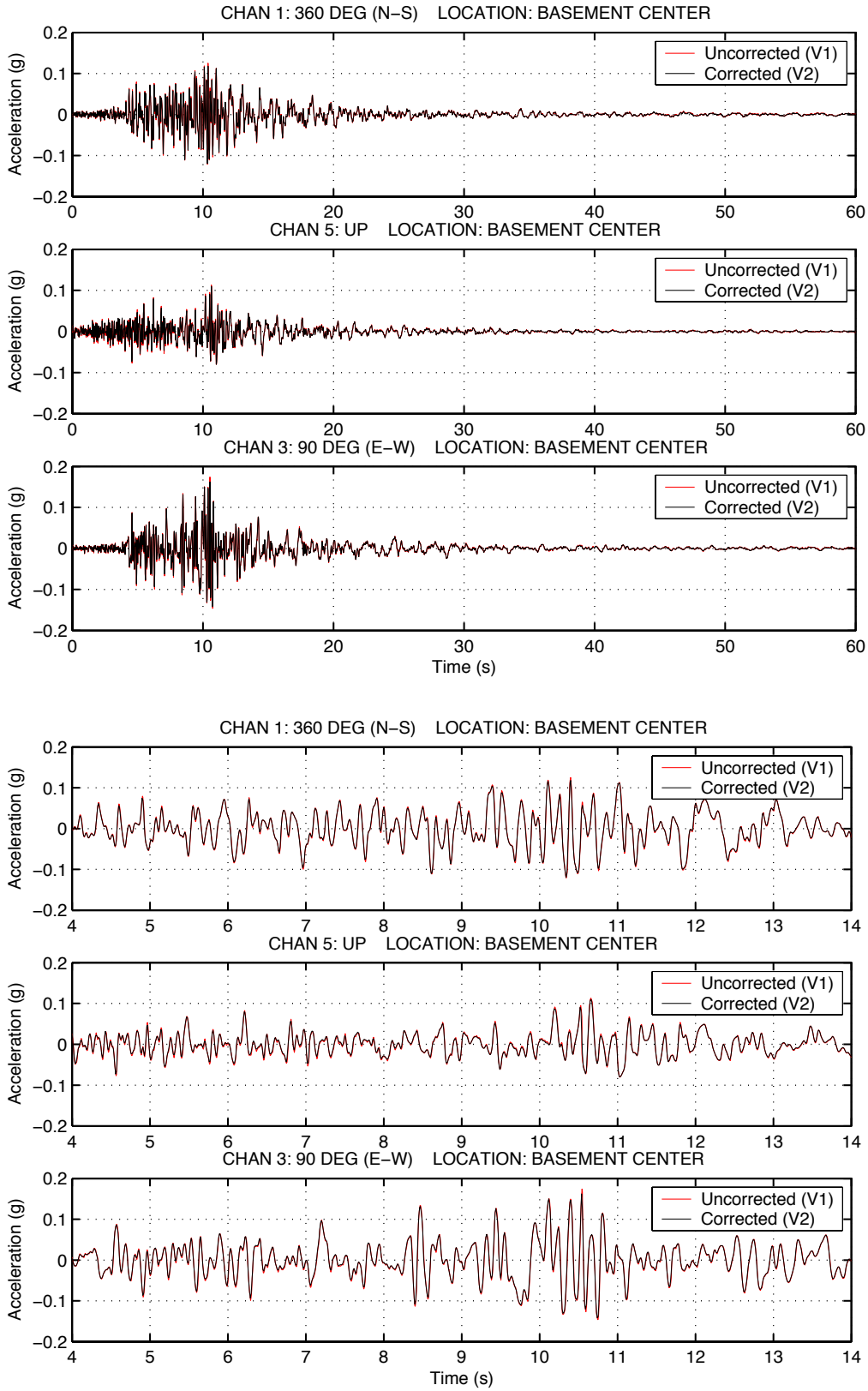

Figure A - 10. Corrected and uncorrected basement acceleration, Alhambra – Office Building #1, full record (top) and close-up of transients (bottom)

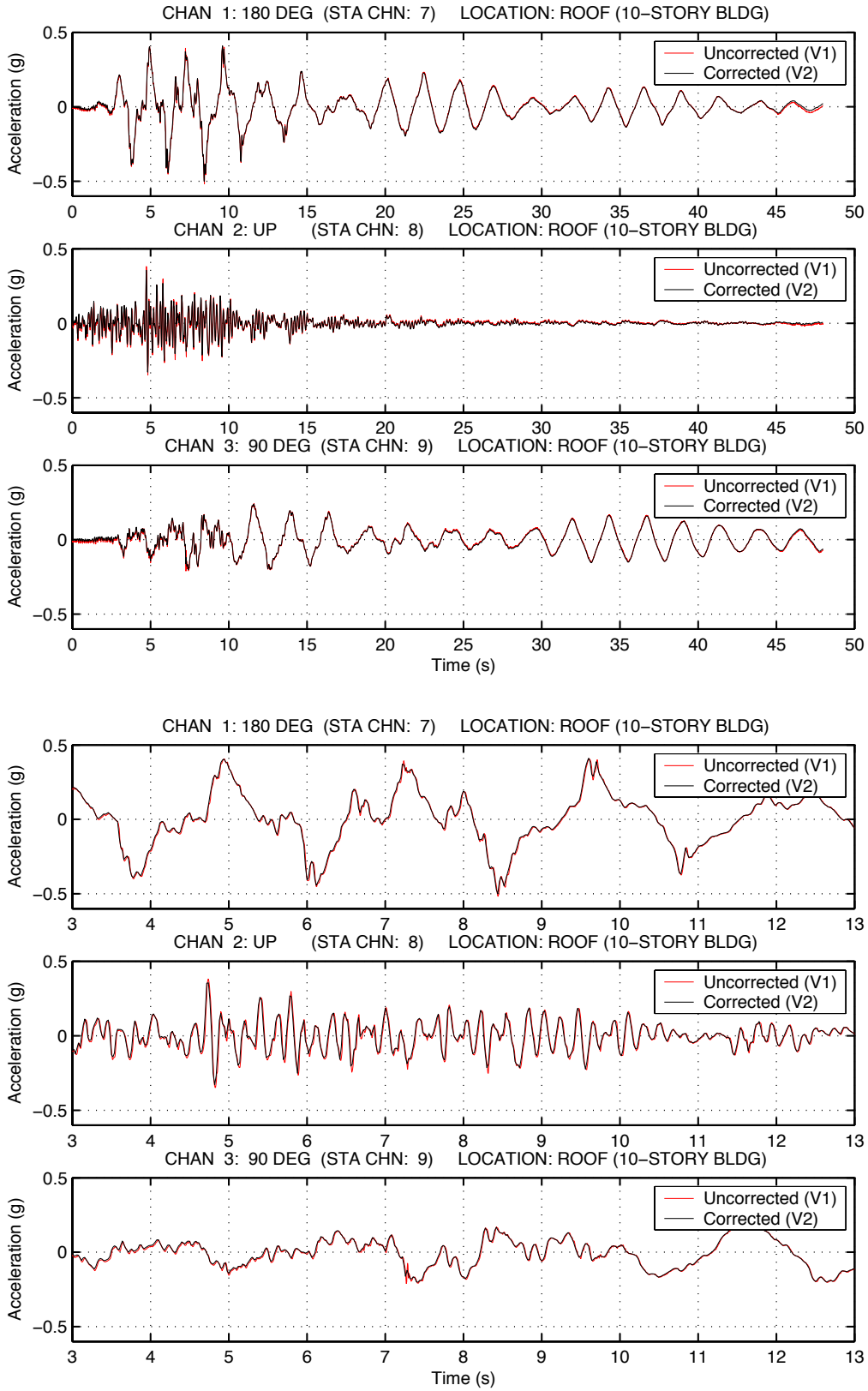

Figure A - 11. Corrected and uncorrected roof acceleration, Tarzana – Ventura #10, full record (top) and close-up of transients (bottom)

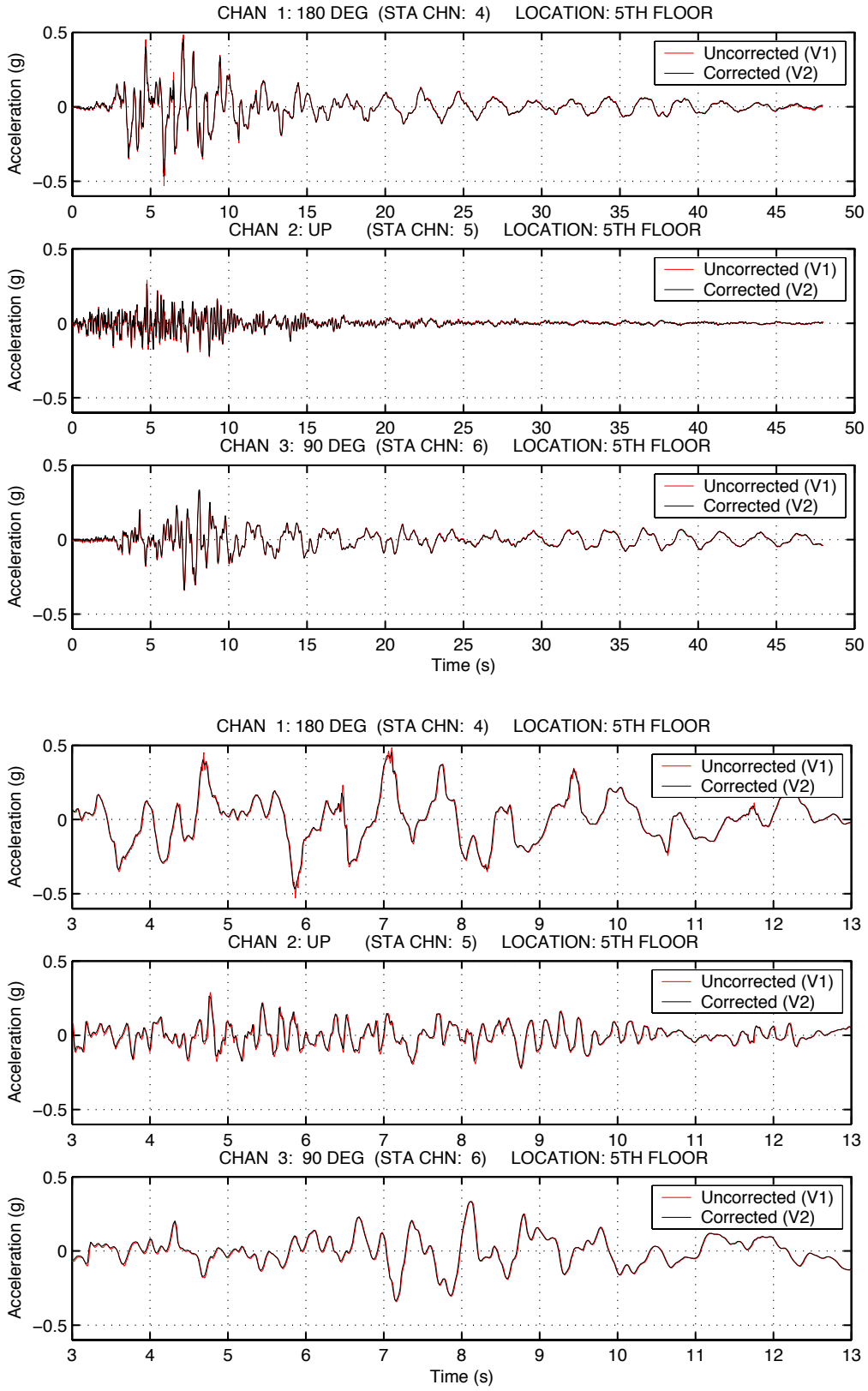

Figure A - 12. Corrected and uncorrected mid-height acceleration, Tarzana – Ventura #10, full record (top) and close-up of transients (bottom)

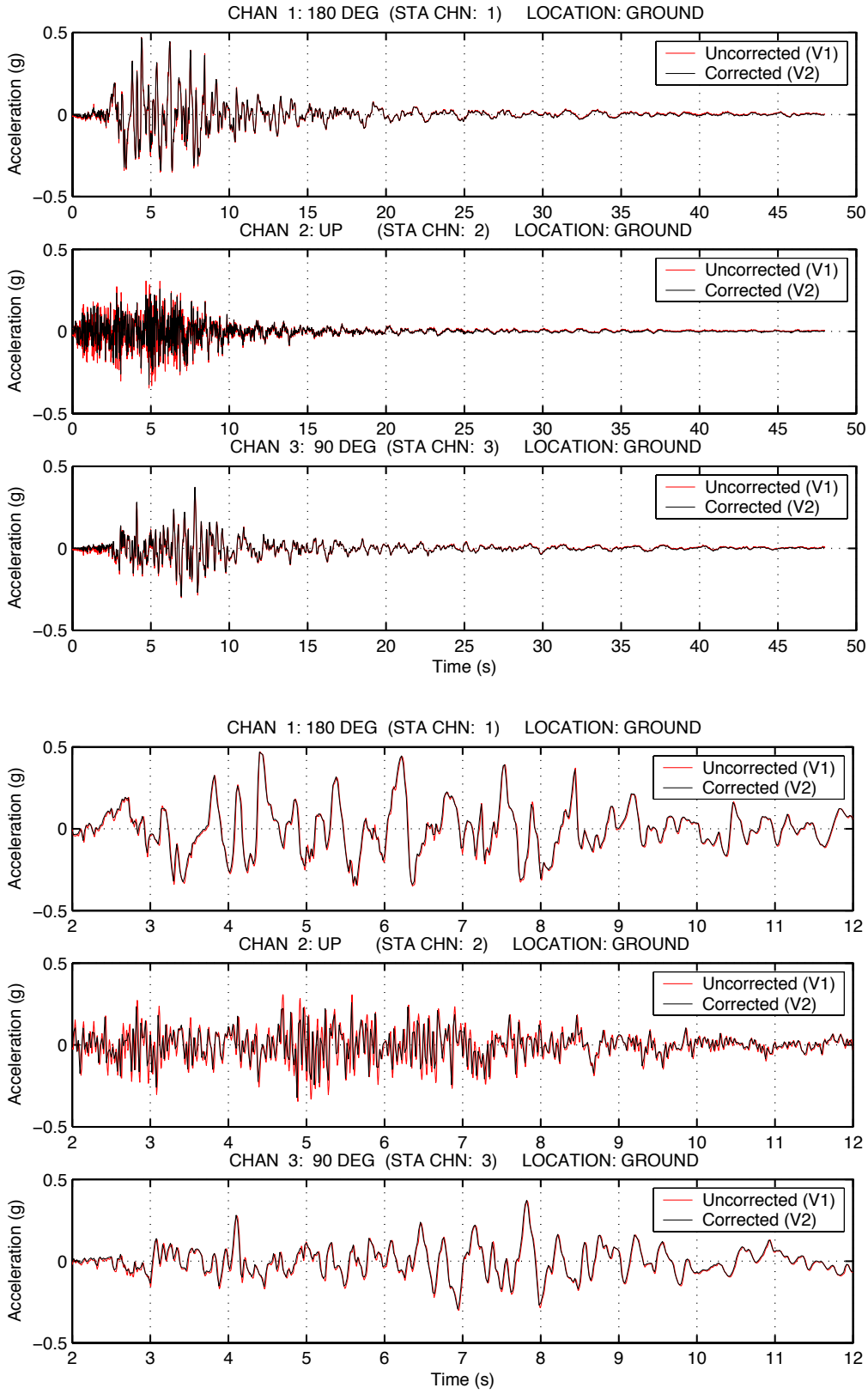

Figure A - 13. Corrected and uncorrected base acceleration, Tarzana – Ventura #10, full record (top) and close-up of transients (bottom)

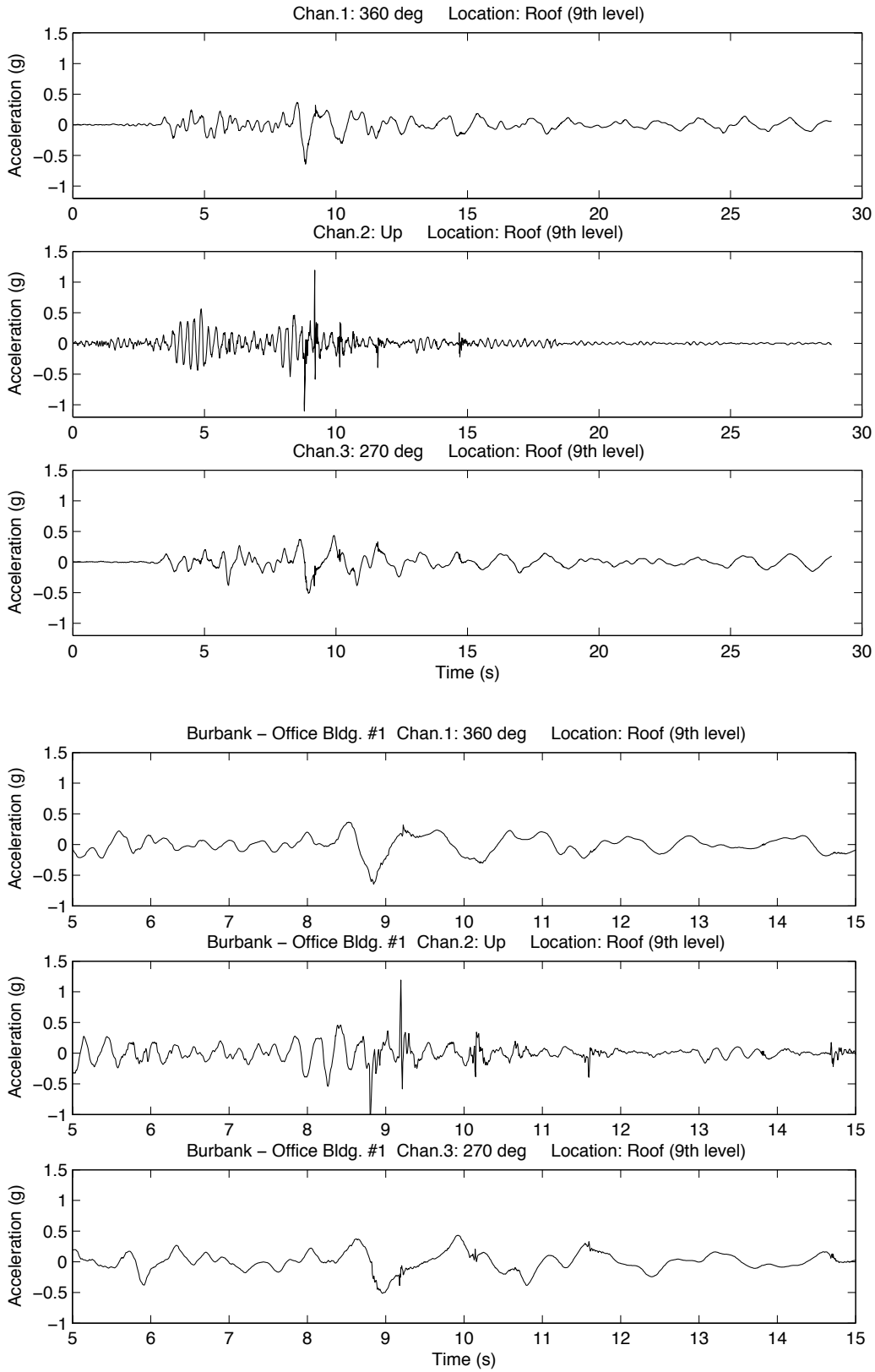

Figure A - 14. Corrected and uncorrected acceleration, Burbank – Office Building #1, full record (top) and close-up of transients (bottom)

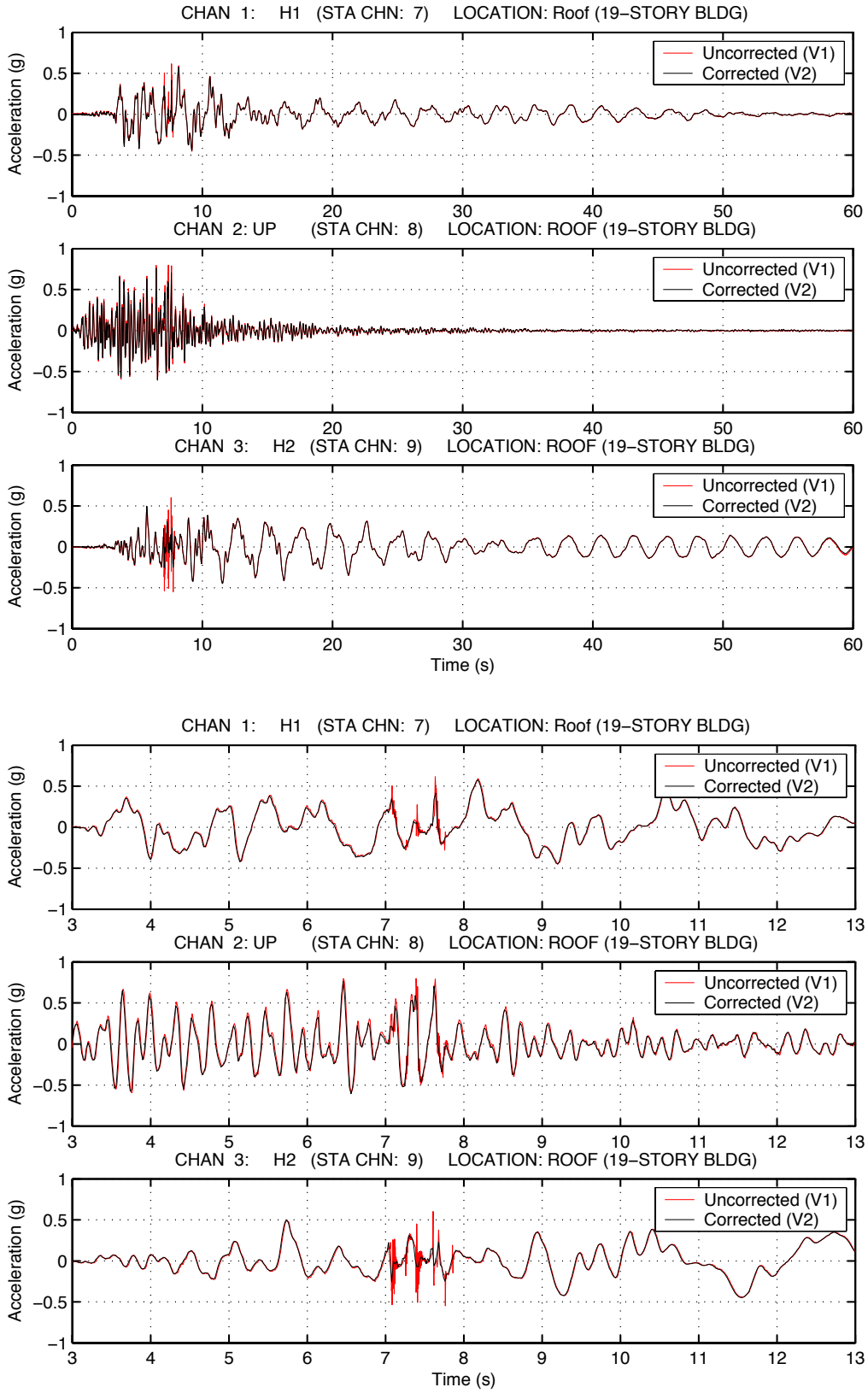

Figure A - 15. Corrected and uncorrected roof acceleration, Encino – Ventura #12, full record (top) and close-up of transients (bottom)

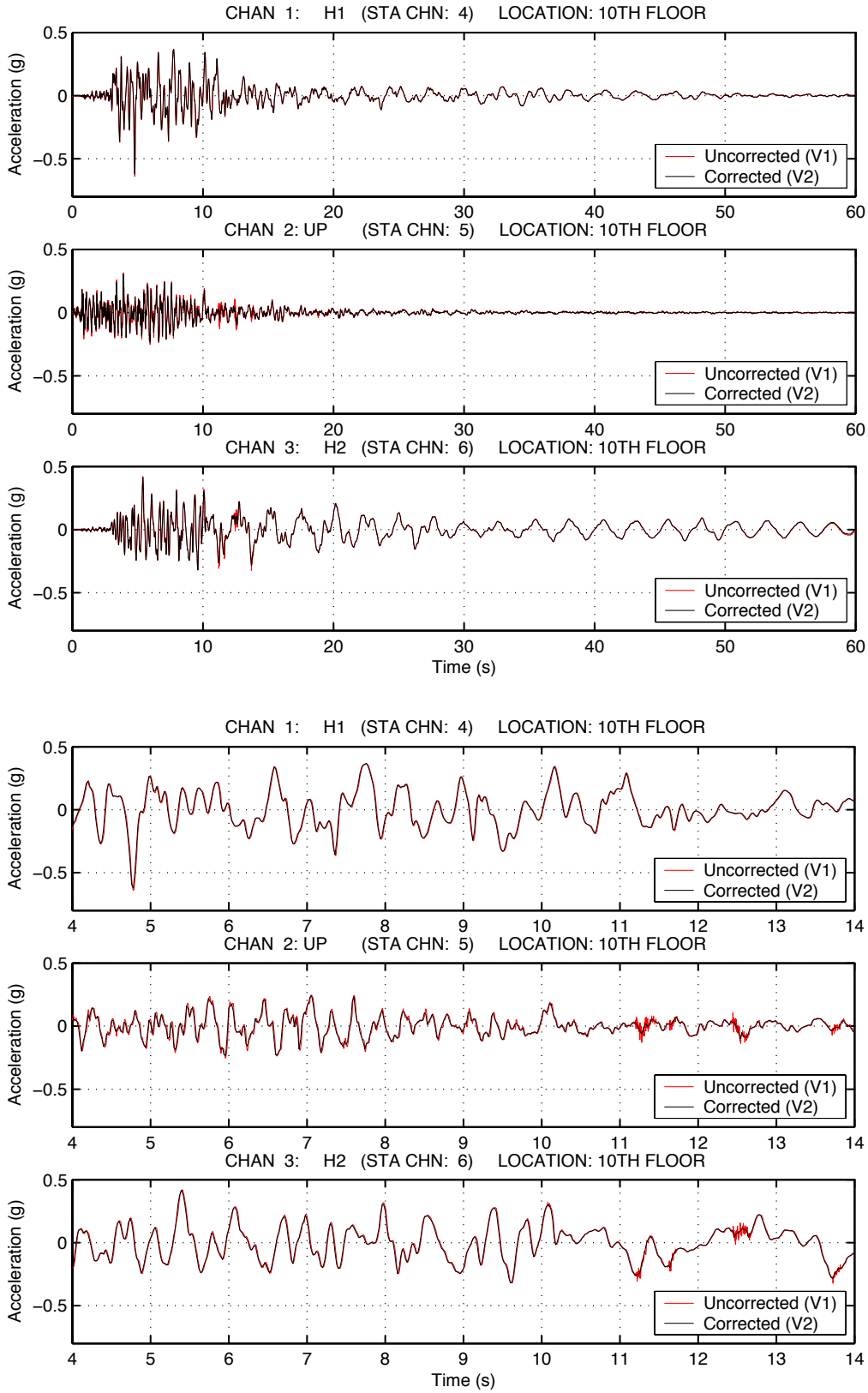

Figure A - 16. Corrected and uncorrected mid-height acceleration, Encino – Ventura #12, full record (top) and close-up of transients (bottom)

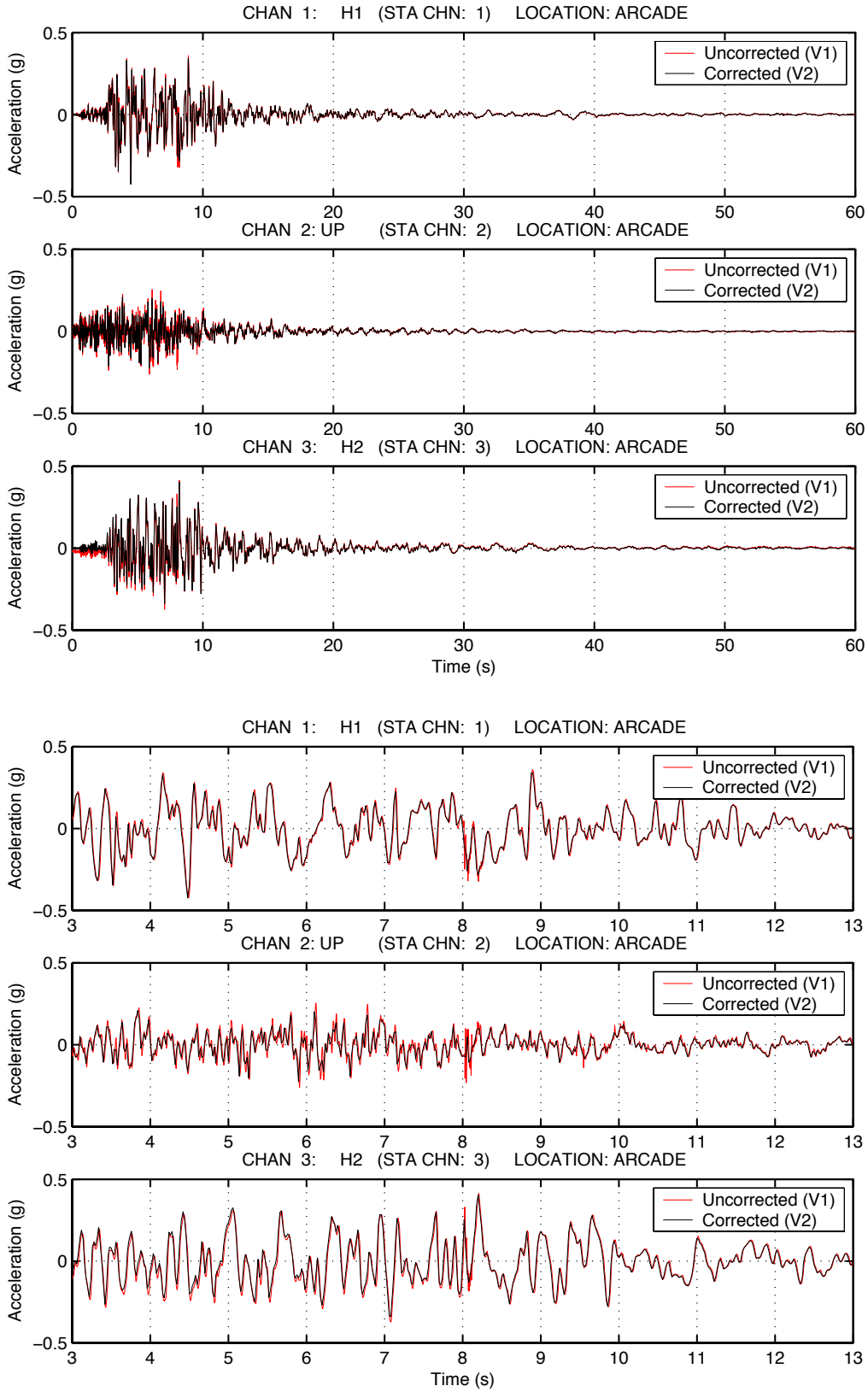

Figure A - 17. Corrected and uncorrected base acceleration, Encino – Ventura #12, full record (top) and close-up of transients (bottom)

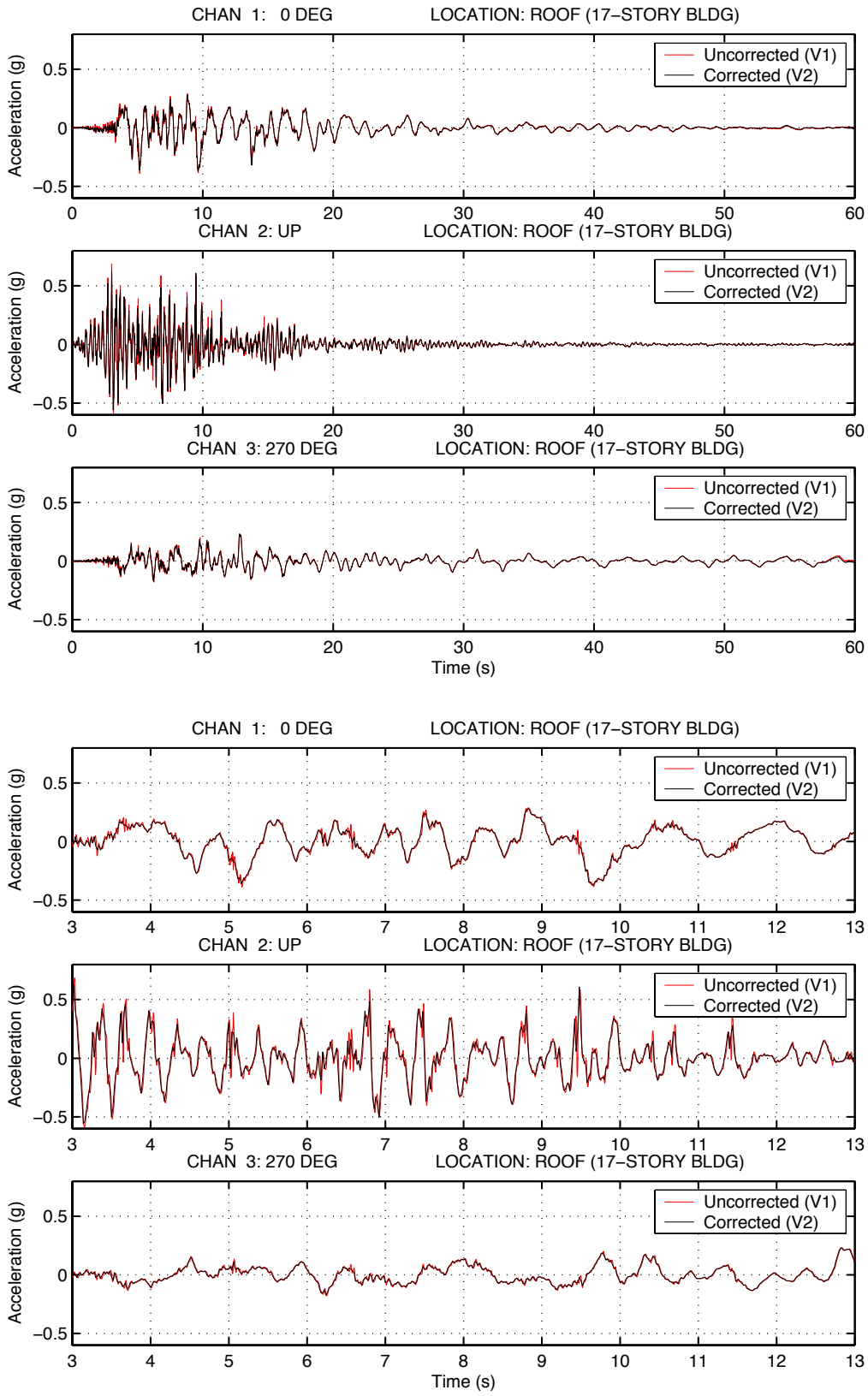

Figure A - 18. Corrected and uncorrected acceleration, Woodland Hills – Canoga #1, full record (top) and close-up of transients (bottom)

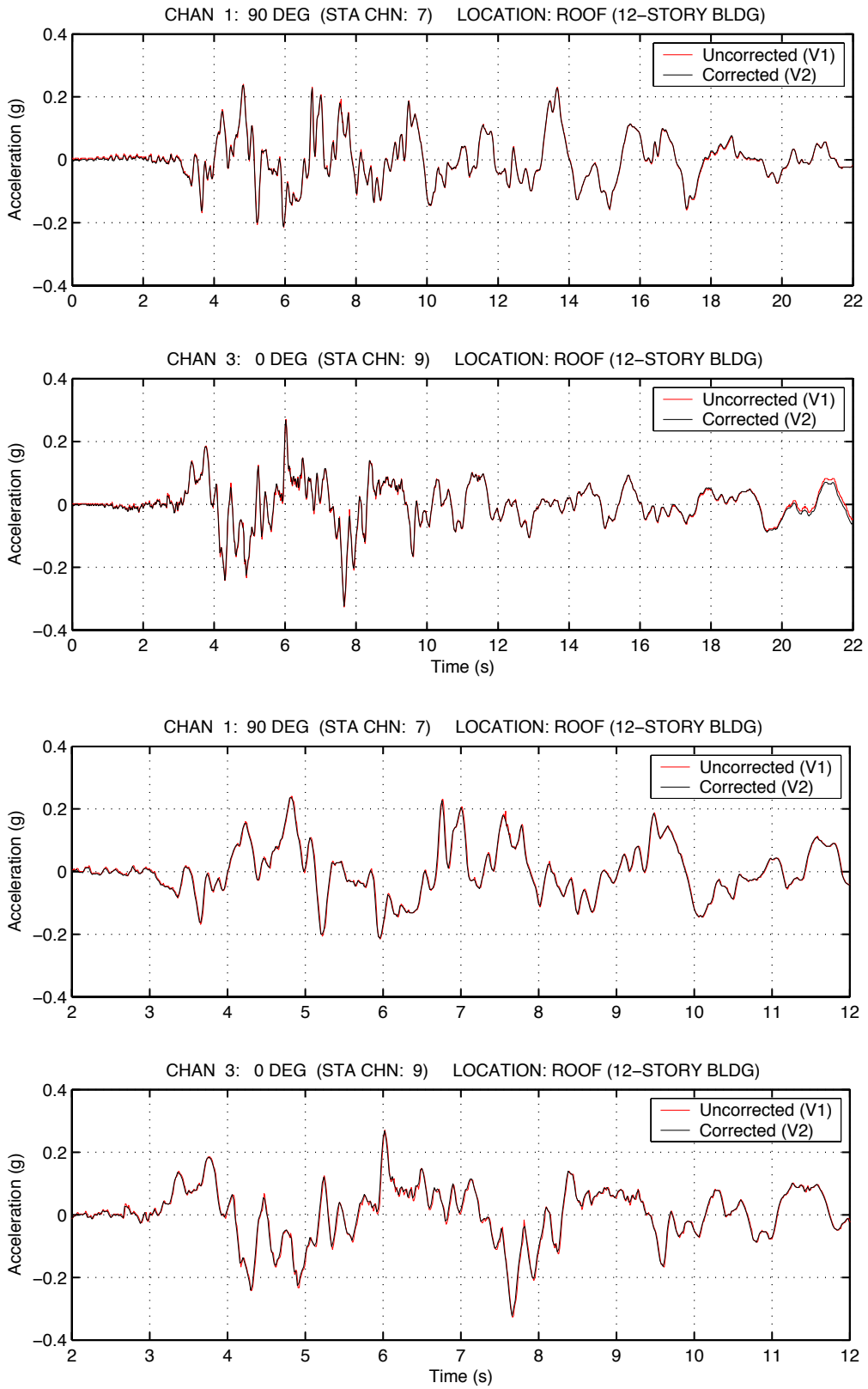

Figure A - 19. Corrected and uncorrected roof acceleration, Woodland Hills – Oxnard #4, full record (top) and close-up of transients (bottom)

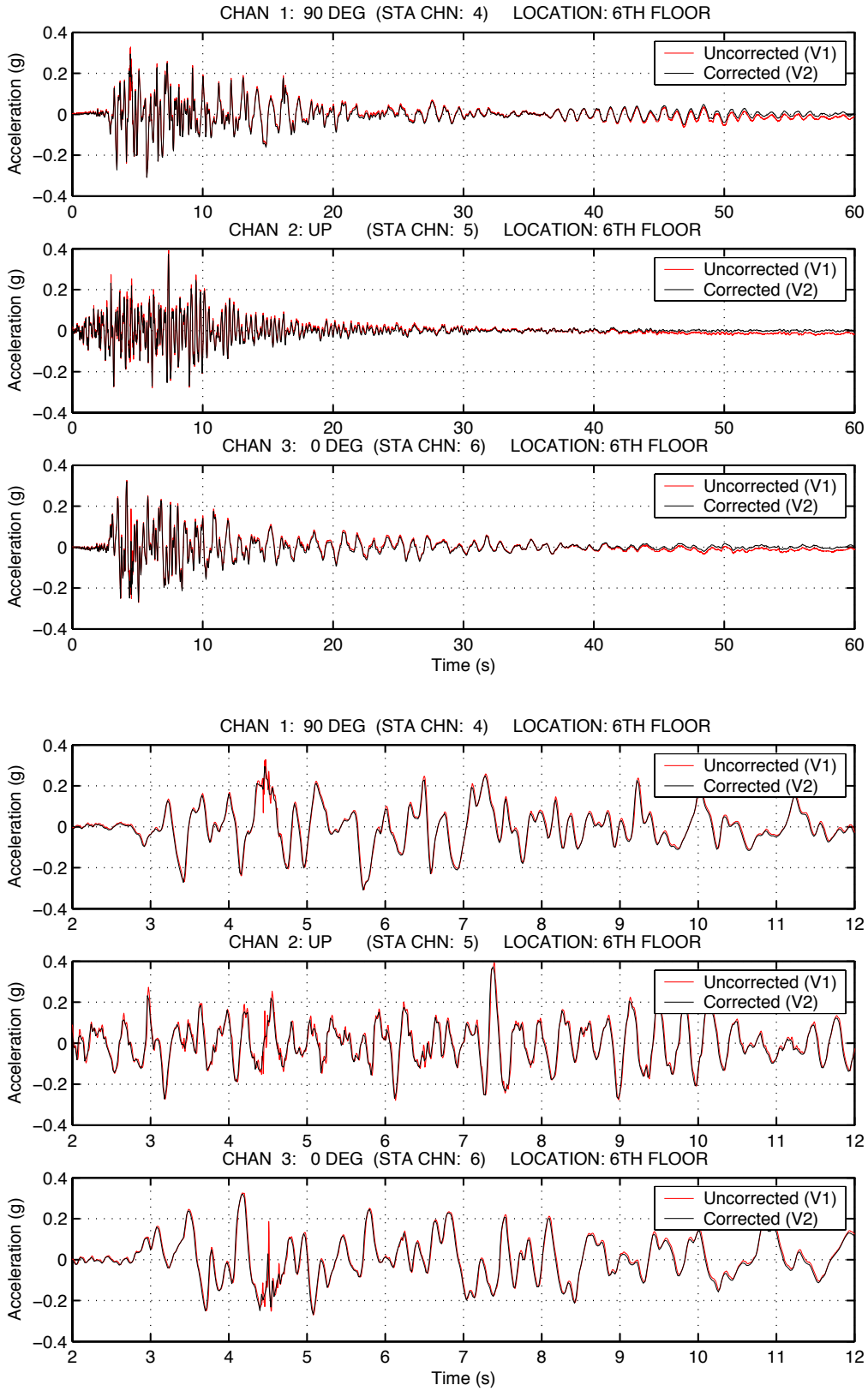

Figure A - 20. Corrected and uncorrected mid-height acceleration, Woodland Hills – Oxnard #4, full record (top) and close-up of transients (bottom)

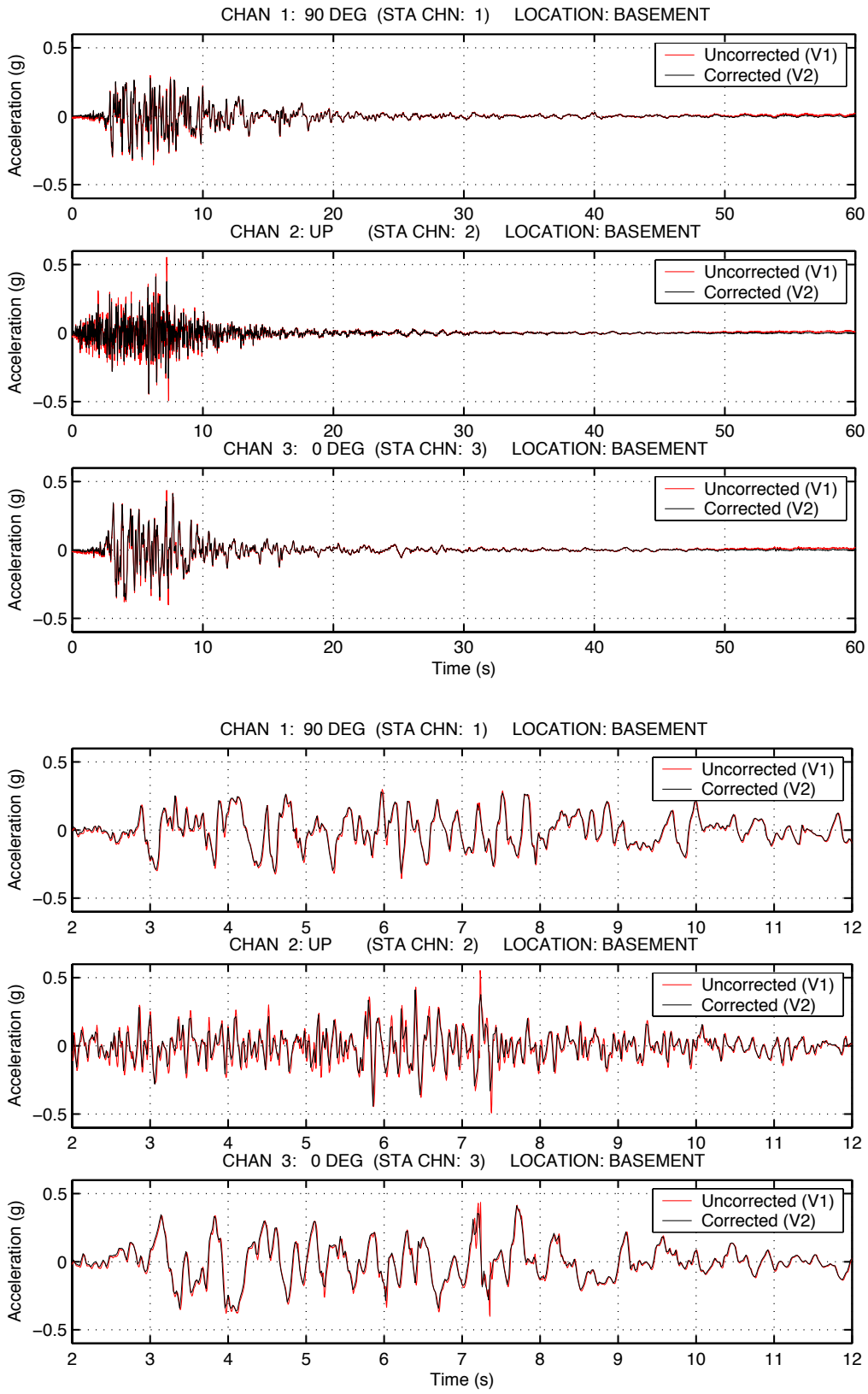

Figure A - 21. Corrected and uncorrected base acceleration, Woodland Hills – Oxnard #4, full record (top) and close-up of transients (bottom)

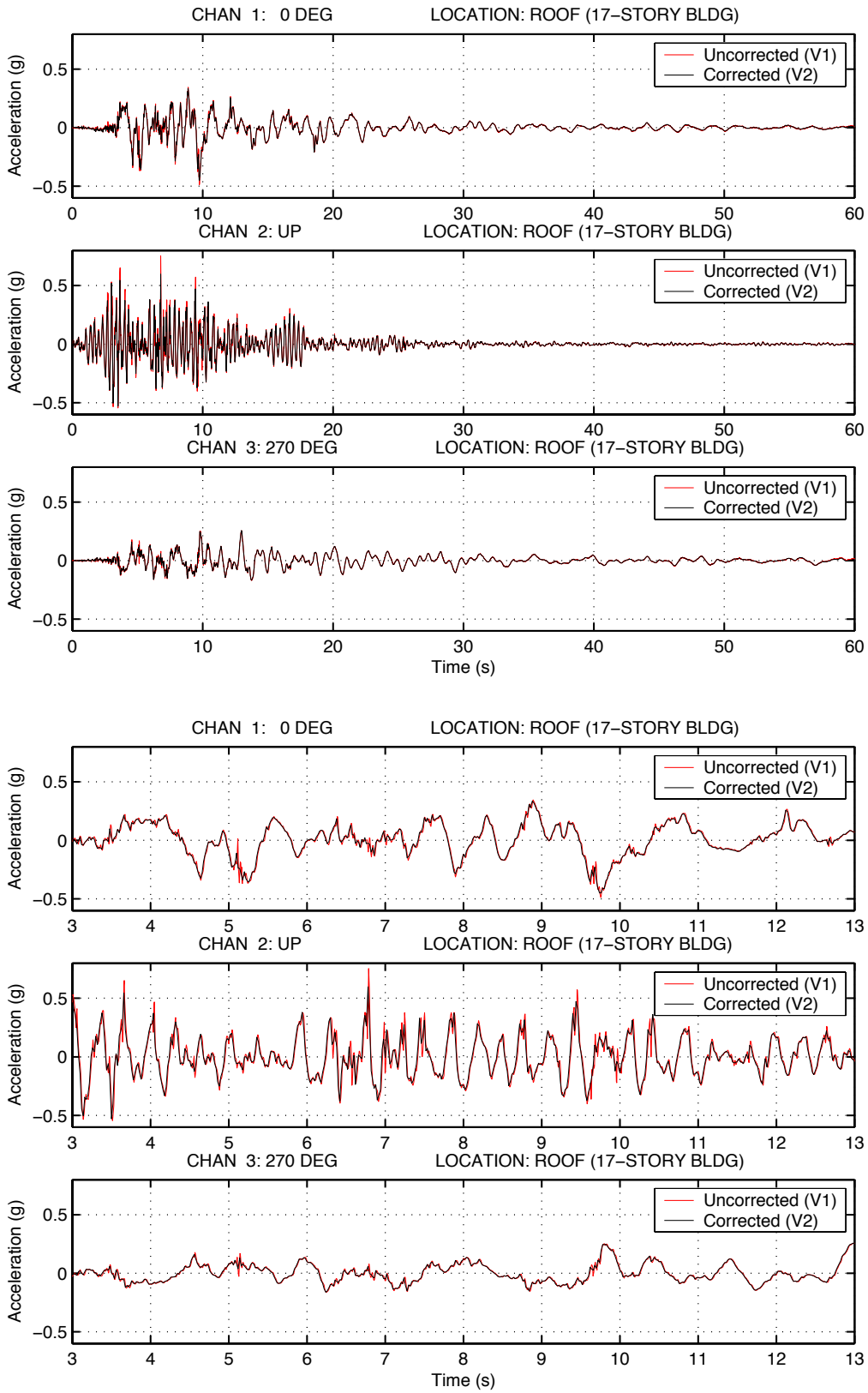

Figure A - 22. Corrected and uncorrected acceleration, Woodland Hills – Canoga #2, full record (top) and close-up of transients (bottom)

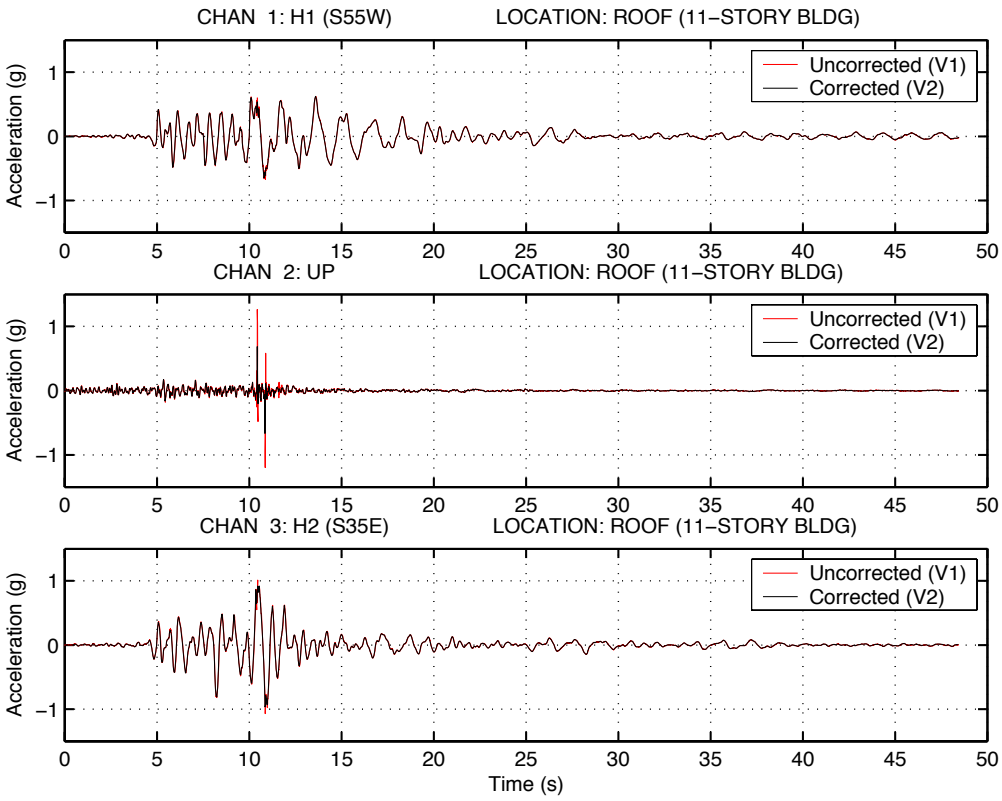

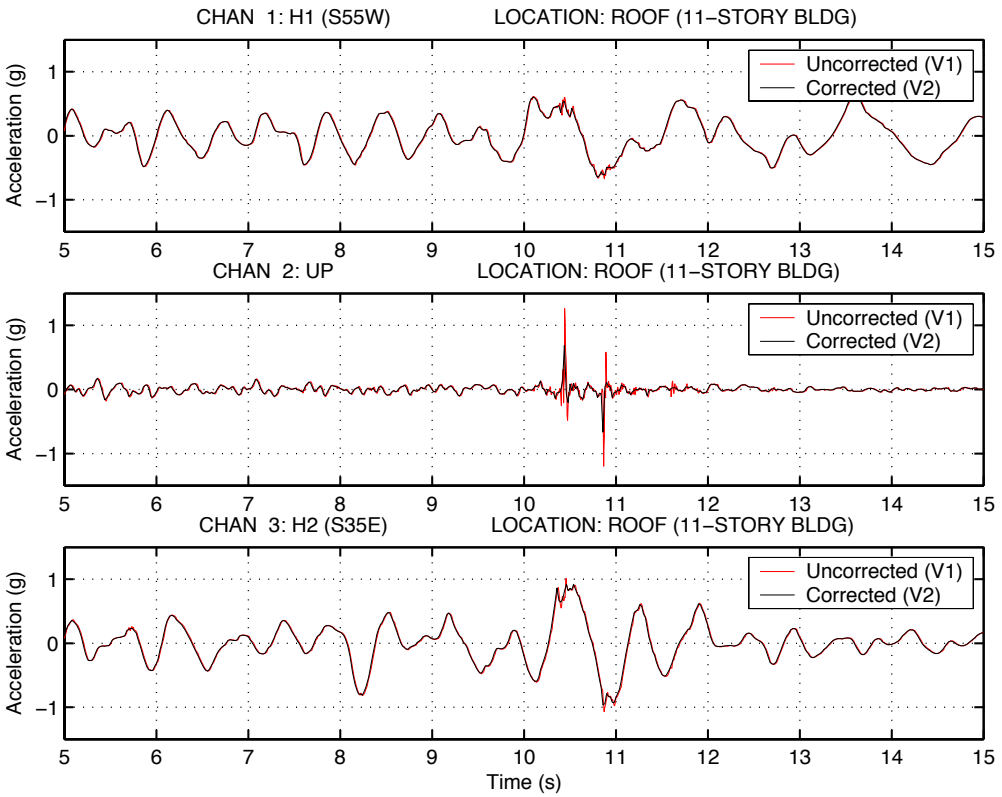

Figure A - 23. Corrected and uncorrected acceleration, Los Angeles – Olympic #2, full record (top) and close-up of transients (bottom)

Set 2a

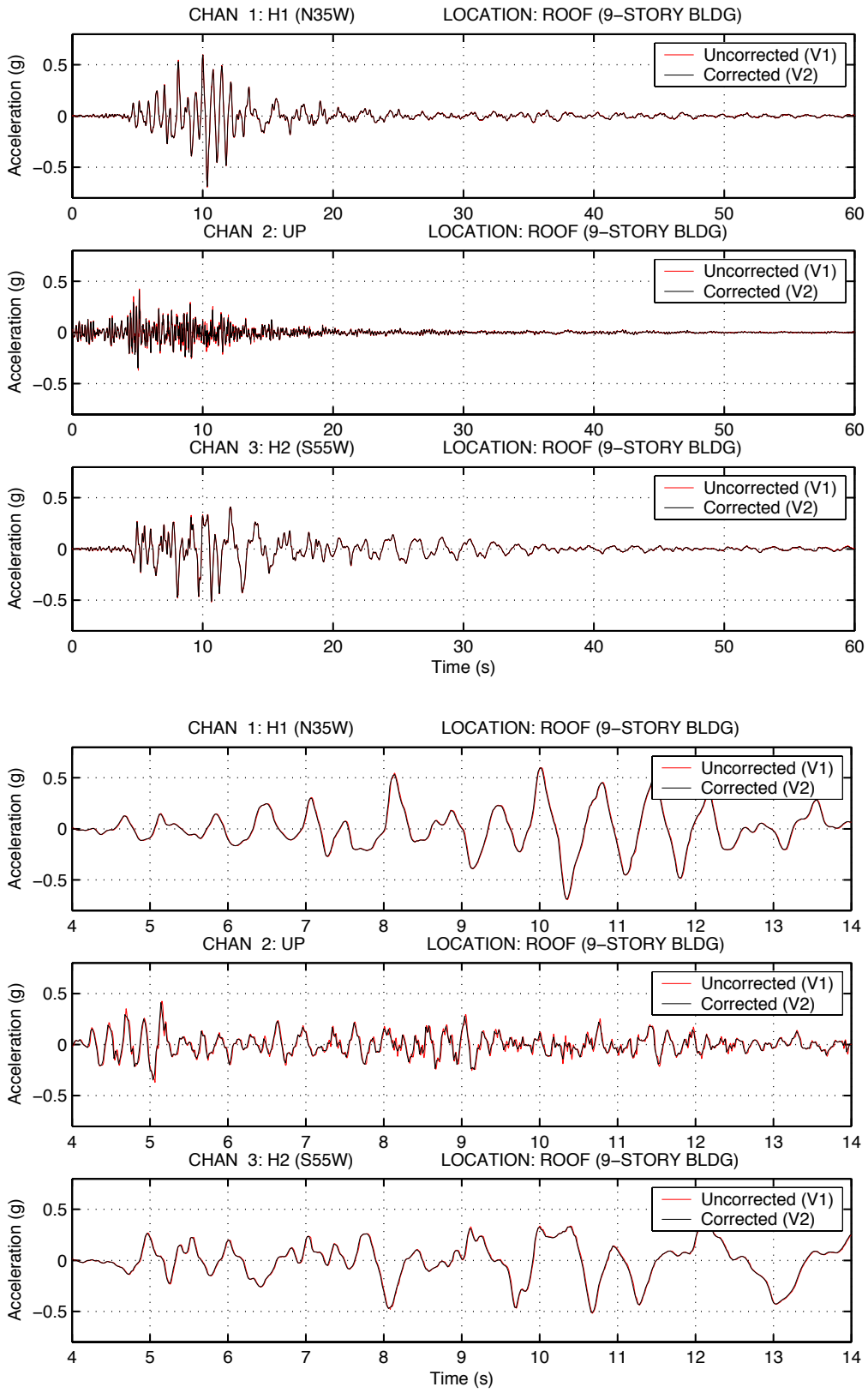

Figure A - 24. Corrected and uncorrected acceleration, Los Angeles – Olympic #1, full record (top) and close-up of transients (bottom)

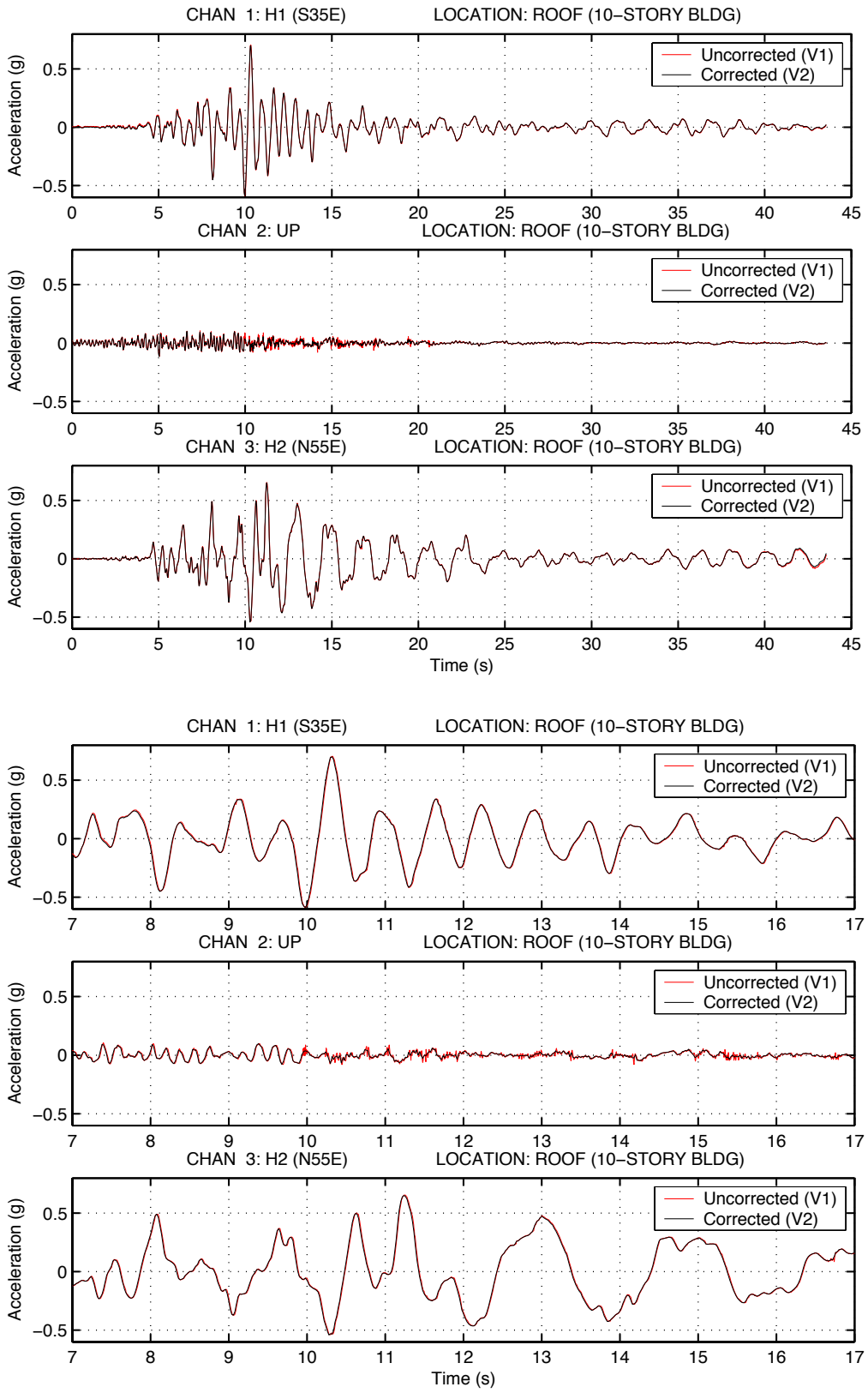

Figure A - 25. Corrected and uncorrected acceleration, Los Angeles – Olympic #3, full record (top) and close-up of transients (bottom)

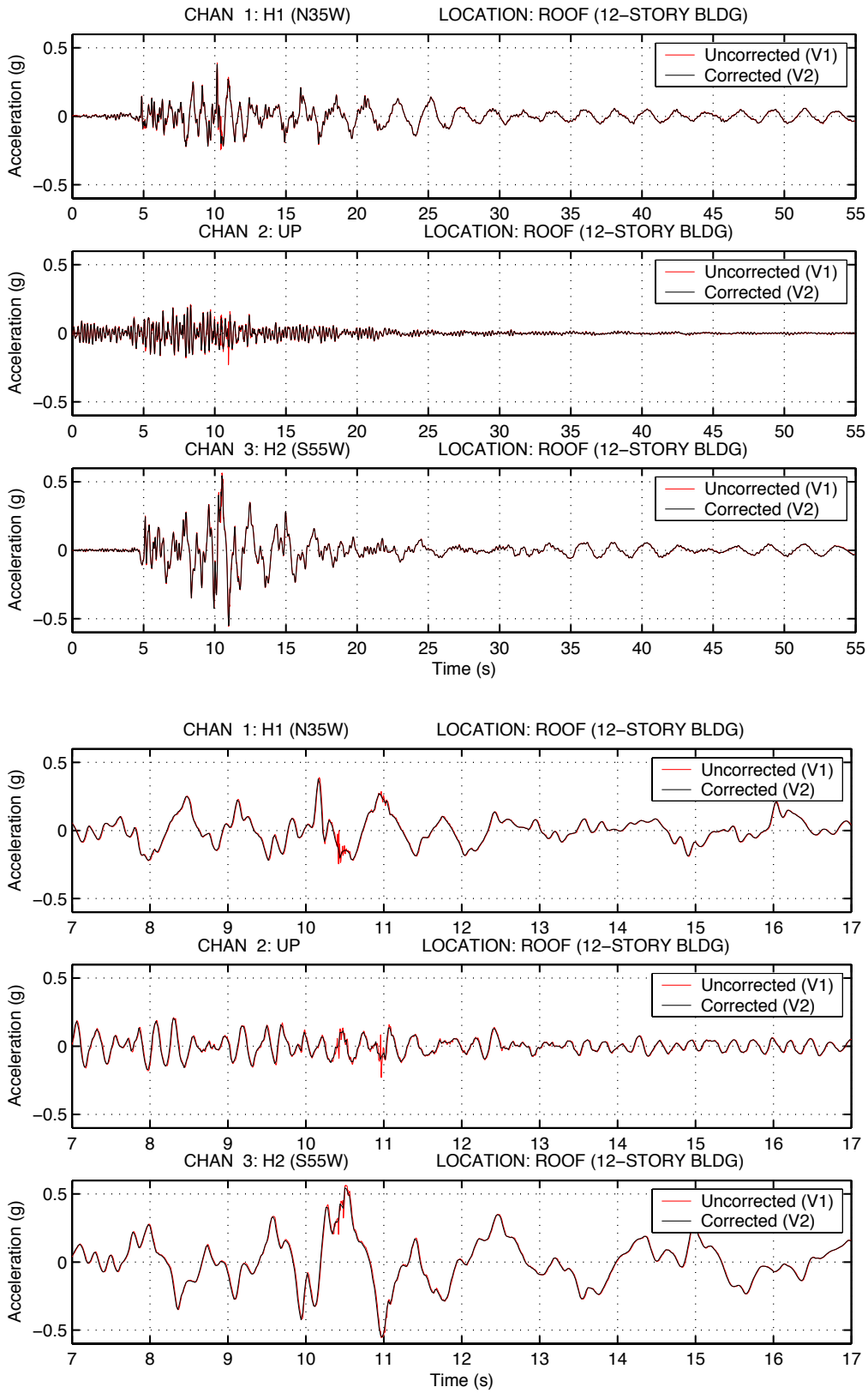

Figure A - 26. Corrected and uncorrected acceleration, Los Angeles – Olympic #4, full record (top) and close-up of transients (bottom)

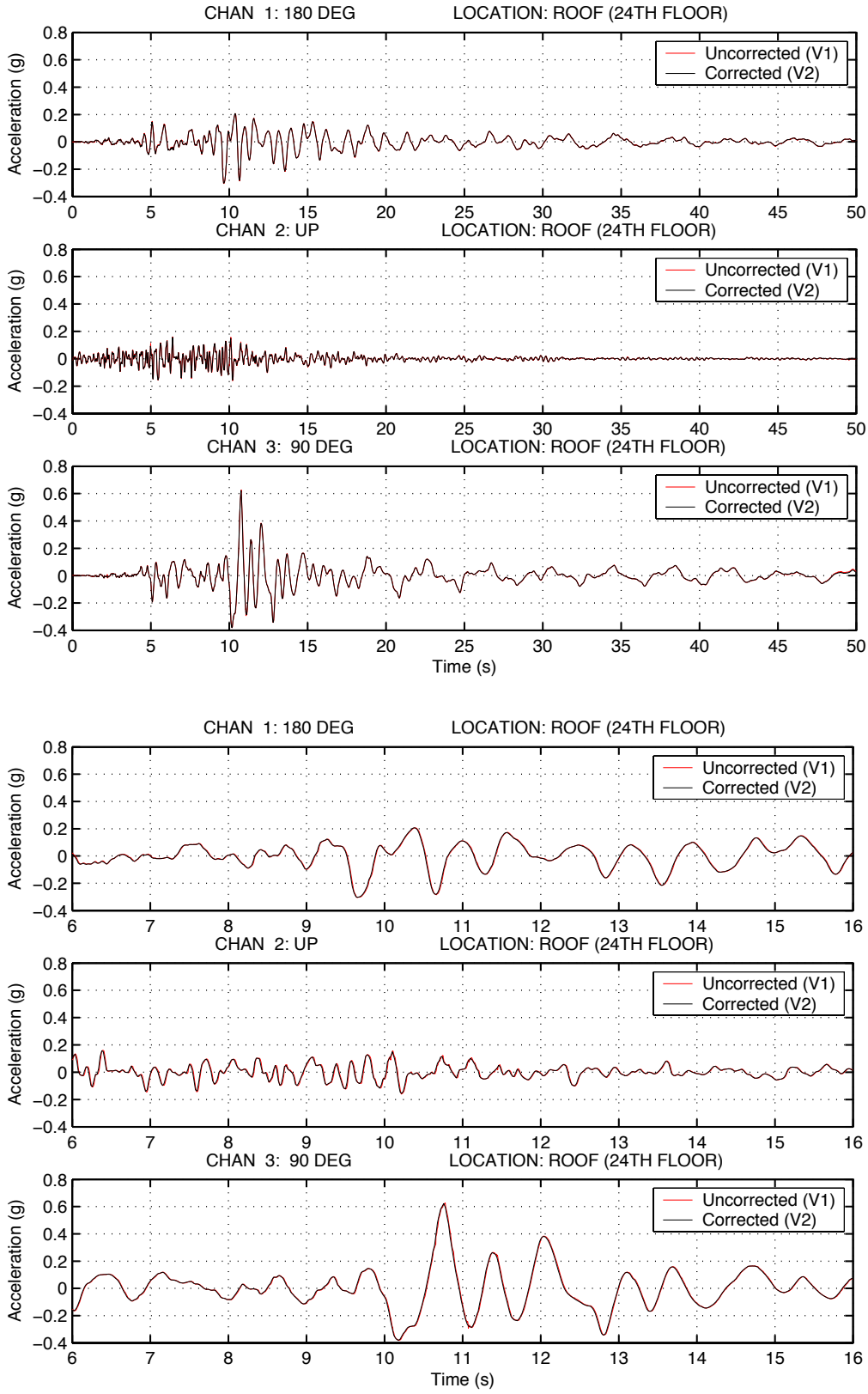

Figure A - 27. Corrected and uncorrected acceleration, Los Angeles – Wilshire #1, full record (top) and close-up of transients (bottom)

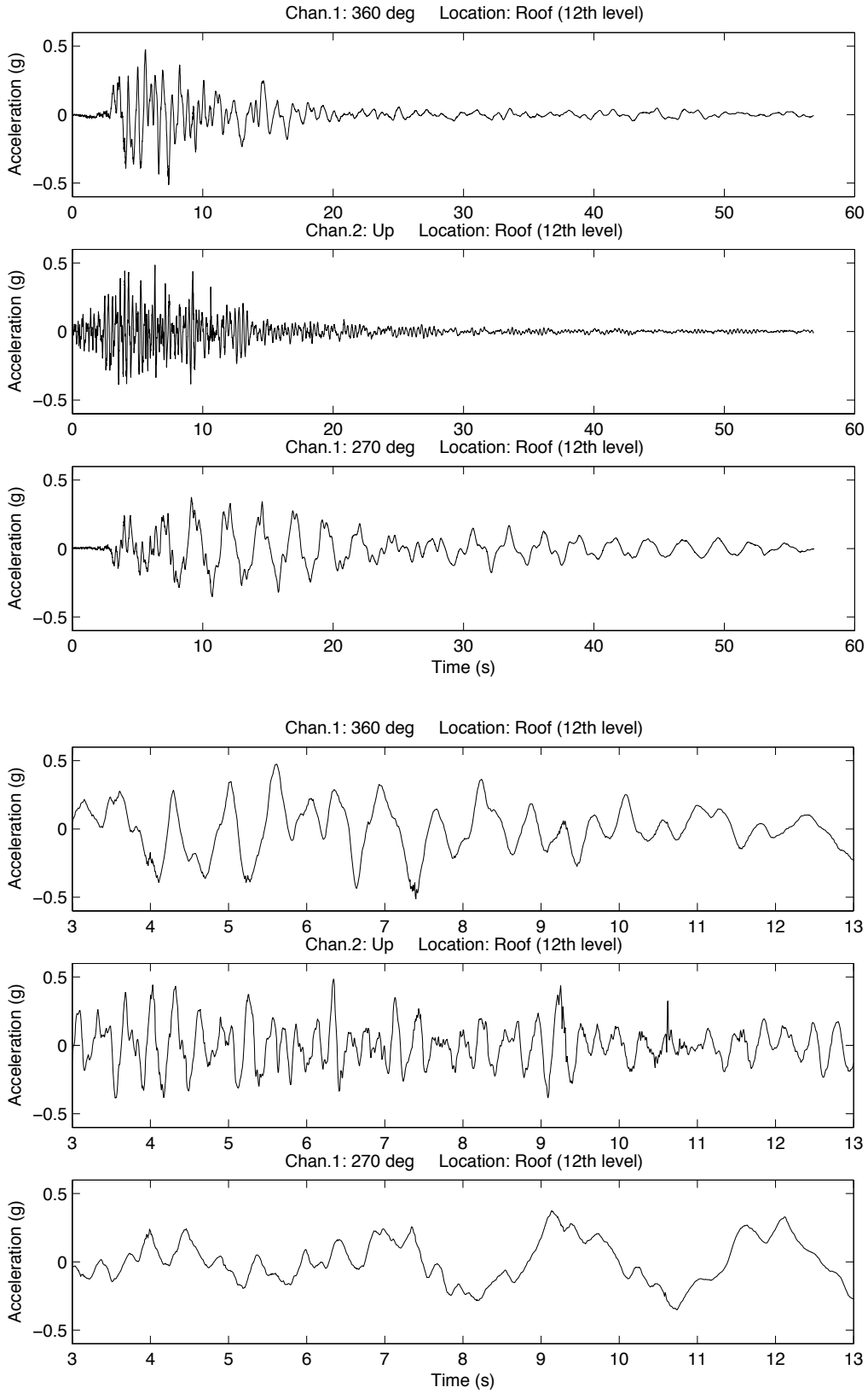

Figure A - 28. Uncorrected acceleration, Woodland Hills – Office Building #1, full record (top) and close-up of transients (bottom)

Set 2b

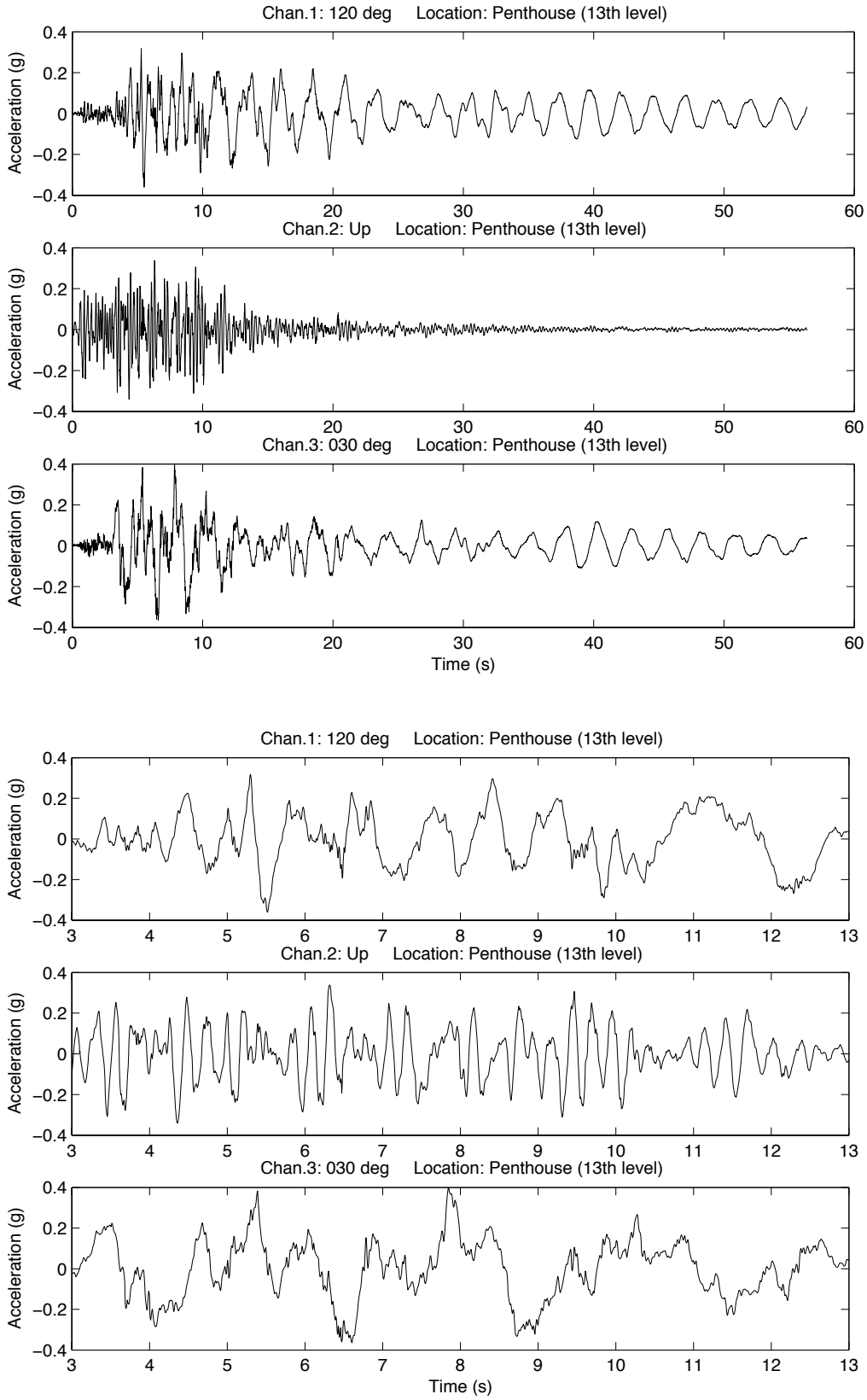

Figure A - 29. Uncorrected acceleration, Encino – Office Building #1, full record (top) and close-up of transients (bottom)

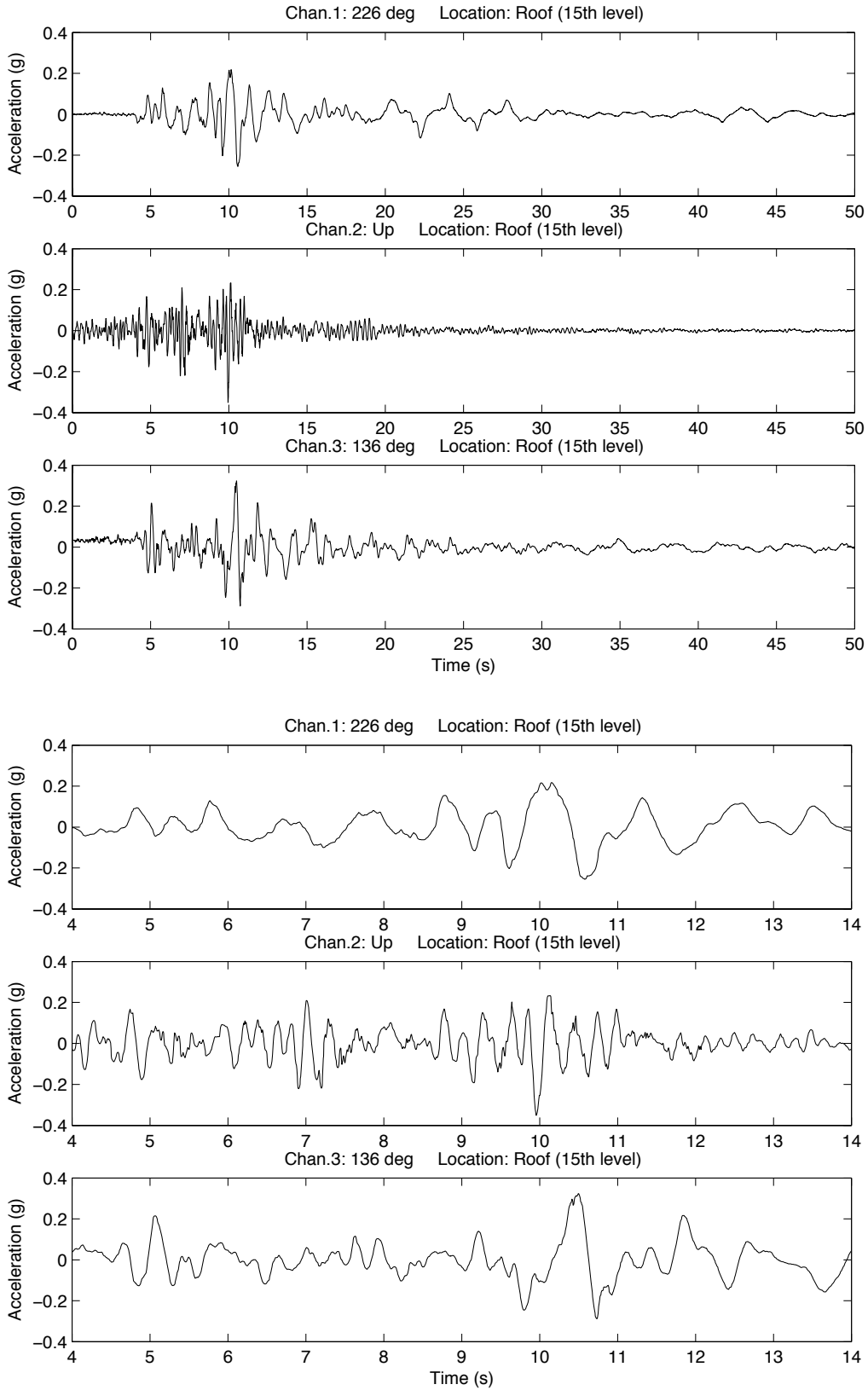

Figure A - 30. Uncorrected acceleration, Los Angeles – Office Building #3, full record (top) and close-up of transients (bottom)

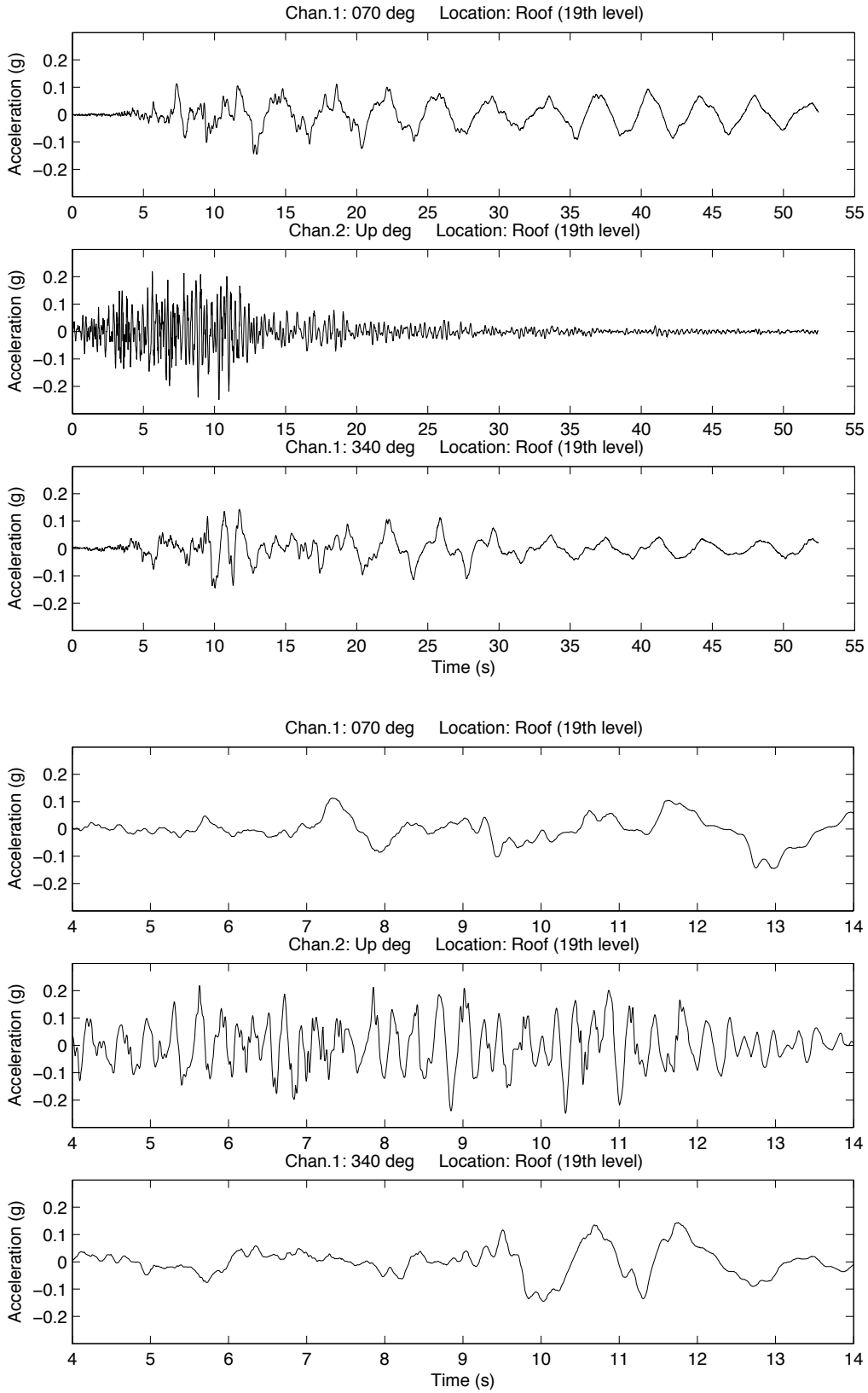

Figure A - 31. Uncorrected acceleration, Los Angeles – Office Building #4, full record (top) and close-up of transients (bottom)

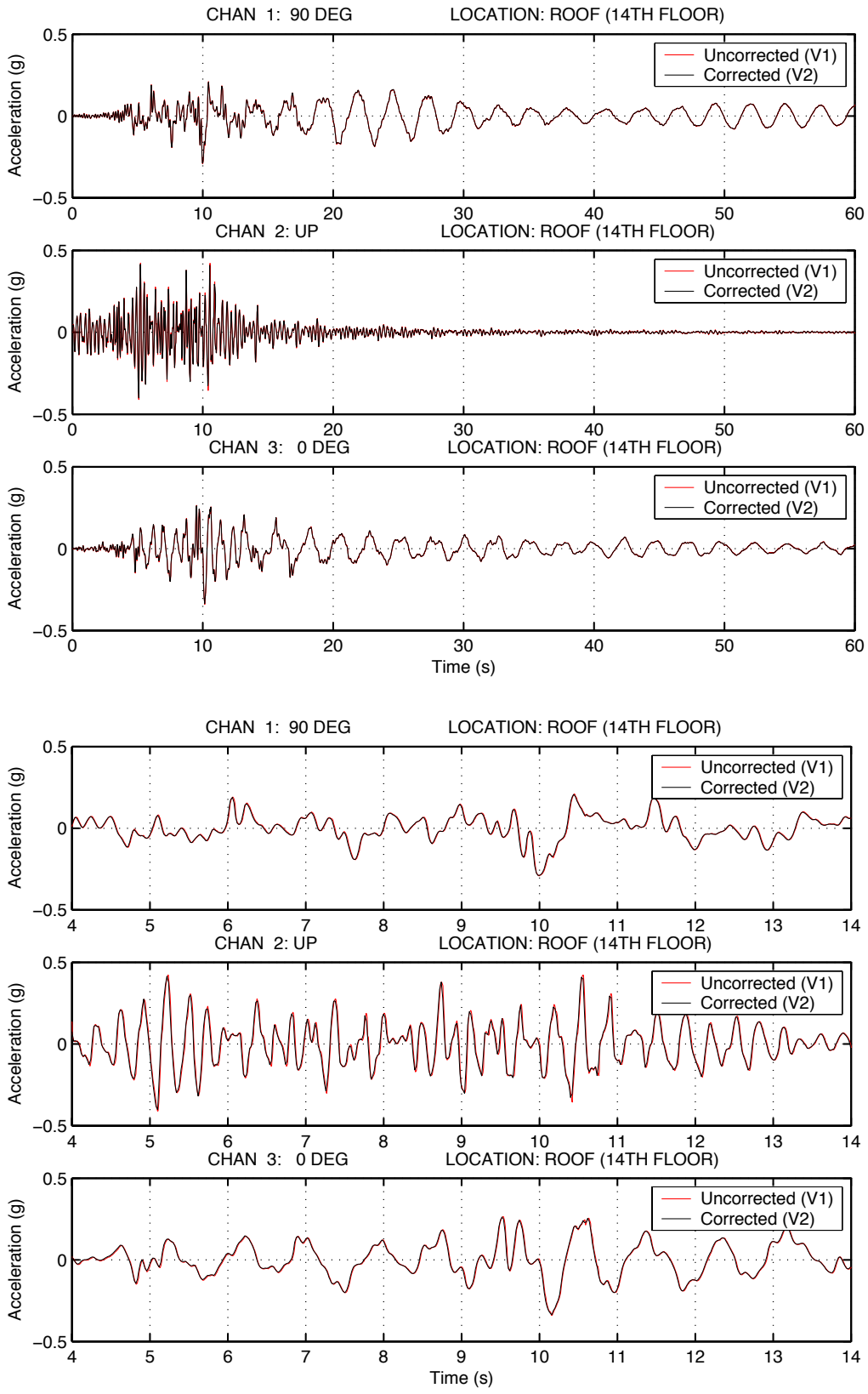

Figure A - 32. Corrected and uncorrected acceleration, Los Angeles – Wilshire #7, full record (top) and close-up of transients (bottom)

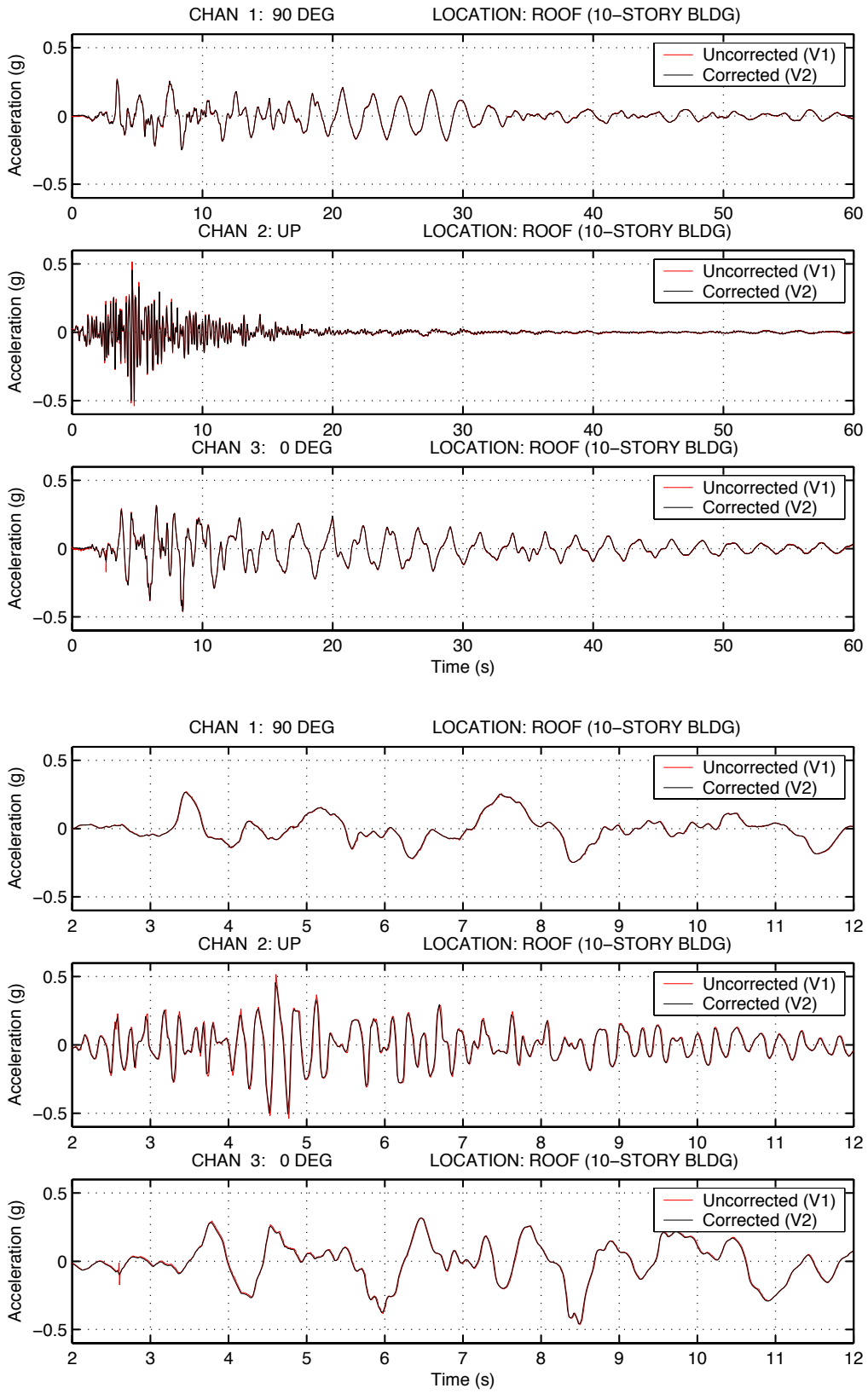

Figure A - 33. Corrected and uncorrected acceleration, Northridge – Oakdale #1, full record (top) and close-up of transients (bottom)

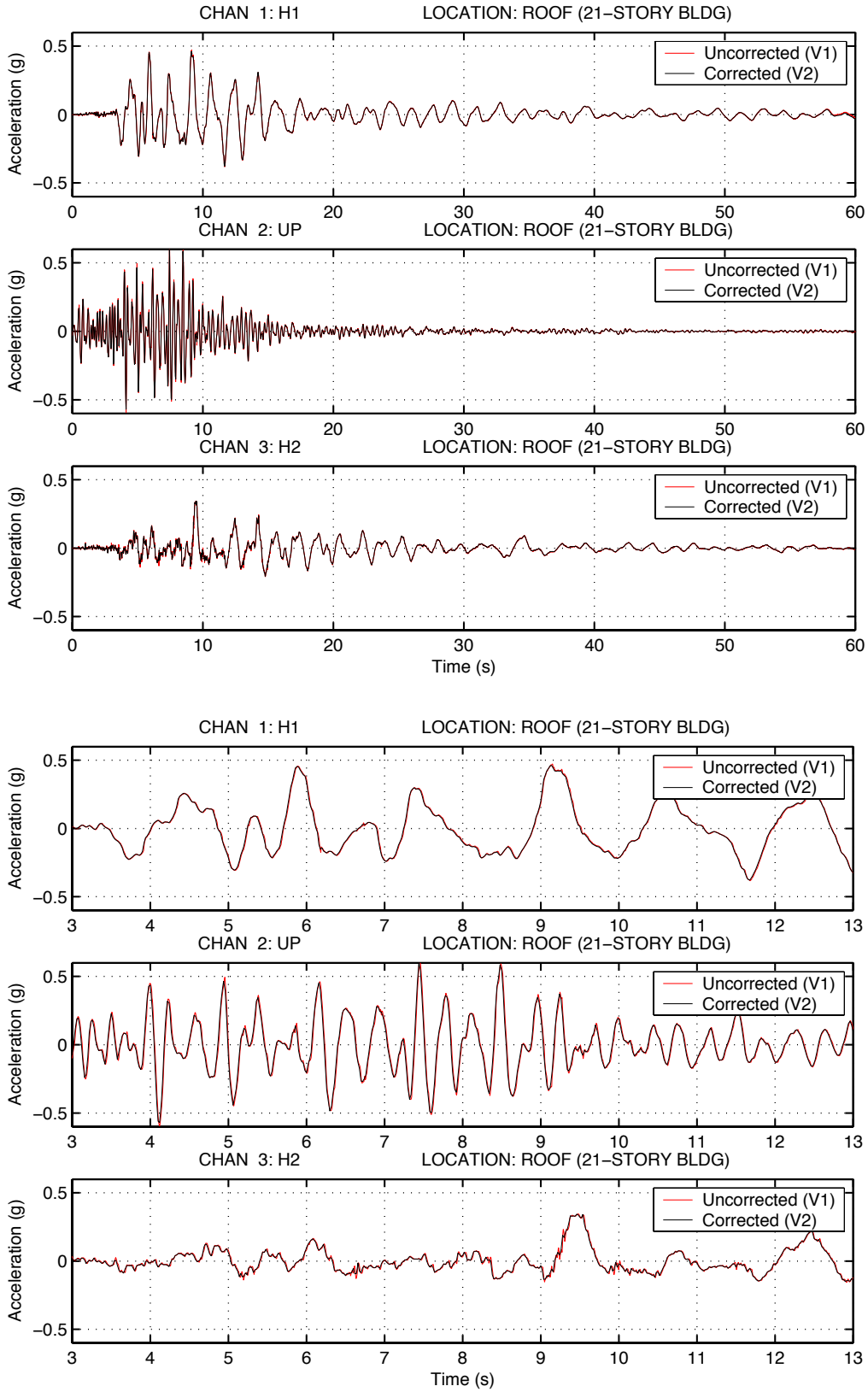

Figure A - 34. Corrected and uncorrected acceleration, Sherman Oaks – Ventura #7, full record (top) and close-up of transients (bottom)

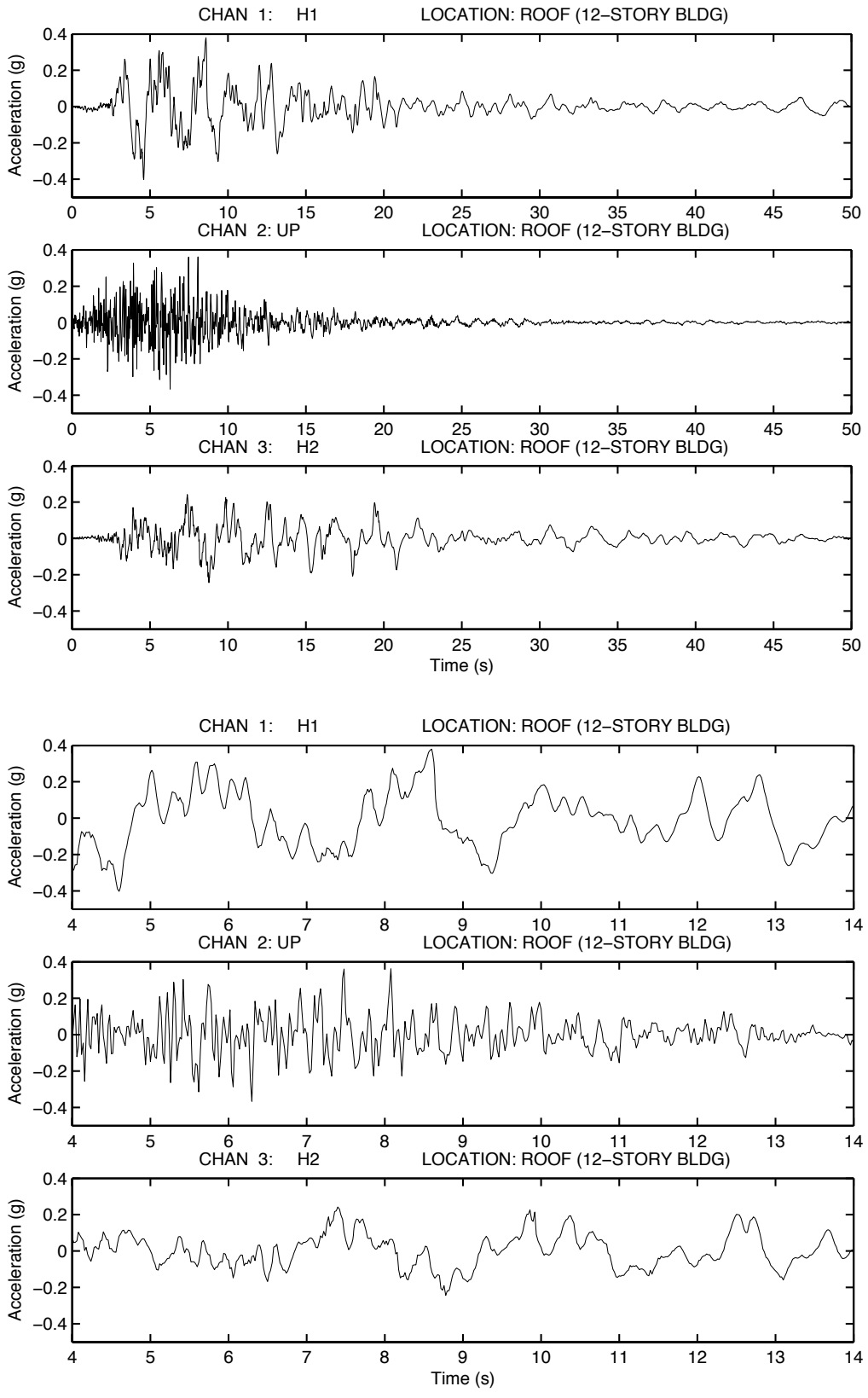

Figure A - 35. Corrected and uncorrected acceleration, Woodland Hills – Oxnard #1, full record (top) and close-up of transients (bottom)

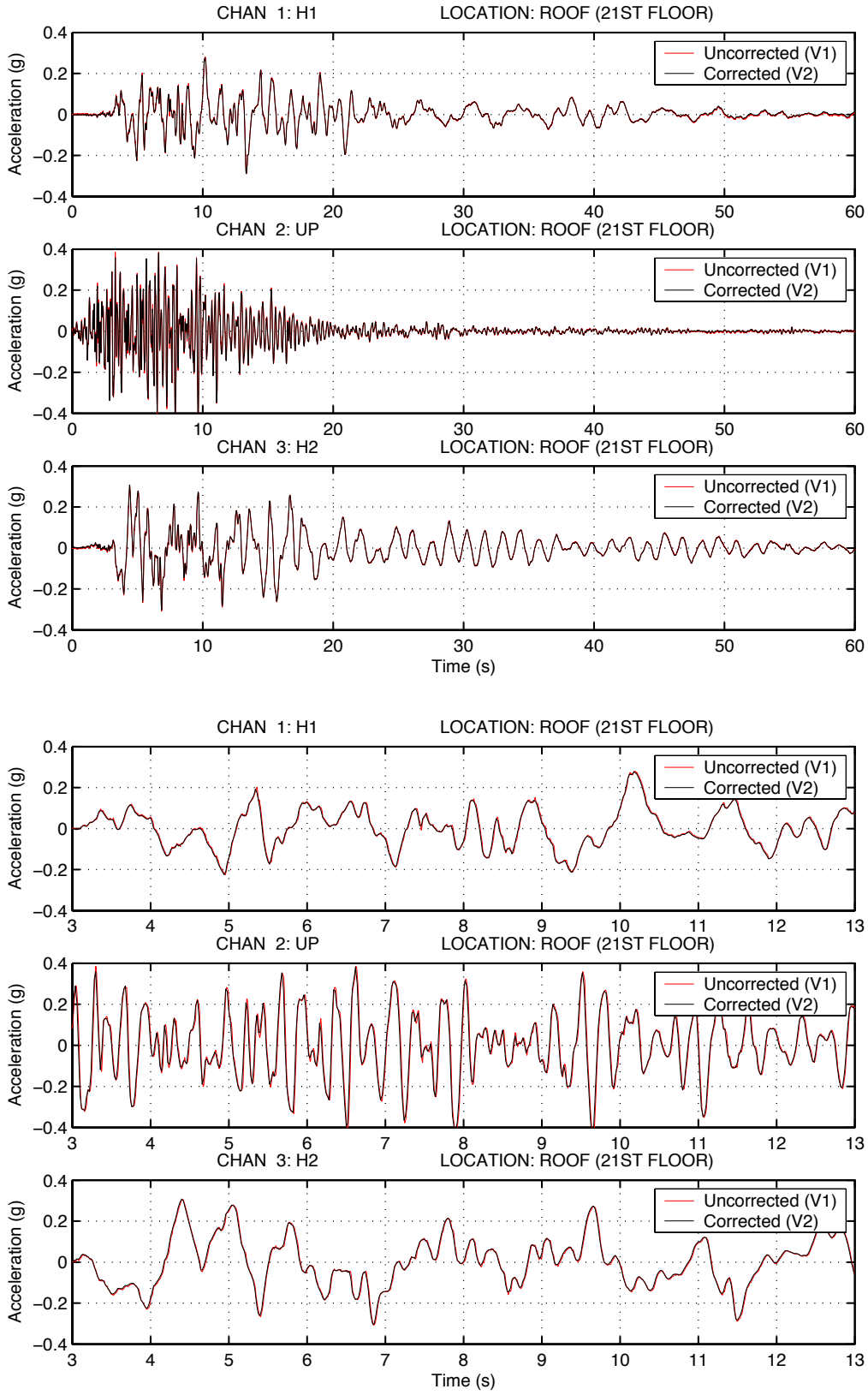

Figure A - 36. Corrected and uncorrected acceleration, Woodland Hills – Oxnard #2, full record (top) and close-up of transients (bottom)

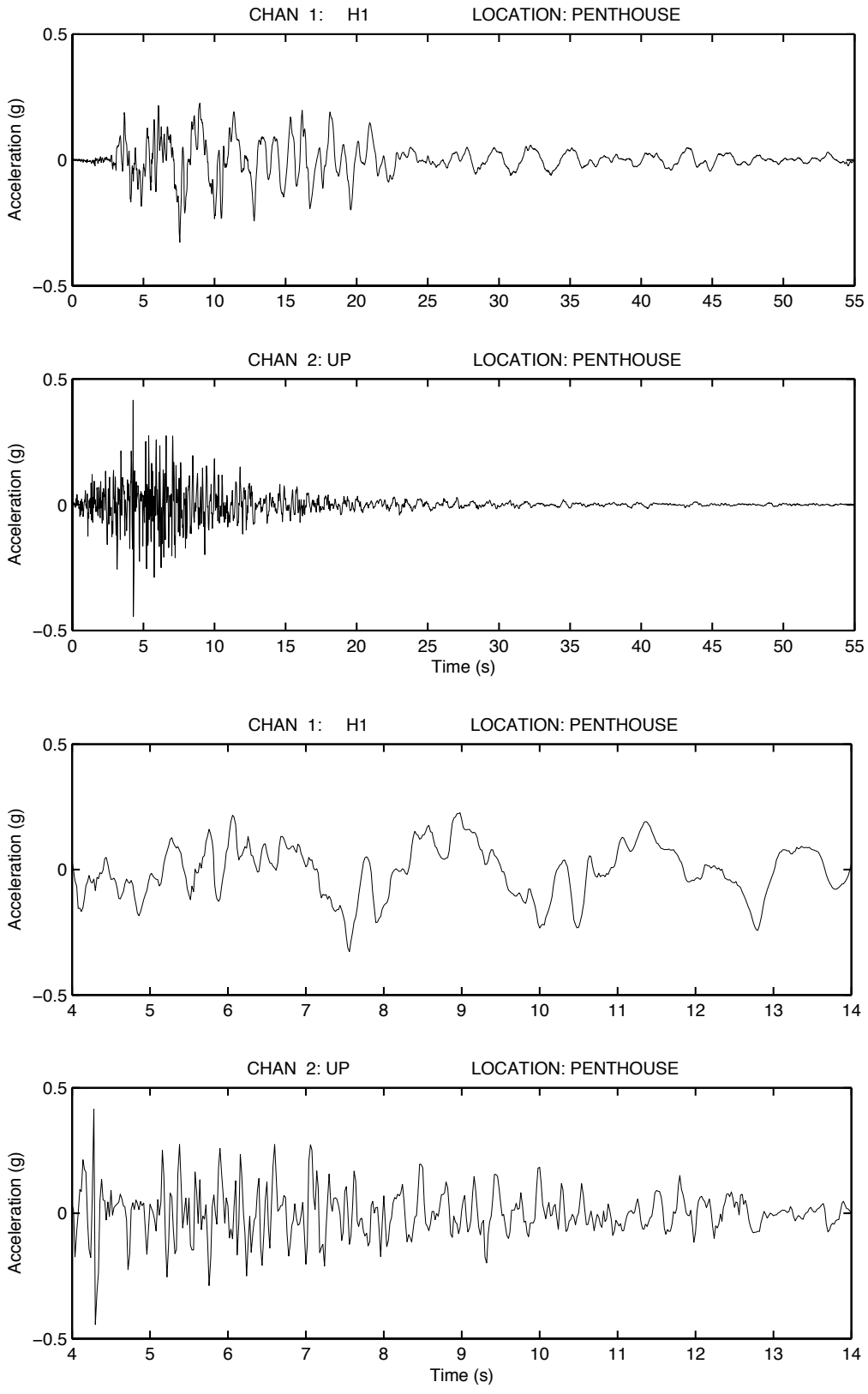

Figure A - 37. Corrected and uncorrected acceleration, Woodland Hills – Oxnard #5, full record (top) and close-up of transients (bottom)